SHORT WAVELENGTH CONE ACTIVITY TO AND THROUGH THE SUPERIOR COLLICULUS

by

Nathan Hall

B.S., University of Pittsburgh, 2007

Submitted to the Graduate Faculty of

The Kenneth P. Dietrich School of Arts and Sciences in partial fulfillment

of the requirements for the degree of

Doctor of Philosophy

University of Pittsburgh

2016

UNIVERSITY OF PITTSBURGH

KENNETH P. DIETRICH SCHOOL OF ARTS AND SCIENCES

This dissertation was presented

by

Nathan Hall

It was defended on

March 22, 2016

and approved by

Daniel J. Simons, PhD, Department of Neurobiology

Marc A. Sommer, PhD, Department of Biomedical Engineering, Duke University

Marlene R. Cohen, PhD, Department of Neuroscience

Matthew A. Smith, PhD, Department of Ophthalmology

Neeraj J. Gandhi, PhD, Department of Bioengineering

Dissertation Advisor: Carol L. Colby, PhD, Department of Neuroscience

SHORT WAVELENGTH CONE ACTIVITY TO AND THROUGH THE SUPERIOR COLLICULUS

Nathan Hall, PhD

University of Pittsburgh, 2016

A key structure for directing saccadic eye movements is the superior colliculus (SC). The SC is thought to be unresponsive to stimuli that activate only short wavelength sensitive cones (S-cones) in the retina. The apparent lack of S-cone input to the SC was recognized as an opportunity to test SC function. The assumption that S-cone stimuli are invisible to the SC has been used in numerous human clinical and psychophysical studies. The idea is that visually guided behavior dependent on the SC should be impaired when S-cone stimuli are used. Behavioral impairment to S-cone stimuli is used to infer the role of the SC in a given behavior. The goal here was to directly test this assumption by recording from single neurons in macaque SC. This hypothesis was tested in three steps. First, the perceptual reports of monkeys were used to psychophysically calibrate stimuli that activate only S-cones. Second, individual SC neurons were tested for visual sensitivity to S-cone stimuli. Finally, express saccades, a behavior known to depend on the SC, were examined physiologically and behaviorally. Both neural activity and SC-dependent behavior are present to S-cone stimuli and depend on the amount of S-cone contrast. These results demonstrate that the SC receives S-cone input, and outputs S-cone dependent behavioral commands. Together the data indicate that S-cone stimuli cannot be used to diagnose SC involvement in behavior.

TABLE OF CONTENTS

LIST OF TABLES

LIST OF FIGURES

PREFACE

I would first like to thank my advisor Dr. Carol Colby for allowing me to pursue my scientific interests and continually pushing me in directions that support my career goals. I also thank my committee for making themselves available to help solve my problems and move my research and analyses in a productive direction. I give special thanks to Dr. Marc Sommer for his willingness to serve as outside examiner and make the trip to Pittsburgh. I thank my colleagues in the CNBC Mellon Institute who always proved themselves to be both friendly and helpful. I specifically would like to thank Dr. Carl Olson for his critical, but always constructive and insightful comments. I especially thank my wife Dr. Roma Konecky, whom I met during my graduate research, and who has continued to endure my scientific reflections and provide invaluable feedback. Finally, I would like to thank my parents, John and Pattie, who are relentless in their support of my endeavors, and who nurtured a healthy scientific intellect and curiosity in me from the very beginning.

1.0 GENERAL INTRODUCTION

Evidence from studies of the oculomotor system have come to the conclusion that it is completely color blind (Schiller, 1998, White et al., 2006). This conclusion appears at odds with our subjective experience: it is easy to make saccadic eye movements to objects of a particular color. Not being able to use color to direct action seems like a failure to maximize the evolutionary advantages of color vision (Mollon, 1989, Dominy and Lucas, 2001). Yet a central structure in the control of saccadic eye movements, the superior colliculus (SC) (Schiller, 1998), does not use color opponent input from the retina. The SC is thought to receive only achromatic, luminance signals.

There are two primary pathways that carry visual information from the retina to the SC. 1) The direct, retinotectal pathway is formed by the axon collaterals of retinal ganglion cells that synapse directly onto SC neurons (Bunt et al., 1975, Hubel et al., 1975). 2) The corticotectal pathway, which travels along retinal ganglion cells to the lateral geniculate nucleus of the thalamus (LGN) before projecting on to primary visual cortex. The primary visual cortex in turn projects extensively to the SC (Kuypers and Lawrence, 1967, Fries, 1984). Early physiology studies found that the retinal ganglion cells forming the retinotectal pathway are not color opponent and are not sensitive to short wavelength sensitive cone (S-cone) activity (Marrocco and Li, 1977, Schiller and Malpeli, 1977, De Monasterio, 1978b). Instead, retinotectal ganglion cells carry luminance information, which originates from long and middle wavelength sensitive cones (L- and M-cones), but not S-cones (Calkins, 2001). The corticotectal pathway carries information originating from

the magnocellular layers of the LGN (Schiller, Malpeli, & Schein, 1979). Neurons in the magnocellular layers also carry only luminance information, summed inputs from L- and M-cones, but not S-cones. The conclusion from these studies is that SC neurons are responsive to achromatic luminance stimuli (arising from L- and M-cones) but not to chromatic stimuli. In addition, they suggest that the SC is not sensitive to S-cone activation at all.

Many psychophysical studies have been based on the assumption that S-cone activation does not drive neurons in the SC. If this were true, the use of S-cone isolating stimuli would be a convenient way to assess collicular function. This strategy was first proposed in an influential behavioral study of SC function (Sumner et al., 2002). Since its inception, this technique has been used to test a broad range of behavioral phenomena for SC dependence. The scope of investigations has ranged from neural mechanisms of blindsight (Leh et al., 2006, Marzi et al., 2009, Alexander and Cowey, 2010) and interhemispheric transfer in patients without a corpus callosum (Savazzi et al., 2007), to inhibition of return (Sumner et al., 2004), nasotemporal asymmetry (Bompas et al., 2008), and the gap effect (Anderson and Carpenter, 2008). The appeal of this method is that the SC can be "lesioned" on a trial by trial basis without any damage to the brain. The idea is to present subjects with either a luminance or an S-cone stimulus on separate trials of a visual-oculomotor task. If behavior (usually saccadic reaction time, or RT) is different in response to the S-cone stimulus, the conclusion is that the phenomenon under study depends on the SC. The argument is that because the SC cannot detect the S-cone stimulus, it cannot generate a behavior that depends on the S-cone stimulus.

No physiological studies of the SC have directly tested whether cells in the SC respond to S-cone stimuli and use them to guide behavior. Studies of SC afferents suggest that they are not color opponent, but color opponency is different from sensitivity and detection. Previous work

has not explicitly tested if SC neurons are affected by S-cone stimuli, and their experimental methods differed tremendously from those currently used in human psychophysics. The experimental goal here was to directly test whether SC neurons can detect S-cone stimuli and use them to drive saccadic behavior. The present experimental methods were designed to replicate those used in human behavioral, psychophysical and clinical research. To test the hypothesis that SC neurons can detect and use S-cone input requires 3 steps. 1) Determine a true S-cone isolating stimulus in macaque monkeys. A true S-cone isolating stimulus varies with retinal location and observer. It must be psychophysically determined. 2) Determine whether SC neurons show visual responses to calibrated S-cone isolating stimuli. 3) Determine whether SC neurons can transform S-cone input into behavioral output. Data from these three steps reveal that S-cone isolating stimuli drive SC neurons and SC-dependent behavior in the same way as luminance stimuli. These findings demonstrate that S-cone stimuli cannot be used to remove, or determine, SC involvement in visual and oculomotor behavior.

2.0 PSYCHOPHYSICAL DEFINITION OF S-CONE STIMULI

Adapted with permission from: Hall NJ and Colby CL (2013).
Psychophysical definition of S-cone stimuli in the macaque. Journal of Vision (13): 1-18.

2.1 INTRODUCTION

2.1.1 The S-cone system

In vision experiments it is often desirable to isolate specific visual processing subsystems. Creating a stimulus that can do this is not straightforward, and typically requires a subject-specific psychophysical calibration. Psychophysical calibrations must be based on perceptual experience—something that is easy to ascertain in human subjects via verbal report. Our goal here was to use the non-verbal perceptual report of monkeys to perform psychophysical calibrations similar to those done in human subjects. The procedure developed allows us to create a stimulus that isolates excitation to a specific cone subsystem.

Photopic vision in Old World primates is driven by the activation of 3 classes of cone receptors in the retina. Blue cones, or S-cones, are those most sensitive to the short wavelengths of visible light. The S-cone system differs from other visual subsystems in a number of important ways. The S-cone system is phylogenetically older (Yokoyama and Yokoyama, 1989) and in many ways peculiar compared to long and middle wavelength sensitive cone systems (L- and M-cones) (Calkins, 2001). For example, S-cone signals are carried by their own, slowly conducting

class of retinal ganglion cell (Dacey and Lee, 1994). Such differences in the processing of S-cone input have made the study of this subsystem the focus of numerous investigations. Stimuli calibrated by the procedure described here can be used to study S-cone systems physiologically by selectively altering excitation of S-cones in macaque monkeys.

2.1.2 S-cone isolating stimuli in humans

Stimuli that selectively activate S-cones (or S-cone isolating stimuli) can be used to study the S-cone system. These stimuli cause no change in L- and M-cone excitation. A true S-cone isolating stimulus differs from one based solely on cone sensitivity spectra mainly because of macular pigment in the eye (Sumner et al., 2002). Macular pigment selectively absorbs short-wavelength, blue light (Snodderly et al., 1984b), where S-cones are most sensitive. The amount of macular pigment absorption depends on the viewer and even varies by retinal location within individuals. These factors make it difficult to construct an S-cone isolating stimulus. S-cone isolating stimuli must be calibrated for individual observers and spatial locations. This requires a calibration procedure to identify S-cone isolating stimuli at desired experimental locations for each subject.

Several studies have adopted a calibration procedure to determine S-cone isolating stimuli. These calibration procedures have all been performed on human subjects and based on the procedure proposed by Smithson et al. (2003). Armed with S-cone isolating stimuli for each individual subject and test location, researchers have investigated a variety of questions about the function of the S-cone system. Behavioral analyses using S-cone isolating stimuli have shown that the S-cone system is slower than other visual systems (Smithson and Mollon, 2004), especially within oculomotor networks (Bompas and Sumner, 2008). In particular, the role of the superior colliculus (SC) has been studied using S-cone stimuli, to which the SC is believed to be blind (De

Monasterio, 1978b, Schiller et al., 1979a, Sumner et al., 2002). These investigations have probed the role of the SC in oculomotor behavior (Sumner et al., 2002, Sumner et al., 2004, Sumner et al., 2006, Anderson and Carpenter, 2008) and clinically in studies of blindsight and interhemispheric transfer (Savazzi and Marzi, 2004, Leh et al., 2006, Savazzi et al., 2007, Leh et al., 2009). These studies of human subjects all share the common theme of isolating the SC by using S-cone isolating stimuli.

2.1.3 S-cone isolating stimuli in non-human primates

All studies using calibrated S-cone isolating stimuli to date have been performed on human subjects. The use of animal models allows collection of neurophysiological as well as behavioral data. Macaque monkeys are excellent models of trichromatic cone mediated vision. Macaque color vision and perception are nearly identical to that of humans as found both psychophysically via behavioral report (De Valois et al., 1974, Huang et al., 2002) and physiologically by studying the spectral sensitivity of the three cone types (Bowmaker et al., 1978, Bowmaker and Dartnall, 1980). The distribution of retinal S-cones is likewise similar in both species, being most numerous around the fovea and forming a semi-regular distribution more eccentrically (Curcio et al., 1987, Bumsted and Hendrickson, 1999). Both humans and monkeys have macular pigment that is most dense near the fovea and decreases toward the periphery (Snodderly et al., 1984a, Snodderly et al., 1984b, Trieschmann et al., 2007). The spatial extent of macular pigment varies between individuals. This variation has lead researchers using psychophysical studies in humans to calibrate S-cone isolating stimuli for each subject and each spatial location used experimentally. Similarities between humans and monkeys in visual processing make it both possible and

necessary to calibrate S-cone isolating stimuli in macaques using procedures like those used in humans.

Our goal was to determine S-cone isolating stimuli in macaque monkeys. Our methods are conceptually similar to those Smithson et al. (2003) proposed for use on human subjects. The similarity between the two procedures provides a critical bridge between previous human psychophysics studies and future work in monkeys using S-cone isolating visual stimuli. We found that it is possible to calibrate S-cone isolating stimuli in macaque monkeys. The colors of these stimuli are similar to those found for humans and likewise depend on the individual observer and spatial location tested.

2.2 MATERIALS AND METHODS

2.2.1 Subjects and data acquisition

Two adult male rhesus monkeys (*macaca mulatta*) were used in these experiments. Animals were cared for and handled in accordance with National Institutes of Health guidelines. The University of Pittsburgh Institutional Animal Care and Use Committee approved all experimental protocols. Monkeys weighed 13 and 8.5 kg (monkey CA and monkey FS, respectively). Both had normal trichromatic color vision as evidenced by their ability to distinguish L-cone isolating stimuli in addition to their ability to resolve S-cone isolating stimuli. During experiments, animals sat in a primate chair with head fixed. Monkeys viewed a CRT monitor at a distance of 30 cm. Eye position was monitored using scleral search coils (Judge et al., 1980) with a Riverbend field driver and signal processing filter (Riverbend Technologies Inc.). Eye position voltages were

continuously monitored online through NIMH Cortex software (provided by Dr. Robert Desimone) and saved for offline analysis on a separate computer running Plexon software (Plexon Inc.). Offline analysis was carried out on custom MATLAB® (Mathworks; Natick, MA) software that detected saccades, trial events and trial outcomes.

2.2.2 Stimulus presentation and control

Stimulus timing and presentation were controlled using NIMH Cortex software. Stimuli were presented on a computer controlled 19" ViewSonic® color CRT monitor at a refresh rate of 85 Hz using an 8 bit DAC with an ATI Radeon™ X600 SE graphics card. To generate stimuli, the monitor was calibrated for color and luminance using a Photo Research PR-655 SpectraScan® spectroradiometer integrated with custom MATLAB® (Mathworks; Natick, MA) software. Actual stimuli used were verified for accuracy in both color and luminance using the same setup. Colors for stimuli were chosen from MacLeod-Boynton (MB) color space (MacLeod and Boynton, 1979) as defined using the Smith and Pokorny cone fundamentals (Smith and Pokorny, 1975). We modified MB space such that the vertical axis represents relative S-cone excitation times 4, as has been done previously (Smithson et al., 2003). Color coordinates in this paper refer to this modified MB color space which we will simply call MB space.

2.2.3 Experimental approach

Our approach takes advantage of "transient tritanopia" (Mollon and Polden, 1975) in a manner first proposed by Smithson et al. (2003). The principle is that sensitivity in the S-cone opponent channel is briefly and selectively decreased after adaptation to a bright yellow background. In

other words, there is a transient blindness to activation of the third, "tritan" cone (or S-cone) channel, i.e. tritanopia. Elevated L- and M-cone channel activity persists after excessive stimulation by the bright yellow background resulting in selective suppression of S-cone opponent pathways. S-cone channel activity must outweigh that of L- and M-cones in order to detect an increase in S-cone contrast. Elevated L- and M-cone activation means that greater S-cone excitation is needed to outweigh them and thus detect an S-cone stimulus—i.e. S-cone detection threshold is increased. One can imagine the afterimage caused by viewing a yellow square, causing the perception of a blue square when looking at a white surface. This perception that everything is tinted blue makes it more difficult to detect blue stimuli. The increase in threshold will be greatest for a stimulus that best matches the exact S-cone isolation point for a given viewer.

The objective of experimental calibration was to determine S-cone isolating stimuli separately for each monkey at 6 spatial locations. An S-cone isolating stimulus will always lie along a tritan confusion line. A tritan line is a line in color space representing a series of colors that are distinguishable only on the basis of S-cone stimulation. Colors along a tritan line represent constant levels of excitation in L-and M-cones, while excitation for S-cones varies. All colors along a subject's tritan confusion line would be perceived as identical were their S-cones suddenly removed. Such a tritan line lies in an equiluminant plane in MB color space.

The equiluminant MB plane (~20.7 cd/m^2) from which our stimuli were chosen is shown in Figure 1. Because the spectral sensitivity of the 3 classes of retinal cones overlaps, an S-cone isolating stimulus, and thus a tritan line, must be determined with respect to a background color. The background and stimulus colors are chosen so that their degree of L- and M-cone excitations are equal. We used the standard equal energy gray (EEG) point (.667, .060) as our background color. Radiating outward from this point are candidate tritan vectors. Candidate vectors are used

to find the actual tritan line and are chosen to be near the theoretical tritan line. The vertical vector represents the theoretical tritan line through EEG in MB space. The bright adapting backgrounds (luminance 53.5 cd/m^2) used were either white (.651, .048) or yellow (.664, .004).

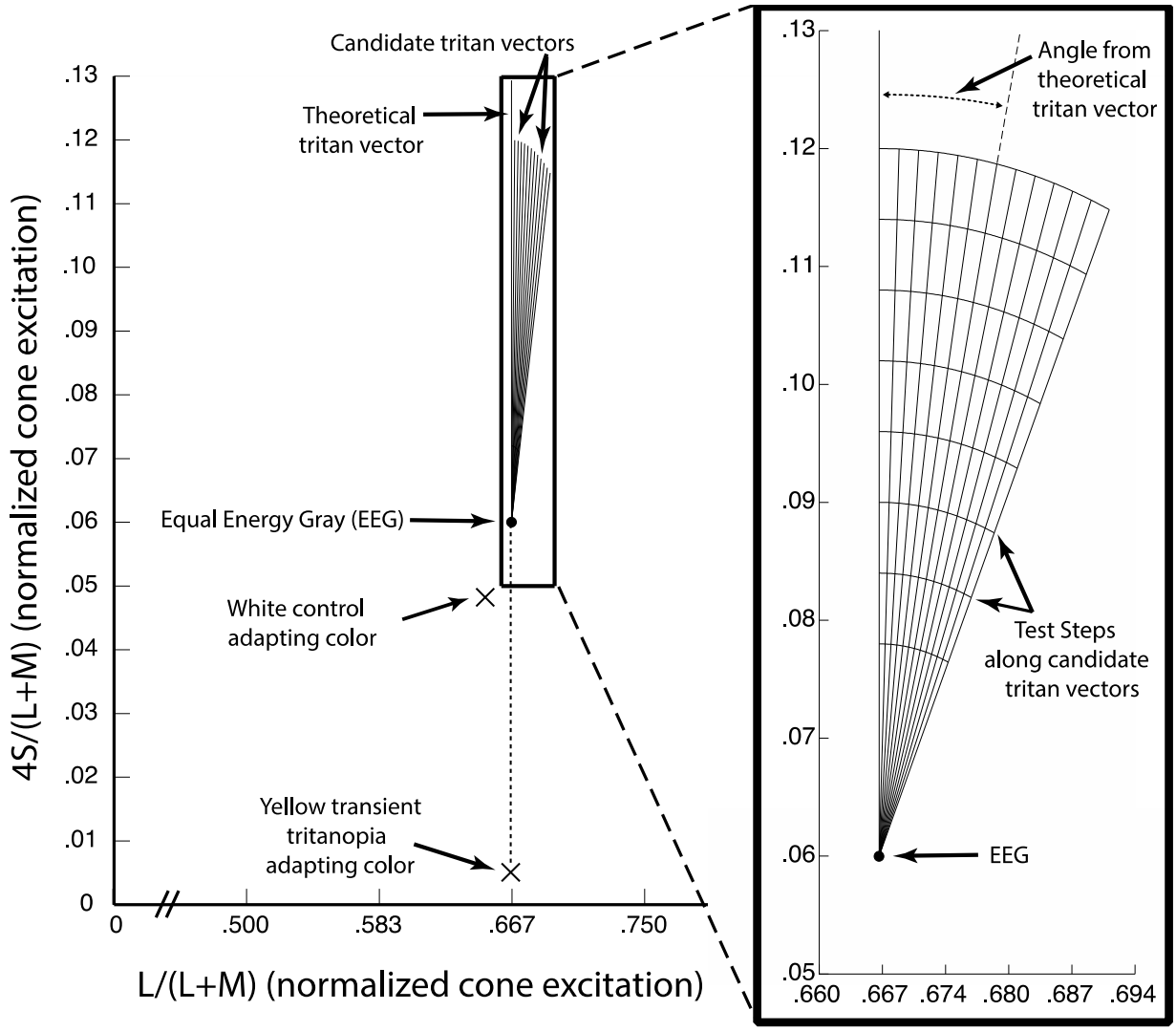

Figure 1. Scaled MacLeod-Boynton color space. The main figure shows the version of MacLeod-Boynton (MB) space used for determining stimulus and background colors. This MB space is scaled so that values for S-cone excitation on the vertical axis are multiplied by 4 to give similar control performance across candidate tritan vectors following the procedure of Smithson et al. (2003). The horizontal axis is truncated as no points outside of those shown were used. EEG (filled circle) was the background color for experiments. The theoretical (vertical) and candidate (angled) tritan vectors tested are shown as lines in the equiluminant plane radiating from EEG. Xs indicate the color coordinates of the adapting backgrounds but signify that they do not lie in the equiluminant plane of the tritan vectors. Adapting backgrounds were much brighter than the plane shown and therefore lie above it along the z-axis rising out of the page. The expanded view on the right details vectors and test steps. Candidate vectors were chosen and labeled as angles from the theoretical line (0^o to 24^o). Curves running across tritan vectors mark the eight test steps. Test steps were increments of 0.006 units in the scaled MB space starting at 0.018 units and measured as distance from

EEG along each vector. Points in MB space used to find detection thresholds lay at the points of intersection between the vectors and test steps.

2.2.4 Task Design

At the start of each trial, a fixation cross was presented on an EEG background and the monkey had 200 ms to acquire fixation (Figure 2). During fixation, the background changed to 1 of 2 possible adapting states. During control trials, the background was bright white. During tritanopia trials the background was bright yellow to induce transient tritanopia. The monkey then fixated for 7600 ms to allow for adequate adaption. This fixation period is much longer than in many primate oculomotor tasks. To encourage monkeys to maintain fixation on this bright background, 1 drop of liquid reward was delivered after 3000 and again after 6000 ms of fixation. Control trials place an upper bound on detection thresholds in the absence of transient tritanopia. They demonstrate that detection thresholds do not change across candidate tritan vectors at contrasts above .018 from EEG. Thresholds are lower in this case because there is no selective desensitization of S-cone channels, i.e. a lack of transient tritanopia. Control and tritanopia trials were run in separate sessions.

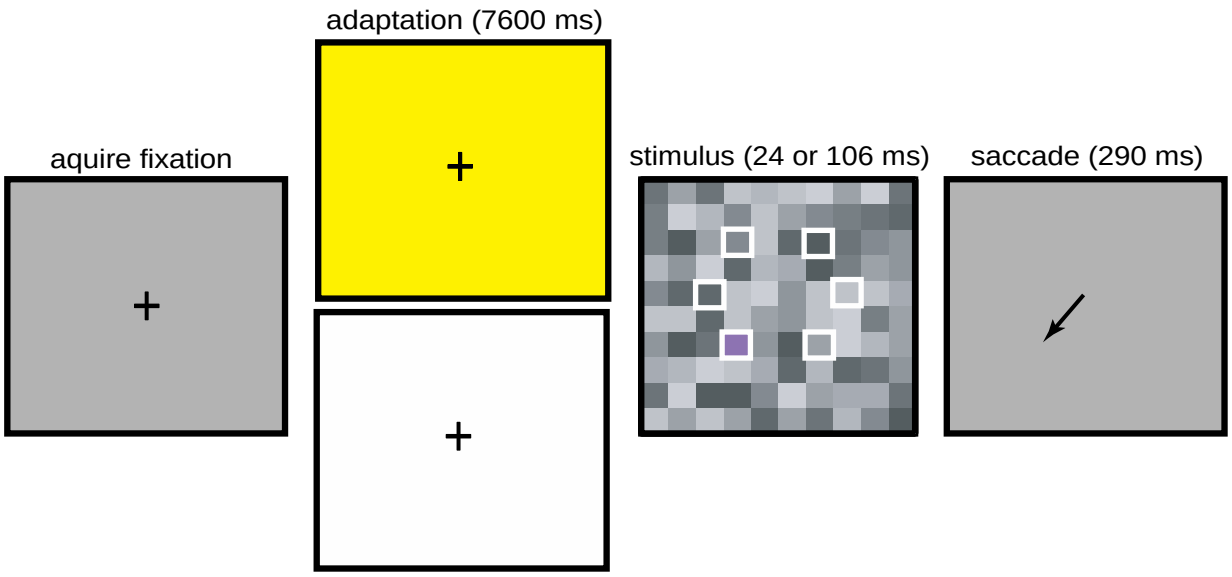

Figure 2. Tritan line calibration task. At the start of each trial, monkeys fixated a central cross on an EEG background. During fixation, a yellow or white bright adapting background was turned on. At the end of the fixation period the fixation cross was turned off and simultaneously a target was presented embedded in a screen of 1^o x 1^o gray squares. The target square appeared randomly in one of six possible locations on each trial (unfilled white squares, not visible to monkeys). Target color was randomly selected on each trial from one of the eight possible test steps. To indicate detection, animals had to initiate a saccade to the location of the target.

After adaptation, the fixation cross was extinguished and simultaneously a $1x1^o$ stimulus target square appeared. This square represented both the test stimulus color and the saccade target. This stimulus target was embedded in a full screen background array of $1x1^o$ gray squares (Figure 2). The square was presented in 1 of 6 possible locations randomly chosen on each trial at 4^o eccentricity for monkey FS and 6^o for monkey CA. Six screen locations were tested for each animal because the identity of the true tritan vector varies by location as well as individual. During a given ~ 2 hour daily session monkeys performed approximately 140-240 trials. Both animals typically performed more trials during the easier control compared to tritanopia sessions. In each session stimulus target colors were chosen from a single candidate tritan vector. Stimulus target color was chosen randomly on each trial. The color was 1 of 8 possible test steps, representing distance from EEG, and chosen to be at the intersection of one of the test step curves with a candidate tritan vector (Figure 1). Luminance of the stimulus target square matched the median

luminance of background squares (approximately 20.7 cd/m^2). All background squares were of the same color (EEG) but their individual luminances were randomly selected on each trial. Individual background squares took 1 of 9 possible luminance values at intervals spaced approximately .5 cd/m^2 apart with range 18.8 to 22.6 cd/m^2. The background array of gray squares served to mask luminance artifacts so that the stimulus target square could be detected only on the basis of chromatic contrast (Birch et al., 1992, Sumner et al., 2002). Background squares were positioned so that the stimulus target square was aligned into the background grid. The display of stimulus target and background squares was presented for approximately 24 ms for monkey CA and 106 ms for monkey FS. Target presentation time was adjusted until detection of the lowest S-cone contrast test step stimulus was near chance (1/6) or well below our 50% detection threshold for each monkey. This was determined during preliminary trials (data not shown) using stimuli from several candidate vectors. The goal was to ensure sigmoidal detection curves, which requires that the lowest contrast stimuli are not reliably detected. From the time of stimulus presentation, monkeys had 290 ms to make a saccade to the location of the target to indicate correct detection of the stimulus. This time window allows sufficient time to saccade to our low contrast stimuli while still encouraging the animals to make rapid decisions. Correct detections resulted in delivery of 5 drops of liquid reward. This large reward was implemented to encourage the animals to indicate a correct detection. This was done at the expense of further limiting the number of trials animals will perform before satiation but was necessary to maintain motivation throughout the long and difficult tritanopia trials.

In this paradigm, animals generally attempted nearly every trial, ensuring a reasonable maintenance of adaptation throughout data collection. Near the end of a session, if the monkey

stopped reliably performing trials or did not attempt trials for a few minutes, data collection was stopped for the day.

2.2.5 Measuring detection thresholds

The task was designed to find detection thresholds along chosen candidate tritan vectors. Detection thresholds were found in a staircase manner using stimuli from the test step points (Figure 3B). The idea was to find the test step, or distance from EEG in MB space, for stimuli on a candidate tritan vector to be reliably detected. During transient tritanopia, the candidate vector with the highest detection threshold is the true tritan line at the tested spatial location. Candidate vectors range from 0^o to 24^o, spaced 2^o apart. We focused on testing candidate vectors from 8^o to 24^o because previous studies using the transient tritanopia method for finding a tritan line have found the true tritan line to lie near this range (Smithson et al., 2003, Anderson and Carpenter, 2008).

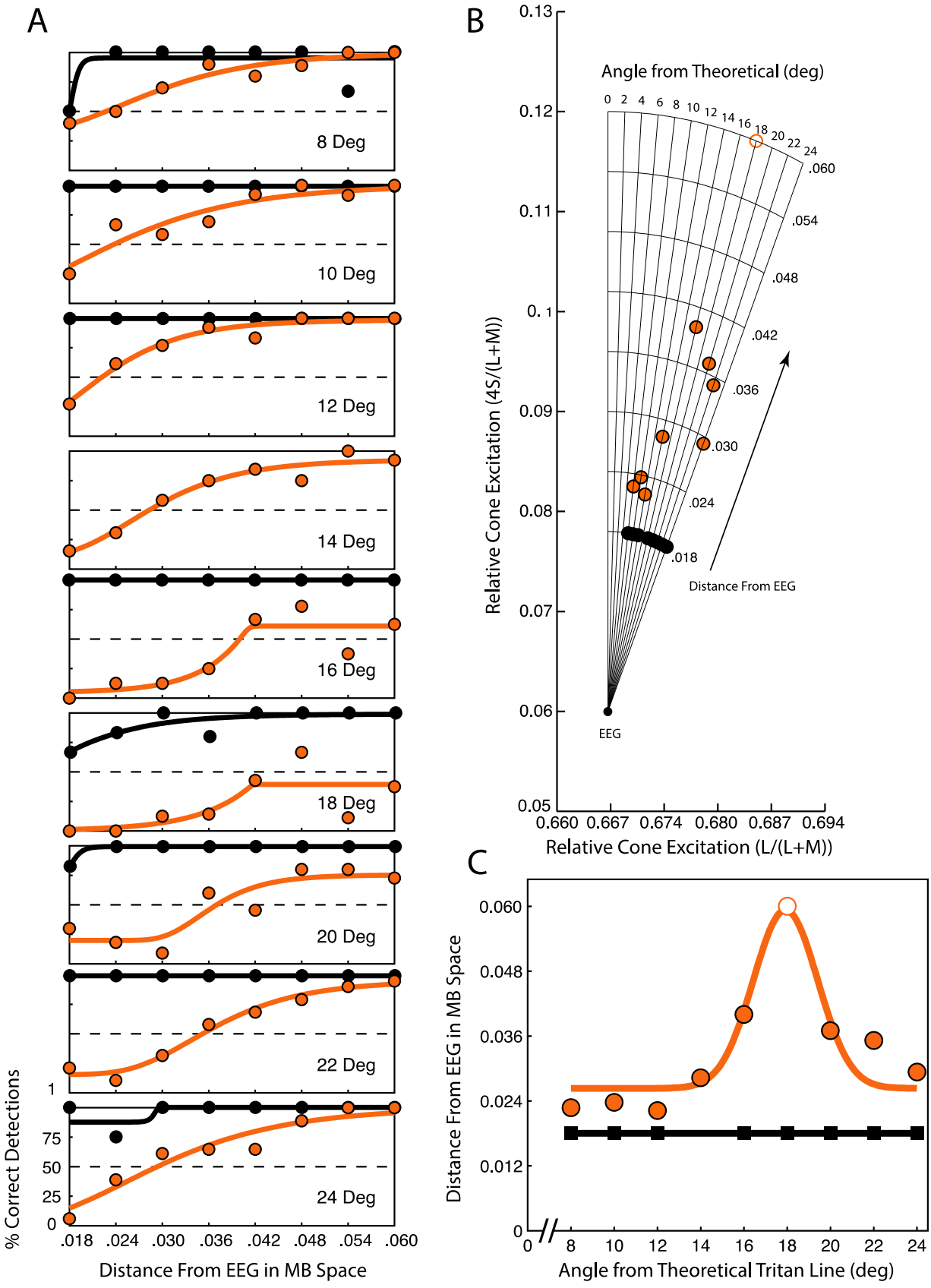
A
8 Deg
10 Deg
12 Deg
14 Deg
16 Deg
18 Deg
20 Deg
22 Deg
24 Deg
% Correct Detections
1
75
50
25
0
.018 .024 .030 .036 .042 .048 .054 .060
Distance From EEG in MB Space
B
Angle from Theoretical (deg)
0 2 4 6 8 10 12 14 16 18 20 22 24
.060
.054
.048
.042
.036
.030
.024
.018
EEG
Distance From EEG
Relative Cone Excitation (4S/(L+M))
0.13
0.12
0.11
0. 1
0.09
0.08
0.07
0.06
0.05
0.660 0.667 0.674 0.680 0.687 0.694
Relative Cone Excitation (L/(L+M))
C
Distance From EEG in MB Space
0.060
0.048
0.036
0.024
0.012
0
0 8 10 12 14 16 18 20 22 24
Angle from Theoretical Tritan Line (deg)

Figure 3. Tritan line calculation from detection thresholds at one spatial location (down left) for monkey FS. Orange circles show data collected after adaptation to the yellow adapting background. Black circles show data collected after adaptation to the white adapting background. **A)** Percent correct detections plotted versus distance of the test step stimulus color from EEG in MB space for 9 candidate tritan vectors. Orange and black curves are the least-squares logistic fits to the data. Dashed horizontal lines at 50 indicate chosen detection percentage threshold. **B)** Detection thresholds computed from the detection curves in A and plotted in scaled MB space. Each point on a candidate tritan vector indicates the detection threshold for that vector as determined from the data in A. **C)** Detection thresholds from B are plotted as a function of the candidate tritan vectors (i.e., angle from theoretical tritan line). Here the vertical axis indicates threshold distance from EEG shown in B while the horizontal axis indicates the candidate vector tested. Data points for tritanopia trials were fitted with a least-squares Gaussian function (orange curve) to determine the peak. Data points for control trials were fitted with a least-squares linear function.

Test steps for finding detection thresholds are indicated by the equally spaced curves spanning candidate vectors (Figure 3B). Moving along a candidate tritan vector away from EEG represents steps of increasing S-cone chromatic contrast. Test steps at greater distances from EEG should become easier to detect as their chromatic contrast from the background increases.

Percent correct was calculated as the ratio of correct stimulus detection trials to attempted trials. A trial was considered attempted if the monkey maintained fixation up to stimulus presentation. Trials aborted before stimulus presentation were not included in the analysis. Trials were considered correct if monkeys made an eye movement to the stimulus location within the allotted 290 ms after stimulus onset. Saccades had to land within approximately a $2x2^{o}$ window centered on the stimulus location to be considered correct. If monkeys made a saccade to any other location or did not initiate a response within 290 ms, the attempted trial was considered an error trial. We included "no response" trials in the analysis as "error" trials because it is unlikely the animals would fail to indicate a detected target. The reward paradigm offers a large reward for correct detection. It is doubtful that the monkeys would perform a long fixation of a bright background for little reward only to choose not to take the large reward offered for correct detection.

Detection thresholds were computed from plots of percent correct target detections vs. stimulus distance from EEG in MB space for each candidate tritan vector (Figure 3A). Moving

along the x-axis represents increasing distance from EEG, i.e. increasing chromatic contrast between the target stimulus and gray background squares. The monkeys' detection percentage generally increased as contrast increased. Behavioral performance in a detection task such as this can be expected to follow a sigmoidal function. We therefore fit a least squares 6 parameter generalized logistic function to the data points as follows.

Equation 1. $$A + \frac{K - A}{(1 + Qe^{-B(x-M)})^{1/v}}$$

The parameters A and K represent the lower and upper asymptotes, respectively. These were constrained to lie between 0 and 1. The parameter M represents the shift of the curve from 0 and was constrained to lie between .018 and .060. The other parameters modify the shape and steepness of the fitted curve and were constrained to be zero or positive. To compute thresholds, we found the point at which the fitted curve reached 50% correct detections (dashed horizontal lines in Figure 3A). The corresponding distance from EEG required for the fitted curve to reach 50% was considered to be the detection threshold for the candidate tritan vector tested (Figure 3A, B). If the fitted curve never reached 50% correct (as in the 18 deg panel of Figure 3A) a threshold of .060 was assigned. Thresholds assigned a value of .060 are indicated by open circles (Figure 3B, C and Figures 4 and 5).

Thresholds were determined separately for tritanopia trials (Figure 3, orange points and curves) and control trials after adaptation to the white background (Figure 3, black points and curves). Threshold values were then plotted as a function of candidate tritan vector angle from zero (Figure 3C). This function is expected to produce a single peak of greatest detection threshold for tritanopia trials. Tritanopia data points were fitted with a least squares 4 parameter Gaussian function as follows.

Equation 2. $$Ae^{-\left(\frac{x-B}{C}\right)^2} + D$$

The parameter A affects the magnitude of the curve and was constrained to lie between .01 and .06. Parameter D indicates the minimum value of the fit and was constrained between 0 and .048. Combined, the constraints on A and D kept the values of the fitted curves within the range of thresholds observed and tested. Parameter C controls the width of the Gaussian function and was constrained between 1.5 and 6.5. This window allowed the curves to rise in correspondence with sharp increases in detection threshold. The parameter B indicates centering of the curve, which is the peak of the fitted function. B was constrained to lie between 8 and 24 in correspondence with our tested range of candidate tritan vectors. The value of B was used to define the peak of the function and thus the tritan vector with greatest threshold.

We characterized goodness of fit for the Gaussian functions by computing the ratio of the root mean square error (RMSE) of the fitted Gaussian and the RMSE of the mean. Values of this RMSE ratio equal to 1 indicate that the mean fits the data as well as the fitted Gaussian. Values less than 1 indicate the Gaussian fit is better than the mean whereas values greater than 1 indicate that the Gaussian fit is worse than the mean. RMSE was computed using degrees of freedom equaling the number of data points tested (9 for monkey FS and 7 for monkey CA) minus the number of model parameters (4 for fitted Gaussians and 1 for the mean).

Control trials were expected to produce flat detection thresholds even below our threshold of .018 as found by Smithson et al. (2003) in human subjects. Therefore these trials were fitted with a least squares linear function. Trials collected for a single candidate tritan vector were combined across sessions for which the same vector was tested. This analysis was performed separately for each candidate tritan vector at each of the 6 spatial locations using each of the 2 adaptation backgrounds for each monkey.

2.3 RESULTS

2.3.1 Detection thresholds indicate the observer's true tritan line

We used a transient tritanopia based paradigm to define S-cone isolating stimuli. In this paradigm, adaptation to a yellow background produces temporary insensitivity to S-cone activation. We measured detection of near S-cone isolating stimuli chosen from candidate tritan vectors during transient tritanopia. The tritan vector is a line in color space along which only S-cone excitation is modulated. We found detection thresholds for each candidate tritan vector at 6 spatial locations in 2 monkeys. To measure detection thresholds, we presented stimuli chosen from along each candidate tritan vector. Stimuli were varied in chromatic contrast in a staircase fashion. Stimulus contrast increases with distance from equal energy gray (EEG) in Macleod-Boynton (MB) space. Stimuli further out are easier to detect than those near the EEG point. The goal of testing these points is to find the minimum distance from EEG required to produce reliable detection along each candidate vector. Greater distance from EEG indicates higher detection threshold and greater transient tritanopia effect. The true tritan line is the candidate tritan vector with the highest detection threshold during conditions of transient tritanopia (i.e. after adaptation to the yellow background). An S-cone isolating stimulus is one chosen from this true tritan line.

Data were collected and analyzed separately for control trials after adaptation to a white background (Figure 3, black points and curves) and tritanopia trials after adaptation to a bright yellow background (Figure 3, orange points and curves). Results are shown for nine candidate

vectors at a single spatial location for monkey FS (Figure 3). The candidate vector on which the orange threshold point is furthest from EEG (the 18° vector in Figure 3B) is the one nearest the true tritan line. When threshold distances are plotted in MB space (Figure 3B) it is clear that contrast must increase the most along the 18° candidate vector to produce stimulus detection. Because transient tritanopia affects sensitivity maximally for true S-cone stimuli, this means the 18° vector is most closely aligned with the animal's true tritan line for this spatial location. Control trials show no detection thresholds above .018 across candidate vectors.

The data shown in Figure 3B are summarized in Figure 3C. Plotting thresholds as shown in Figure 3C makes it is easier to see the peak threshold value. In this example a 17.9° tritan vector has the highest detection threshold as given by the peak of the Gaussian fit. Therefore a 17.9° tritan vector is the true tritan line for monkey FS at this location in space.

2.3.2 Determining spatially specific tritan lines

True tritan lines were determined for 6 spatial locations. Detection thresholds were calculated iteratively for each candidate tritan vector, spatial location, and monkey (Figures 4 and 5). This nested procedure of computing detection thresholds was performed separately for control trials and tritanopia trials. In each daily session a single candidate vector was tested across all 6 locations on either control or tritanopia trials. Each point represents performance measured across all sessions in which a particular candidate vector was tested. Large panels show data collected at the 6 spatial locations indicated by the central illustration.

Both animals displayed steady stimulus detection (black squares) during control trials as indicated by a flat fit with a linear least squares function (black lines). For all locations except Figure 5, lower left and Figure 4, upper left, detection during control trials exceeded 50% even at

the lowest stimulus contrast tested. This constrained these trials to flat lines at .018 units from EEG and placed an upper bound on detection threshold in the absence of transient tritanopia. Separate analyses demonstrate that thresholds did not systematically vary across candidate tritan vectors during control trials as shown in human subjects (Smithson et al., 2003). In contrast, detection threshold was markedly increased above .018 during transient tritanopia (orange circles) and thresholds systematically varied across test vectors with a peak for a specific candidate vector value as indicated by the least squares Gaussian fits (orange curves). Increased threshold after adaptation to the yellow compared to white control background demonstrates that transient tritanopia is taking place. This is true across spatial locations and candidate vectors for both monkeys. Peaks of detection threshold on orange curves indicate the true tritan line at that spatial location.

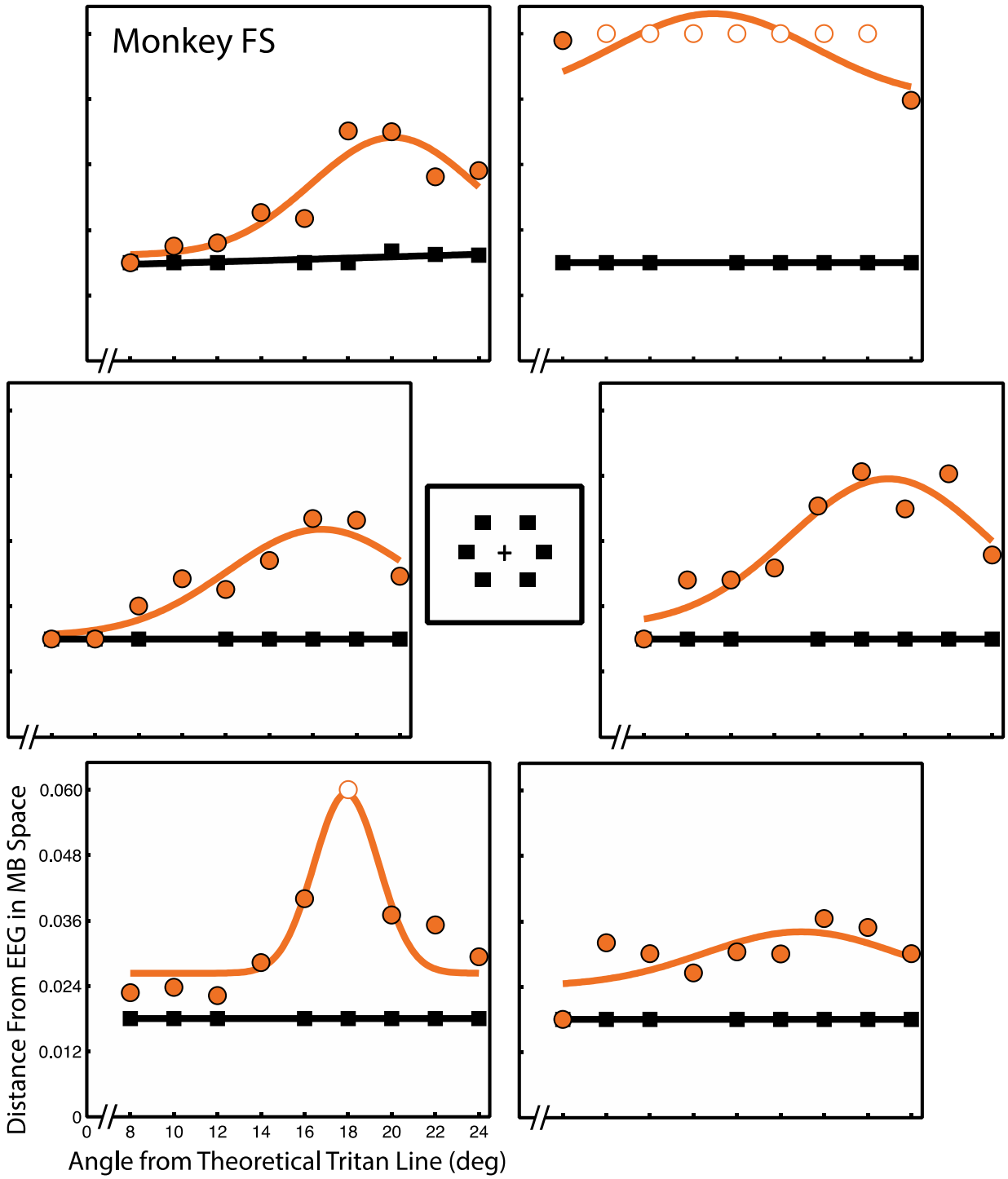

Figure 4. Detection thresholds for monkey FS. Each panel shows detection thresholds for monkey FS at one of the 6 spatial locations tested. All locations were 4º eccentricity. Vertical axes represent detection threshold as distance from EEG in scaled MB space. Horizontal axes indicate candidate tritan vector angle. Orange circles indicate data collected during tritanopia trials. Orange curves show least squares Gaussian fits. Gaussian peaks indicate the angle of greatest threshold increase and thus reveal true S-cone isolating stimuli. Black squares indicate data collected during control trials after adaptation to the white background. Black lines show least-squares linear fits.

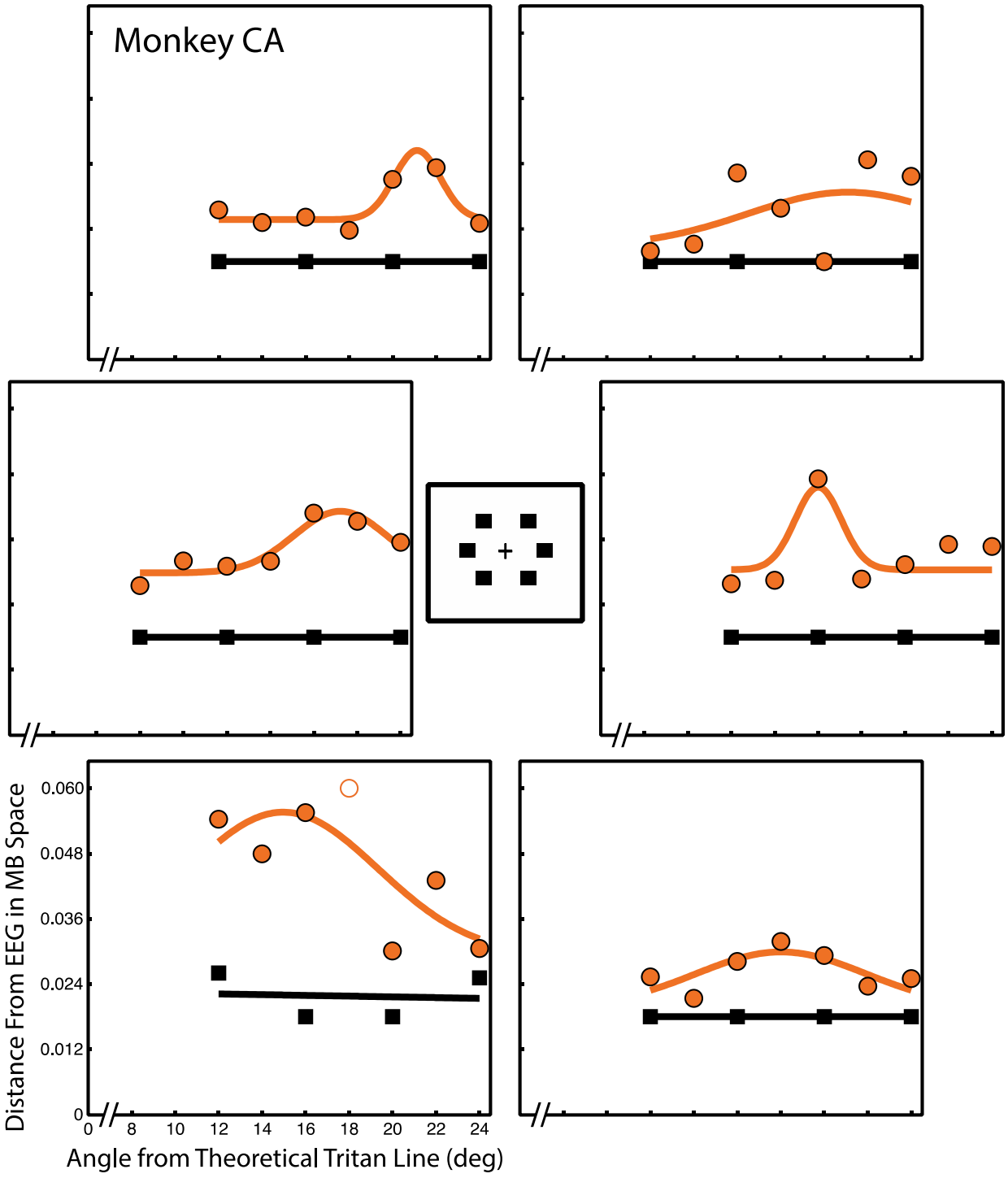

Figure 5. Detection thresholds for monkey CA. Same format as Figure 4. All locations were 6° eccentricity.

A few stimulus locations did not produce clear results. Monkey FS rarely detected the target, regardless of contrast, during transient tritanopia for the up right location (Figure 4, top right panel). There was no clear relation between contrast and detection so there are no meaningful thresholds for candidate vectors. Thresholds appear similarly and extraordinarily elevated across all candidate vectors. The fitted curve at the down right location is also relatively flat without an evident peak (Figure 4, bottom right panel). For monkey CA, the down left location (Figure 5 bottom left panel) and the up right location (Figure 5 top right panel) both contain considerable variation from point to point. For the up right location, this is largely due to the low threshold outlier point for the 20 degree candidate vector. Data point variation from the fitted curve is especially problematic for the down left location where the control data are also more variable than at the other locations. This indicates that monkey CA did not perform accurately during trials at this location even during the easier control trials. These unreliable control trials suggest that transient tritanopia trials at this location may also be unreliable. In these instances, the RMSE ratio is near or above 1 at these locations, indicating a poor fit (Table 1). The RMSE ratio at the down right location for monkey CA is equal to 1, indicating that the Gaussian fit is no better than a flat line at the mean. This flatness is due to the relatively low threshold elevation at this location.

The remaining locations (7/12) in both monkeys produced good Gaussian fits that reveal threshold peaks indicative of the true tritan line with corresponding low threshold control trials. A summary of true tritan lines for each monkey at each location in space is shown in Table 1. These angles are given as the peaks of the fitted Gaussian function (parameter B in equation 2).

Table 1. Calibrated tritan vectors by monkey and location. Summary of calibrated tritan axes as determined from Gaussian fit function peaks for both monkeys at all spatial locations. Tritan axes are given in clockwise degrees angular rotation from the theoretical tritan vector. Numbers in parentheses indicate goodness of fit for each Gaussian calculated as the ratio between RMSE fit and RMSE mean. Smaller numbers indicate better fit. Values near one indicate poor fits. *- Indicates the peak at this location was largely arbitrary and not fitted to reliable data.

Location	Monkey FS		Monkey CA	
Up Right	14.9 *	(1.3057)	21.1	(1.2857)
Straight Right	19.2	(0.4765)	16.0	(0.7941)
Down Right	19.0	(0.9060)	18.0	(1.0000)
Down Left	17.9	(0.4040)	15.0	(0.9333)
Straight Left	20.4	(0.4462)	21.2	(0.5000)
Up Left	20.1	(0.4550)	21.1	(.04091)

2.3.3 Behavioral Analysis

We wanted to know whether the variability in detection threshold distance across locations could be related to bias on the part of the monkeys. We analyzed saccade endpoints to determine whether bias was present in the animals' behavior. Bias should appear as a preference to choose certain target locations more or less often than others on error saccade trials. During these trials, the monkeys typically appear to guess a potential target location. Bias toward a particular location might result in decreased detection thresholds at that location as the animal is more likely to correctly "guess" that target location even though he did not detect the target. Conversely, bias away from a particular location might result in increased detection thresholds.

We plotted saccade endpoints for correct and error trials in order to examine the monkeys' performance and location bias (Figure 6). To quantify performance and bias we used Chi-Squared

tests of homogeneity. Within a given trial type (individual panels in Figure 6) the endpoint distribution was compared to the expected (unbiased) proportion of 1/6 at each location. Distributions were also compared between trial types. These comparisons were followed by post hoc multiple comparisons between corresponding locations using the Goodman procedure (Goodman, 1964, Franke et al., 2011) with p-value = .05.

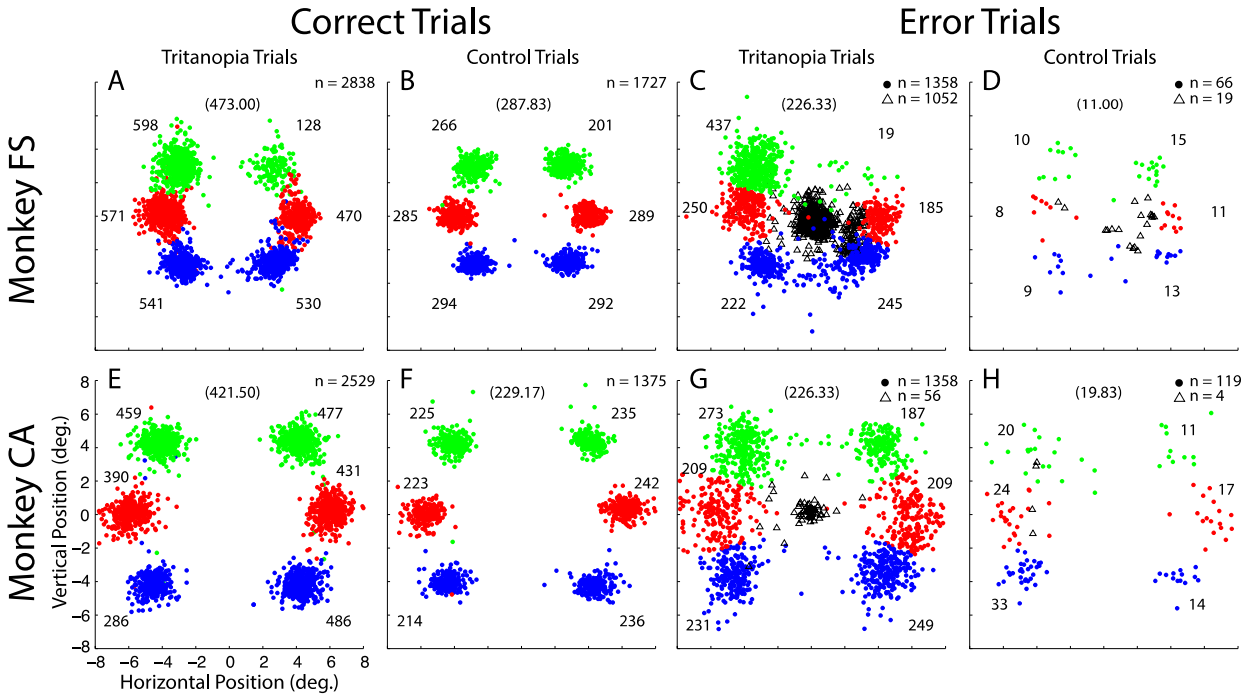

Figure 6. Saccade endpoints during tritanopia and control trials. Endpoints are shown for all candidate tritan vectors and stimulus contrasts. Colored circles indicate trials in which a saccade was attempted. Color code for correct trials shows endpoints corresponding to target presentations at each of six locations. Endpoints far away from their colored cluster are due to occasional eye position drift but represent correct decisions and are placed in the analysis with their corresponding cluster. The average position of correct saccade endpoints for each location was used to classify error endpoints. Error saccade endpoints were classified as being directed to one of the six possible target locations based on the nearest endpoint during correct trials. Numbers near each cluster give the number of endpoints. Numbers in parentheses at the top of each panel give the expected (unbiased) number of endpoints for each location. The unfilled black triangles show eye position 300 ms after target presentation for error trials in which no saccade was attempted.

We set the unbiased proportion at 1/6 for attempted saccade trials because monkeys typically made saccades to locations at or near potential target locations even when they did not detect the target (Figure 6C and G). This is especially true in monkey CA, who had very few no

response error trials (Figure 6G, H black triangles). In contrast, monkey FS exhibits a large number of no response tritanopia trials (Figure 6C, black triangles). As one might expect, the largest number of these (360) occurred after target presentations at the up right location, which he was strongly biased against. It is reasonable to assume that his unbiased performance would lie near the expected value of 1/6.

We found that correct performance of monkey FS during tritanopia trials (Figure 6A) was not equal for all locations ($p < .0001$). Monkey FS rarely performed correctly on up right trials and exceeded expectation on up left trials. This correct performance distribution is similar to his location bias as evidenced by error trials (Figure 6C) in which he showed bias ($p < .0001$) away from the up right location and toward the up left. In an effort to discover whether error saccade bias is predictive of correct performance, we directly compared correct trials to error trials. We found that the difference between correct and error trial bias lies only in bias being less extreme at the upper locations during correct compared to error trials (both locations, $p < .05$). This is largely because monkey FS almost never chose the up right target unless he was correct. The distributions both trend in the same direction, suggesting that bias played a role in his performance.

Monkey CA also showed unequal performance across locations ($p < .0001$) during correct transient tritanopia trials (Figure 6E). This difference is largely due to a low number of correct detections at the down left location. Monkey CA further showed bias during error trials (Figure 6G, $p < .001$). Interestingly, bias during error trials was strongest away from the up right location and toward the up left location. This bias does not predict the performance seen during correct trials. Error trial bias significantly differed from correct trial performance at the up right and down left locations (both locations, $p < .05$). At these locations where performance and bias are at odds, it appears monkey CA was simply not good (down left) or very good (up right) at detecting the

target. His performance at the remaining locations did not differ from his error trial bias. This can be seen in slightly better performance at the up left and down right locations (Figure 6E) corresponding to his small bias to these locations (Figure 6G).

Bias was much less evident during the easier control trials. Monkey FS still exhibits non-uniform correct performance (Figure 6B, $p < .001$), which is again strongest away from the up right location. Enhanced performance at the up left location is no longer evident. Monkey CA showed no variability in location performance (Figure 6F, $p = .8039$). During control error trials (Figure 6D) no bias was observed for monkey FS ($p = .6860$). This distribution differed significantly from his biased selections during tritanopia error trials ($p < .0001$) as he increased selection to the up right target and decreased it to the up left one (both $p < .05$). Error control trial bias was present for monkey CA (Figure 6H, $p = .0078$) and this bias differed from that during tritanopia error trials ($p = .0181$). The bias change between tritanopia and control trials was not significant for any individual location comparison and does not materialize in his unbiased correct performance.

Any bias observed in these data is inherent to the animals' behavioral patterns and preferences. With the exception of the down-left location for monkey CA, both animals performed very accurately for all locations during control conditions (Figures 4 and 5, black squares), after adaptation to the white background. They also demonstrate far less bias during these control trials. Therefore, the origin of any bias cannot be explained by scotoma or major visual deficit at these areas.

Endpoint biases revealed in this analysis do not reliably predict calibration quality at a given location. The only major exception is the very strong bias of monkey FS away from the up right location, which resulted in so few detections that the calibration could not really be performed

there. His bias to the up left target may explain the slightly lower threshold peaks at this location, though the effect appears small (Figure 4). His bias does not account for his decreased detection thresholds to the down right location, to which he showed no bias. Monkey CA's (Figure 5) tritanopia error bias toward the up left target may have also slightly decreased the threshold peak for the up left location. However, his elevated thresholds for the down left target would not be predicted from his tritanopia error trials, which show no bias away from this location. Monkey CA also shows rather flat thresholds for the up right target, which would not be predicted based on his bias away from this location. These results suggest the monkeys were simply unusually good or bad at detecting targets in some locations. Perhaps a larger range of candidate tritan vectors would have revealed a threshold peak.

Both monkeys show variability in performance and error saccade bias across spatial locations. Behavioral biases are only able to explain calibration performance in extreme cases. There is a trend for biased locations to show decreased or elevated detection thresholds at some locations. However, deviations in performance across locations cannot be reliably predicted based on bias observed during error trials. For bias to affect our estimated tritan vectors independent of location would require the monkeys to be biased in a test vector direction dependent manner. This seems unlikely as the rapid stimulus presentation gives the monkeys little time to react and individual vectors were tested across days. This suggests that bias plays little or no role in our calibration results at most locations tested.

2.4 DISCUSSION

We have shown that S-cone isolating stimuli can be defined in monkeys by taking advantage of transient tritanopia. Transient tritanopia occurs after adaptation to a bright yellow background. It produces selective desensitization to S-cone input, which can be used to determine an observer's true tritan line. Our method is modeled after the technique introduced by Smithson et al. (2003) to identify tritan lines in human subjects. This method for finding a tritan line and determining truly S-cone isolating stimuli has never before been performed on non-human subjects. The ability to stimulate S-cones selectively in awake behaving monkeys is important for two reasons. This approach will allow future behavioral studies on responses to S-cone stimuli in monkeys to have direct relevance to previous psychophysical work in humans. Further, defining S-cone isolating stimuli in monkeys allows physiological studies not possible in humans.

2.4.1 Methodological differences from calibrations in humans

The transient tritanopia calibration procedure described here differs in 3 main ways from those previously used on human subjects (Sumner et al., 2002, Smithson et al., 2003, Smithson and Mollon, 2004, Sumner et al., 2004, Sumner et al., 2006, Anderson and Carpenter, 2008, Anderson et al., 2008, Bompas et al., 2008, Bompas and Sumner, 2008). First, our procedure requires that subjects indicate detection by performing a saccade to a single briefly presented target embedded in luminance noise. In contrast, many human studies have used verbal report to indicate detection of Ishihara rings of stimuli. To determine thresholds, we fit psychometric curves indicating percent correct stimulus detection. These curves were used to determine the point at which the stimulus was reliably detected by the animals.

A second difference from the procedures used in humans is that we did not use an initial adaptation period to induce transient tritanopia. We began each experimental session by running approximately 10 trials using the standard 7.6 second adaption to a yellow background at the beginning of each trial. After these initial trials, data collection was begun using the same trial parameters. To maintain adaptation, data were collected only so long as animals were reliably performing trials. Previous calibrations in humans assume that subjects will continue to perform trials so long as it is asked of them, with little error or unattempted trials. These human studies used an initial adaptation period of 1-2 minutes to induce transient tritanopia. After initial adaption, trials were run with about 7.6 seconds of adaptation per trial to maintain transient tritanopia. We found that the initial adaption prolongs the already more difficult task of calibrating a tritan line in monkeys. Adaptation would need to be repeated if the monkey did not perform the task for several trials. Our method produced sufficient adaptation for transient tritanopia without initial adaption. In both animals, detection thresholds were clearly elevated after adaption to the yellow compared to white background.

A third difference was the method used for luminance calibration. We photometrically calibrated our S-cone stimuli for equiluminance with the background. Several previous studies have instead used psychophysical luminance calibration, such as the minimum motion procedure for determining equiluminance (Anstis and Cavanagh, 1983). We did not psychophysically calibrate equiluminance for 3 reasons. 1) Our preliminary results with the minimum motion technique in one monkey (data not shown) were inconsistent at the eccentric locations of our stimuli as has been reported previously in monkeys (Logothetis and Charles, 1990). Additionally, this psychophysically estimated equiluminant point ultimately differed little from measured photopic equiluminance. 2) Psychophysical luminance calibration results can depend on spatial

and temporal properties of the stimulus (Anstis and Cavanagh, 1983, Cavanagh et al., 1987, Logothetis and Charles, 1990) and vary with eccentricity (Bilodeau and Faubert, 1997). 3) The equiluminant point differs from one neuron to the next (Schiller and Colby, 1983). This implies that in any future physiological experiments using the S-cone calibration technique presented here, stimulus luminance would need to be calibrated before recording each individual neuron. We reasoned that any small measurement inaccuracy would be masked by using luminance noise that varied over a relatively wide range of values (+/- 2 cd/m^2) from the target luminance. We found that omitting psychophysical luminance calibration simplifies the procedure while still producing results dependent on chromatic contrast.

2.4.2 Comparison to calibrations in humans

Our calibration results in 2 monkeys are similar to tritan line calibrations in humans (Smithson et al., 2003, Anderson and Carpenter, 2008). These previous studies found that actual tritan lines are typically shifted toward red (clockwise rotation of the vector from theoretical), as expected (Sumner et al., 2004). Across 4 subjects, Anderson and Carpenter (2008) identify tritan lines of 10.6^o, 11.8^o, 14.5^o and 17.7^o clockwise rotation from the theoretical line. With 2 subjects, Smithson et al. (2003) found tritan lines of 7.8^o and 9.5^o clockwise rotation when using an adaption background similar to ours. Tritan lines in monkeys were actually rotated slightly further, but critically, they trend in the same direction. They ranged from 15.0^o to 21.2^o rotation in monkey CA and 17.9^o to 20.4^o rotation in monkey FS (Table 1), excluding the unattempted location (Figure 4, upper right).

The difference in calibrated tritan lines between humans and monkeys might be attributable to eccentricity and corresponding macular pigment density. The two studies above both used

annular stimuli that spanned an entire visual quadrant. Furthermore, the stimulus annulus covered an area from 3° to 5° eccentricity. Here we tested stimuli that were single points centered at either 4° or 6° eccentricity. Macular pigments in humans and monkeys have similar absorption spectra and a higher density near the fovea. However, it appears that human macular pigment may extend further from the fovea than in monkeys (Snodderly et al., 1984a, Snodderly et al., 1984b, Trieschmann et al., 2007). A lower density of macular pigment in the periphery and/or more eccentric test locations would result in the observed greater shift toward red in the calibrated tritan line seen in our animals.

2.4.3 Differences between locations and animals

Calibrated tritan lines in both monkeys were qualitatively very similar. They ranged from 15.0° to 21.2° rotation in monkey CA and 17.9° to 20.4° rotation in monkey FS (Table 1), excluding the unattempted location (Figure 4, up right). Individual variations at successfully calibrated locations are to be expected. S-cone isolating stimuli vary between observers due to variations in macular pigment, lens optical density, cone sensitivity and chromatic aberration (Sumner et al., 2004). Both monkeys showed evidence of bias toward or away from 1 to 2 locations, particularly during the more difficult transient tritanopia trials. Although bias can explain variability in calibration quality at some locations, it cannot account for all of them, particularly the flatter curves for monkey CA up right and monkey FS down right. At these locations where bias does not play a major role, it appears the monkeys were simply too effective at target detection to produce good calibrations. Nonetheless, a peak is evident and this could possibly be accentuated by altering specific trial parameters that would increase detection threshold. For example, increasing the strength of transient tritanopia by brightening the adaption background would likely make targets

more difficult to detect. Alternatively, decreasing target presentation time has a similar effect. Unfortunately, changes like these would in turn make target detection at other locations more difficult as well. We wanted to keep trial parameters identical for each test location so that target location was unpredictable. The parameters chosen here sought a balance that would produce good results at as many locations as feasible.

2.4.4 S cone contributions to visual subsystems

Signals from the 3 cone types are carried from retina to the brain by different classes of ganglion cells that largely maintain segregation through the thalamus and into cortex. This segregation leads to a number of visual subsystems. One intriguing instance of such segregation is the pathway for luminance perception (Lee, 2011). Luminance perception arises from addition of signals from L- and M-cones, but not S-cones (Eisner and MacLeod, 1980). Luminance perception in primates has been linked to the magnocellular layers of the LGN (Lee et al., 1988, Lee, 2011). Neurons in the magnocellular layers of the LGN sum inputs from L-and M-cones but rarely or not at all from S-cones (Field et al., Schiller and Malpeli, 1978, Derrington et al., 1984, Sun et al., 2006). S-cone signals are carried by their own class of retinal ganglion cell, which projects almost exclusively to the koniocellular LGN layers (Dacey and Lee, 1994, Hendry and Reid, 2000, Klug et al., 2003, Dacey, 2004, Dacey et al., 2005, Tailby et al., 2008a). However, it is possible that S-cone input to the magnocellular LGN is simply weaker than that of L- and M-cones (Derrington et al., 1984, Ripamonti et al., 2009). With calibrated S-cone isolating stimuli, L- and M-cone input can be held constant using an isoluminant gray background while changes in the S-cone opponent direction are manipulated by presenting a calibrated S-cone stimulus. The ability to define S-cone stimuli

in monkeys affords the opportunity to test aspects of segregated S-cone processing physiologically in a novel way.

2.5 CONCLUSIONS

The perceptual reports of non-human primates can be used to perform psychophysical calibrations of S-cone isolating stimuli. S-cone isolating stimuli can be calibrated separately at several spatial locations for individual monkeys. These S-cone isolating stimuli were determined by finding a stimulus whose detection threshold was maximally elevated during transient tritanopia. This calibration is specific to both location and animal. S-cone stimuli were successfully determined at most locations tested in each monkey. This technique in monkeys will allow physiological tests of S-cone function not previously possible. It provides a direct link to calibrations in previous human studies which should allow it to elucidate the neural foundations of phenomena such as blindsight that have attracted great interest yet remain unresolved.

3.0 S-CONE STIMULI ACTIVATE SUPERIOR COLLICULUS NEURONS

First published in: Hall NJ and Colby CL (2014). S-cone visual stimuli activate superior colliculus neurons in old world monkeys: implications for understanding blindsight. Journal of Cognitive Neuroscience (26): 1234-1256.

3.1 INTRODUCTION

Blindsight is an enigma. Patients with lesions in primary visual cortex (V1) are unable to describe or perceive stimuli in their blind field, yet they retain the ability to detect, localize and discriminate unseen stimuli (Sanders et al., 1974, Weiskrantz, 2004, Cowey, 2010). This perplexing phenomenon has been demonstrated in both humans and monkeys (Cowey and Stoerig, 1995, Moore et al., 1995, Stoerig and Cowey, 1997, Gross et al., 2004). Many researchers have investigated the capabilities and mechanisms of blindsight yet the pathways involved remain only partially understood (Leopold, 2012).

Multiple cortical and subcortical structures contribute to blindsight. Projections from the superior colliculus (SC) to extrastriate cortex play a critical role in producing neuronal visual responses in the absence of V1 (Gross, 1991). The SC and extrastriate visual cortex are both crucial for blindsight (Vaughan and Gross, 1969, Goebel et al., 2001, Weiskrantz, 2004, Yoshida et al., 2008, Cowey, 2010). A possible blindsight pathway requires the lateral geniculate nucleus of the thalamus (LGN). The SC and retina project to the LGN, which projects directly to extrastriate cortex. When the LGN is inactivated in awake, behaving monkeys that have V1 lesions, extrastriate activation and blindsight behavior are both abolished (Schmid et al., 2010,

Leopold, 2012).

An important strategy in studies of blindsight in humans has been to block visual input to the SC psychophysically. It is widely believed that the SC does not receive input from short wavelength sensitive cones (S-cones) in the retina (Sumner et al., 2002). The reasoning is that by using S-cone stimuli, visual pathways that depend on the SC should be blocked or impaired. Several studies have used S-cone stimuli to test whether the SC mediates blindsight in humans (Leh et al., 2006, Marzi et al., 2009, Alexander and Cowey, 2010, Leh et al., 2010, Tamietto et al., 2010). Experimental paradigms have ranged from target detection to fMRI activation. The results have demonstrated selective impairments when S-cone stimuli are used as compared to luminance stimuli. The conclusion is that the SC is likely to be responsible for visual abilities demonstrated by blindsight patients

Beyond blindsight, many behavioral studies have been based on the assumption that S-cone isolating stimuli do not drive cells in the SC. If this were true, the use of S-cone isolating stimuli would be a convenient way to assess collicular function. This strategy was first proposed in an influential behavioral study of SC function (Sumner et al., 2002). Since its inception, this technique has been used in a number of human psychophysical studies of the SC. The appeal of this method is that the SC can be "lesioned" without any damage to the brain, making it useful in healthy human subjects. Many studies using S-cone stimuli have found differences in behavioral responses to S-cone as compared to luminance stimuli. When behavioral effects are observed, the interpretation is that the SC must play a critical role in the affected behavior.

The original idea that the SC is blind to S-cone isolating stimuli is based on anatomical and physiological studies. Early physiology studies found that SC neurons and the retinal ganglion cells that form the retinotectal pathway are not color opponent and are not sensitive to S-cones

(Marrocco and Li, 1977, Schiller and Malpeli, 1977, De Monasterio, 1978b). The corticotectal pathway in turn carries information originating only from the magnocellular layers of the LGN. Neurons in the magnocellular layers carry summed inputs from long and middle wavelength sensitive cones (L- and M-cones), but not S-cones. Single neurons in monkey superior colliculus are silenced when the magnocellular layers of the LGN are inactivated (Schiller, Malpeli, & Schein, 1979). The conclusion is that SC neurons should be responsive to achromatic luminance stimuli but not to chromatic stimuli.

No single neuron studies have directly tested whether cells in the SC respond to individually calibrated S-cone isolating stimuli. Studies of SC afferents only make clear that these afferents are not color opponent, and not whether SC neuronal responses are affected by calibrated S-cone isolating stimuli. One recent study reported neuronal sensitivity in the SC of macaques to colored stimuli (White et al., 2009). Another has reported the absence of S-cone input in the marmoset SC (Tailby et al., 2012). Our goal was to test directly whether S-cone isolating stimuli can activate single cells in the SC of awake behaving macaque monkeys under conditions that explicitly replicate those used in human behavioral and clinical research. Surprisingly, our data show that S-cone specific stimuli produce robust activation of SC neurons.

3.2 MATERIALS AND METHODS

Two adult male rhesus monkeys (*macaca mulatta*) were used in these experiments. Animals were cared for in accordance with National Institutes of Health guidelines. The University of Pittsburgh Institutional Animal Care and Use Committee approved all experimental protocols. Monkeys weighed 13 and 8.5 kg (monkey CA and monkey FS, respectively). Both had normal trichromatic

color vision as evidenced by their ability to make saccades to L- cone and S-cone isolating stimuli (data not shown).

Each monkey underwent sterile surgery to implant an acrylic cap with an embedded head restraint bar, scleral search coils, and a recording chamber as described elsewhere (Dunn et al., 2010). We used MRI to guide correct placement of the SC recording chambers, which were positioned posteriorly on the midline at an angle of 40^{o}. The SC was located approximately 25-30 mm below the surface of the brain.

3.2.1 Data Acquisition

During experiments, animals sat in a primate chair with head fixed. Monkeys viewed a CRT monitor at a distance of 30 cm. Eye position was monitored using scleral search coils (Judge et al., 1980) with a Riverbend field driver and signal processing filter (Riverbend Technologies Inc.). Eye position voltages were continuously monitored online through NIMH Cortex software (provided by Dr. Robert Desimone) and saved for offline analysis of saccades on a separate computer running Plexon software at a sampling rate of 1000 Hz (Plexon Inc., Dalls, TX). Neuronal spiking activity was recorded using tungsten microelectrodes (Frederick Haer, Bowdoinham, ME) inserted into the SC through stainless steel guide tubes stabilized in a nylon grid system (Crist Instruments). Voltage signals were amplified, filtered, and sorted using on and offline template-matching and principal component analysis (Plexon Inc., Dalls, TX). The collicular surface was physiologically identified by the sudden appearance of light sensitive neuronal activity as the electrode was advanced. At deeper locations eye movement related activity was observed. Visual and motor receptive fields were in agreement with known SC maps (Goldberg and Wurtz, 1972, Schiller and Stryker, 1972). Trial types, events, and outcomes were

monitored with Cortex software and stored with neuronal spike data at 40 kHz using Plexon hardware and software.

3.2.2 Stimulus Presentation and Control

Stimulus timing and presentation were controlled using NIMH Cortex software. Stimuli were presented on a 19" ViewSonic® color CRT monitor at a refresh rate of 85 Hz using an 8 bit DAC with an ATI Radeon™ X600 SE graphics card. To generate stimuli, the monitor was calibrated for color and luminance using a Photo Research PR-655 SpectraScan® spectroradiometer integrated with custom MATLAB® (Mathworks; Natick, MA) software. The accuracy of the calibration was verified by independently measuring the spectral composition of all stimuli used. Stimulus colors were chosen from MacLeod-Boynton (MB) color space (MacLeod and Boynton, 1979) as defined using the Smith and Pokorny cone fundamentals (Smith and Pokorny, 1975).

3.2.3 Stimuli and Background

We presented stimuli defined by either luminance or S-cone contrast. In MB space, S-cone excitation is isolated along a vertical vector, perpendicular to the L- and M-cone excitation axis, known as the tritan vector. The actual tritan vector varies across individuals and spatial locations due to variations in cone density and macular pigment (Snodderly et al., 1984a, Snodderly et al., 1984b, Sumner et al., 2002, Hall and Colby, 2013). We presented S-cone stimuli chosen from psychophysically calibrated tritan vectors determined separately for each spatial location and each animal described as described in CHAPTER 2 (Hall and Colby, 2013). We were able to identify 4 location specific tritan vectors in monkey FS and 4 in monkey CA using this procedure. Neurons

in the SC with receptive fields corresponding to these calibrated locations were targeted in each animal and all stimulus presentations took place at these calibrated locations.

The calibrated tritan vector for each monkey and spatial location examined was rotated to the right of the theoretical vertical tritan line in MB space. Calibrated tritan vectors were brought into congruence with standard MB space by linearly transforming their MB values such that the calibrated tritan vector extends vertically and orthogonal to the standard L- and M-cone excitation axis.

Stimuli were presented on an equal energy gray (EEG) background of luminance noise (Birch et al., 1992, Sumner et al., 2002). The background was a full screen array of 1 x 1^{o} squares whose color was EEG but whose individual luminances changed at random every 4 monitor frames (~47 ms). This flickering background removes potential artifacts created by stimuli that are not exactly equiluminant with the background. Stimuli presented on such a background are therefore detectable only through contrasts falling outside the range of the noise. The luminance of the squares was uniformly distributed across 9 possible values ranging from 18.78 to 22.55 cd/m^2, spaced in increments of approximately 0.5 cd/m^2. The mean background luminance across all possible values was 20.73 cd/m^2, with mean color coordinates in MB space of (.66692, .01493) as compared to the theoretical value (.66667, .01500).

The goal of our experiment was to test SC neuronal responses to S-cone specific stimuli. We converted stimuli to DKL contrast space in order to make the effects of contrast in color opponent channels explicit (Derrington et al., 1984, Brainard, 1996). The mean color and luminance of the background noise in MB space was used as the basis point to convert stimuli to DKL space. This procedure gives stimulus contrasts with respect to the mean color and luminance of the EEG noise background. Conversion to DKL space gives contrasts corresponding to the

luminance mechanism (L + M), the L- and M-cone opponent mechanism (L - M) and the S-cone opponent mechanism [S - (L + M)], i.e. the S-cone isolating direction. Following the procedure described by Brainard (1996), we normalized DKL space such that a stimulus isolating a specific mechanism in DKL space with unit pooled cone contrast (i.e. the length of the 3-D vector in cone contrast space equals one) would correspond to a contrast of 100%. This normalization procedure has the advantage that it is independent of observer and experimental setup. We define the DKL coordinate contrasts for each mechanism as a vector of the form (L+M, L-M, S-(L+M)). In these terms, the minimum contrast of the luminance noise background was (-16.2298, 0.0091, 1.0320) and the maximum was (15.3497, -0.0402, -0.2187).

Three stimulus types were presented on the background array of squares: luminance, high contrast S-cone, and low contrast S-cone. Stimuli were 1 x 1^{o} squares embedded in the luminance noise background. The luminance contrast stimulus (24.92 cd/m^2) isolates the luminance mechanism (35.1922, 0.1817, 0.5641). This stimulus is more than double the maximum luminance contrast of the noise background. The other 2 stimuli activated the S-cone opponent mechanism. One was a high S-cone contrast stimulus whose DKL coordinates across all 3 mechanisms ranged from (-5.4318, 0.0157, 95.7475) to (-8.7634, -0.1684, 95.9704). The other was a low S-cone contrast stimulus whose DKL coordinates ranged from (-2.7450, 0.0462, 28.3539) to (-6.2916, -0.2824, 29.5714). Both S-cone stimuli slightly decreased DKL luminance contrast and contained only small, inconsistent contrasts in the DKL L-M-opponent mechanism. Such small and inconsistent deviations in mechanisms other than the S-cone opponent channels would not be expected to produce consistent effects on neurons. Luminance and L-M-opponent contrasts remained within the range covered by the background noise. S-cone stimuli presented on the noisy background were therefore detectable only on the basis of S-cone contrast, and are thus S-cone

isolating stimuli. The high contrast S-cone and luminance stimuli were chosen to be similar to those found in previous human psychophysics research. The low contrast S-cone stimulus was chosen to lie near the luminance stimulus and far from the high contrast S-cone stimulus in total cone contrast.

In 10 neurons we additionally tested neuronal responses to an L-cone stimulus as defined in DKL space (data not shown). SC neurons were responsive to the L-cone stimulus, as found previously (White et al., 2009). This confirmed that our results are not specific to S-cone stimuli or a subpopulation of SC neurons, but that SC neurons can be broadly activated by all cone inputs.

3.2.4 Behavioral Tasks

We used a standard memory guided saccade task to identify neurons with receptive fields at locations at which tritan vectors had been previously calibrated in CHAPTER 2 (Hall and Colby, 2013). We tested each SC neuron in 2 tasks. We used the memory guided saccade task to classify neurons as visual or visuomotor. We then used a fixation task to measure neuronal responses to the luminance and to high and low contrast S-cone stimuli. During previous S-cone calibration sessions, S-cone stimuli were behaviorally relevant because they served as saccade targets for the animals. In the fixation task of these experiments, no response was required after stimulus presentation.

3.2.4.1 Memory Guided Saccade (MGS) Task

During MGS trials, the stimulus and fixation point were maximum monitor intensity white (63.15 cd/m^2) presented on a dark background (< 0.01 cd/m^2). These stimuli represent the maximum contrast possible with our monitor. At the beginning of each trial a 1 x 1^o fixation cross appeared

and the monkey fixated for 200-400 ms. While maintaining fixation, a 0.5^{o} diameter circle was presented in the recorded neuron's receptive field for 4 frames (~47 ms). Monkeys were required to maintain fixation for an additional 300-500 ms after stimulus presentation before the fixation cross was turned off, cueing the animals to make a saccade to the remembered location of the target. Saccades within approximately 1.5^{o} of the target location were rewarded with a drop of liquid. Data for the MGS task were collected in a block of 20 trials before the fixation task and a block of 20 trials after the fixation task.

3.2.4.2 Fixation Task

At the beginning of each trial, a 1 x 1^{o} black (< 0.01 cd/m^{2}) fixation cross was presented as the luminance noise masking background was introduced. Animals fixated the central cross for 200-400 ms (Figure 7, left panel) after which one of the three stimulus types was presented. The stimuli appeared for 4 frames (~47 ms) synchronously with the change in the luminance noise background (Figure 7, center panel). The figure shows the high contrast S-cone stimulus, outlined in white for clarity. This outline was not present during the actual task. All three stimuli were subjectively difficult for a human observer to detect. After stimulus presentation, animals were required to continue fixating for an additional 200-400 ms to receive a liquid reward. After the additional fixation period, the luminance noise and fixation cross were turned off and the intertrial interval (ITI) began (Figure 7, right panel). During the 400 ms ITI, an EEG screen approximately equal to the average background noise (-0.7879, 0.0000, 0.4667) was displayed. This procedure minimizes the contrast between the ITI background and the luminance noise background onset. The ITI screen also served to maintain the animals in a primarily photopic visual state because its luminance was relatively high (20.66 cd/m^{2}). Fixation trials were run in a separate block from the MGS task. The three stimulus types were presented randomly interleaved with 20 presentations

of each stimulus type. Stimuli were presented in the recorded neuron's receptive field at the calibrated tritan vector locations for each animal. Possible stimulus locations were located radially from fixation at an eccentricity of 4º for monkey FS and 6º for monkey CA.

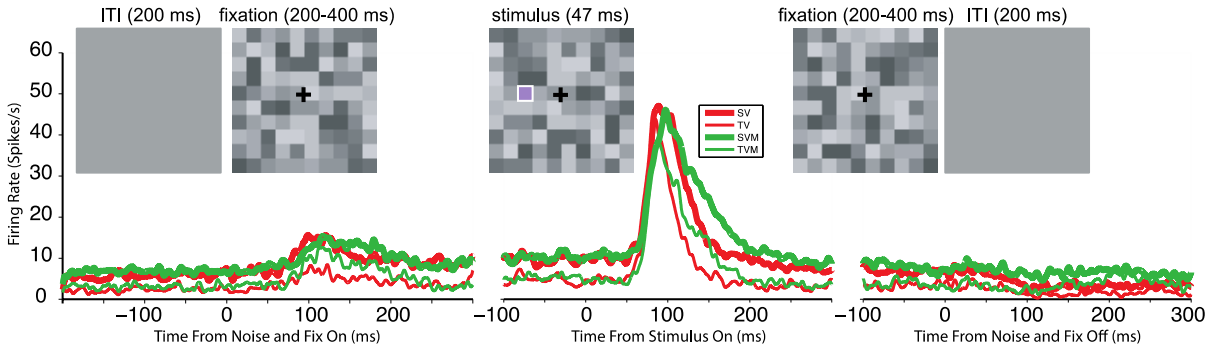

Figure 7. Fixation task and average neuronal responses to luminance noise and stimuli. Upper schematics show fixation task timing and paradigm. Center task schematic shows only the presentation of the high contrast S-cone stimulus highlighted with a white outline, which is not presented during the actual task. Neuronal responses are average spike density functions across all three stimulus types. Neurons were classified as sustained visual (SV), transient visual (TV), sustained visuomotor (SVM), and transient visuomotor (TVM). Left: During the ITI the screen is steady EEG. The luminance noise background is turned on, and at the same time a fixation cross appears. Middle: After 200-400 ms of fixation, a stimulus appears in the recorded neuron's receptive field. The stimulus was either a high contrast S-cone, low contrast S-cone, or luminance contrast. Right: The animal fixates for an additional 200-400 ms after stimulus presentation to receive a liquid reward.

3.2.5 Data Analysis

We analyzed trial event timing, eye position and spike timing. All analyses were carried out offline using custom MATLAB® software (Mathworks; Natick, MA).

3.2.5.1 Neuron Classification

Neurons were classified by responses during the MGS task. Average neuronal firing rate during the baseline epoch (-100 to 0 ms before stimulus presentation) was compared with average activity

during the visual response epoch (30 to 130 ms after stimulus presentation) and saccade epoch (-50 to 50 ms after saccade onset, defined as the time at which eye velocity first exceeded 30^{o}/s). Of 194 neurons recorded, 178 showed a significant visual response (one-sided t-test, $p < .05$) and were included in further analysis. Of these neurons, 91 also had a significant saccade related response (one-sided t-test, $p < 0.05$) and were classified as visuomotor neurons. The remaining 87 neurons were classified as visual.

Visual and visuomotor neurons were further classified as having transient or sustained visual responses by computing a transience index. Previous studies have measured transience by comparing peak firing rate during a defined response epoch to average activity in the following epoch (Schiller and Malpeli, 1977, White et al., 2009). Our sample contained many cells exhibiting a strong response to stimulus offset as well as stimulus onset (e.g., figure 8, row 2). Neurons with clear on-off responses were generally transient in nature. Their on response must end before the off response begins in order to produce a distinct off response. Due to their off response, these cells have high levels of activity in the epoch following the initial response. Using previous approaches (Schiller and Malpeli, 1977, White et al., 2009), such neurons were often classified as sustained neurons even though their responses appeared very transient. We therefore used a different method for determining transience based on the Fourier transform of each neuron's spike trains. We binned the spike trains (0.1 ms time bins, i.e. 10,000 Hz sampling rate) of each neuron from -200 to 300 ms after stimulus presentation across all 40 trials of the MGS task and performed a fast Fourier transform on the average spike train. From the Fourier transform, we computed the average power at frequencies from 2 to 100 Hz as the baseline power. This frequency band was chosen because it contains spiking activity from neurons with high baseline firing rates (strong low frequency components) and neurons with low, spurious baseline firing

rates (strong high frequency components). We then computed the average power at frequencies from 13 to 30 Hz as the stimulus power. This stimulus frequency band was chosen because it captures our stimulus frequency of 21.25 Hz (refresh rate divided by stimulus frames, i.e. 85/4) and encompasses the frequency power exhibited by neurons whose responses closely tracked stimulus presentation with on and/or off responses. Transience indices were then computed as the ratio: (stimulus power) / (stimulus power + baseline power). Thus a neuron whose average baseline power was equal to its average stimulus power would have a transience index of 0.5. Neurons with transience indices > 0.5 were classified as transient and those ≤ 0.5 were classified as sustained.

Neurons in the superficial layers of the SC have visual responses that are generally transient (Schiller and Koerner, 1971, Marrocco and Li, 1977, White et al., 2009). In the present study, 20/31 visual neurons classified as transient were confirmed to lie near the collicular surface (less than 1 mm). Visual neurons deeper than 1 mm had sustained or transient responses, and at greater depths visuomotor neurons predominated.

3.2.5.2 Spike Density Function

Average spike density functions were computed by placing spikes across all trials from all neurons in 0.1 ms bins. The resulting non-normalized histogram was then convolved with a Gaussian kernel using a 2 ms standard deviation and values were converted to firing rates in spikes per second.

3.2.5.3 Neuronal Response Latency

Neuronal response latency was determined by finding the time to half height of the peak response for each neuron (Lee et al., 2007). To find the peak response, we computed the SDF for each

neuron but using a 5 ms Gaussian kernel, which produces greater smoothing and reduces spurious results. We identified the time of SDF peak firing rate in the window from 40 to 150 ms after stimulus onset. The peak time was used to find the last point in time the SDF crossed threshold before reaching its response peak. Threshold was set at half the peak value plus the average SDF rate from 200 to 0 ms before stimulus onset. The time at which the firing rate last crossed threshold before reaching its peak was defined as neuronal response latency. For some neurons the response to one of the stimulus types was absent, or very small, so that an accurate half height could not be determined in the prescribed window. We required that a response latency was determined for all 3 stimulus types to eliminate any bias caused by not including latency to all stimulus types from all neurons. Neurons whose response latency to all 3 stimulus types could not be determined were omitted from further latency analysis (15/56 SV, 8/31 TV, 12/66 SVM and 7/25 TVM neurons were omitted).

3.2.5.4 Contrast Sensitivity Indices

For each neuron we measured how its responses differed across the 3 stimulus types. To do this we computed 2 contrast sensitivity indices: a high vs. low S-cone contrast sensitivity index and a high S-cone vs. luminance contrast sensitivity index. These indices were computed as: (HighS – LowS)/(HighS + LowS) and (HighS – Luminance)/(HighS + Luminance) where HighS, LowS and Luminance indicate the mean firing rate of the neuron to the respective stimulus types. The mean responses were computed from spikes in the interval 40-200 ms after stimulus presentation. These indices provide a measure of each neuron's change in response to the stimulus types compared. Values of zero indicate equal response and positive values indicate stronger response to the high contrast S-cone stimulus.

3.2.5.5 Statistical Analyses

In the analyses on mean firing rates, we computed the mean firing rate for each neuron in the window from 40-200 ms after stimulus presentation. When using peak firing rates, we chose the same peak used for the latency analysis: maximum firing rate of the SDF for a single neuron in the window from 40-150 ms after stimulus onset. Peak firing rates were analyzed because, by definition, sustained neurons have longer responses than transient neurons. This could lead to a systematic bias toward sustained neurons exhibiting greater mean responses when comparisons are made across cell classes. We report analyses on peak firing rates primarily to make across class comparisons and include the same analyses on mean firing rates for comparison.

For comparisons across trials within a single neuron, we used 1-way ANOVA on mean firing rates of single trials. For comparisons of firing rate across neurons within a class, we found the mean response of each neuron across trials and used a 1-way repeated measures ANOVA to account for the firing rate differences across neurons. For comparisons of neuronal response latency across neurons within a class, we used the non-parametric Friedman test, which is comparable to a 1-way repeated measures ANOVA.

To compare population firing rates of all neurons across classes (SV, TV, SVM-and TVM), we performed a 2-way ANOVA on both mean and peak firing rate with factors of cell class and stimulus type. This procedure allowed us to compare across all neurons in an unbalanced design and gives a measure of the interaction effect between cell class and stimulus type. The interaction statistic is used to test whether neurons in different classes responded differently to the 3 stimulus types. To compare neuronal response latency across classes, we wanted to continue using non-parametric tests and so chose to compare the latency across all 4 classes one stimulus type at a time. To this end we used the Kruskal-Wallis test, which is comparable to a 1-way ANOVA. All

post-hoc comparisons were made using Tukey's honestly significant difference test for multiple comparisons, denoted HSD. For correlation analyses we used Pearson's correlation coefficient and the t statistic for significance testing.

3.3 RESULTS

We found that single neurons in macaque superior colliculus (SC) are activated by S-cone isolating stimuli. We measured the visual response characteristics of SC neurons to a luminance and two S-cone contrast stimuli, a high and low S-cone contrast. The prevailing hypothesis is that SC neurons cannot be activated by any S-cone isolating stimulus. We tested responses to two different S-cone contrasts because if SC neurons truly respond to S-cone contrast, their responses should change as S-cone contrast changes. We used a luminance noise background to eliminate luminance artifacts during a fixation task (figure 7, upper schematics). Stimuli were presented at screen locations at which S-cone isolating stimuli had been previously calibrated in each animal. At the beginning of each trial, SC neurons responded weakly to the onset of the luminance noise background (figure 7, lower plots). After the response to onset of the checkered background, neurons slowly adapted their firing rates, as shown previously for repeatedly stimulated SC neurons (Cynader and Berman, 1972, Marrocco and Li, 1977, Boehnke et al., 2011). After adaptation SC neurons exhibited sustained firing rates slightly above the baseline response during the intertrial interval. Presentation of a visual stimulus embedded in the luminance noise elicited a large visual burst. In the sections below we report how S-cone specific contrasts affected single unit responses, average activity, peak activity and neuronal response latency.

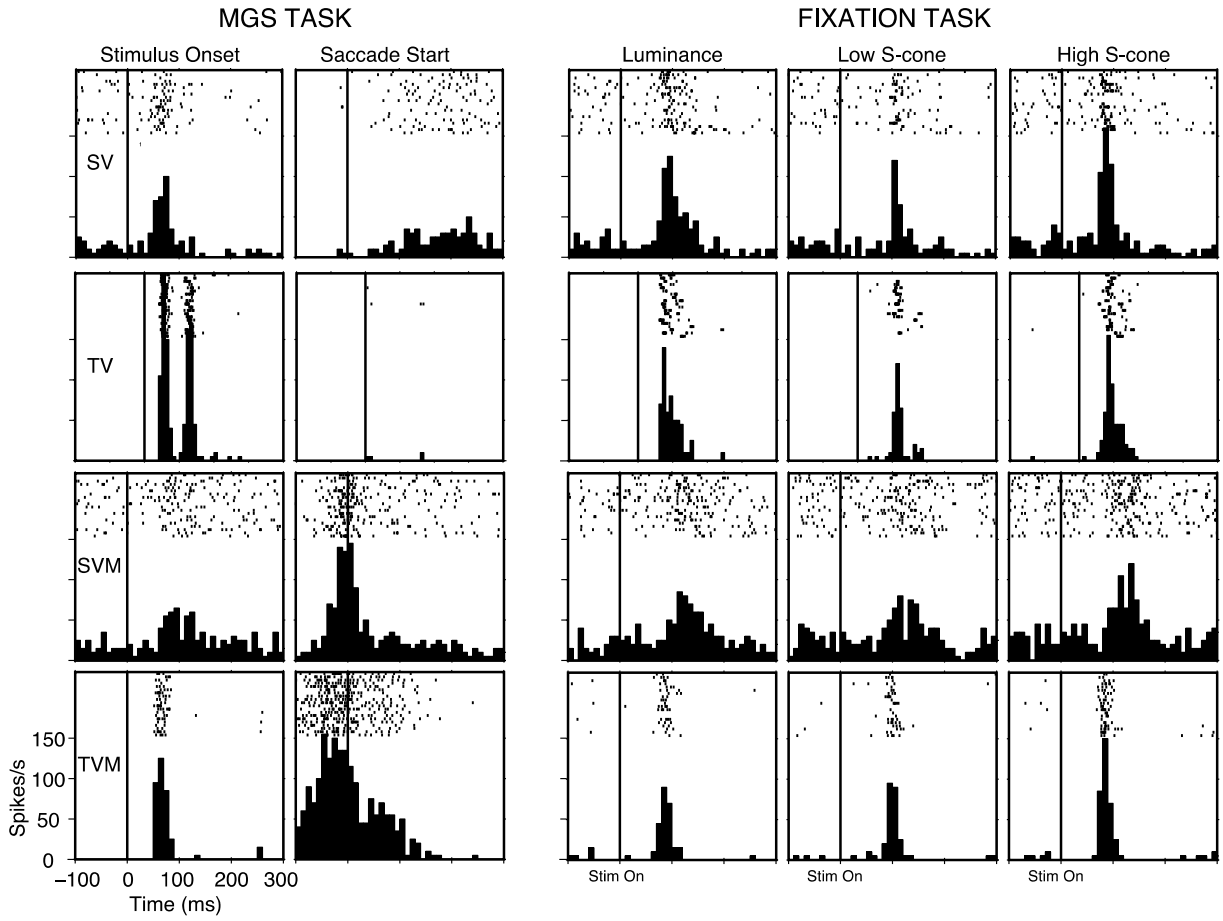

Figure 8. Rasters and histograms from example neurons in each of the four cell classes. The MGS task was used to classify neurons (left columns). Neuronal response to the three stimuli were then recorded during the fixation task (right columns).

3.3.1 Single Neurons Respond to S-cone Stimuli

We divided SC neurons into 4 classes. First we used the memory guided saccade (MGS) task to classify neurons as visual or visuomotor. Of 194 neurons recorded, 178 showed significant visual

responses during the MGS task. Of these, 91 showed significant saccade responses and were classified as visuomotor. The remaining 87 were classified as visual. Second, we classified neurons as either sustained or transient based on their visual response profile in the MGS task. Neurons from all 4 cell classes responded to the luminance and S-cone contrast stimuli.

Characteristic responses of neurons from each class are shown in figure 8. The example sustained visual (SV) neuron (figure 8, top row) responded to stimulus onset and had no response during the saccade in the MGS task. In the fixation task, this neuron fired less to the low contrast S-cone stimulus than to the luminance and high contrast S-cone stimuli (1-way ANOVA, HSD, both $p < 0.05$). The transient visual (TV) neuron (figure 8, second row) showed very brief responses to both stimulus onset and offset. Like the SV neuron, this TV neuron fired less to the low contrast S-cone stimulus than the other 2 stimuli ($p < 0.05$). The example visuomotor (SVM and TVM) neurons (figure 8, bottom 2 rows) had saccade related activity in the MGS task. The TVM neuron responded more briskly to stimulus presentation than did the SVM neuron. The example visuomotor neurons were sensitive to all 3 stimulus types but did not significantly distinguish among them ($p > 0.05$). Similar response patterns were observed across the population of SC neurons (Table 2). A total of 56/178 visual neurons responded significantly more to high than to low S-cone contrast stimuli. Most of the other neurons responded to all stimulus types but response differences did not reach significance. The 2 S-cone stimuli were closely matched in their luminance contrast, differing only in their ability to excite S-cone sensitive visual inputs. These data show that most SC neurons respond to S-cone stimuli and that the activity of many SC neurons significantly distinguishes S-cone contrast.

Table 2. Number of neurons in each class that discriminated stimulus types. High and Low refer respectively to the high contrast and low contrast S-cone stimulus responses. Lum refers to the luminance stimulus response. Counts in the Total column are the total number of neurons in each of the four classes. Counts in the Total Sig column are the number of neurons that showed significant response differences to the three stimulus types (one-way ANOVA, $p < .05$). The three rightmost columns show the number of neurons in each class with significant differences in mean response between the stimulus types indicated in the top row (post hoc, Tukey's HSD, $p < .05$). Neurons in the three rightmost columns are subsets of Total Sig but are not mutually exclusive.

Class	Total	Total Sig	High > Low	High > Lum	Lum > Low
SV	56	26	18	6	13
TV	31	12	9	2	6
SVM	66	23	18	4	13
TVM	25	14	11	6	4

3.3.2 All Cell Classes are Sensitive to S-cone Contrast

We asked whether each class of SC neurons was able to discriminate the 3 stimulus types. The average spike density function responses to each stimulus for neurons in the 4 classes are shown in figure 9. All classes exhibited differential mean responses to the 3 stimulus types that were highly significant (repeated measures 1-way ANOVA, each $p < 0.0001$). Average firing rate for each class strongly and significantly differentiated between the high and low contrast S-cone stimuli (all classes, HSD, $p < 0.001$). In addition, all classes preferred the luminance stimulus to the low contrast S-cone isolating stimulus (SV, TV and SVM-neurons, HSD, $p < 0.001$; TVM-neurons, HSD, $p < 0.05$). We conclude that each class of neurons, taken as a whole, modulate their response with S-cone contrast.

3.3.3 Stimulus Response Modulation is Similar Across Cell Classes

We were especially interested in whether the different neuron classes responded differently to each stimulus type, as has been previously reported for luminance and color stimuli (White et al., 2009). To see how response modulation might differ across the 4 cell classes we performed a 2-way ANOVA on the mean neuronal responses using factors of stimulus type and cell class. To assess whether all cell classes were similarly modulated by the 3 stimulus types we looked at the interaction between class and stimulus. The result was highly non-significant ($p = 0.999$) suggesting that the 3 stimuli were treated uniformly by all 4 cell classes.

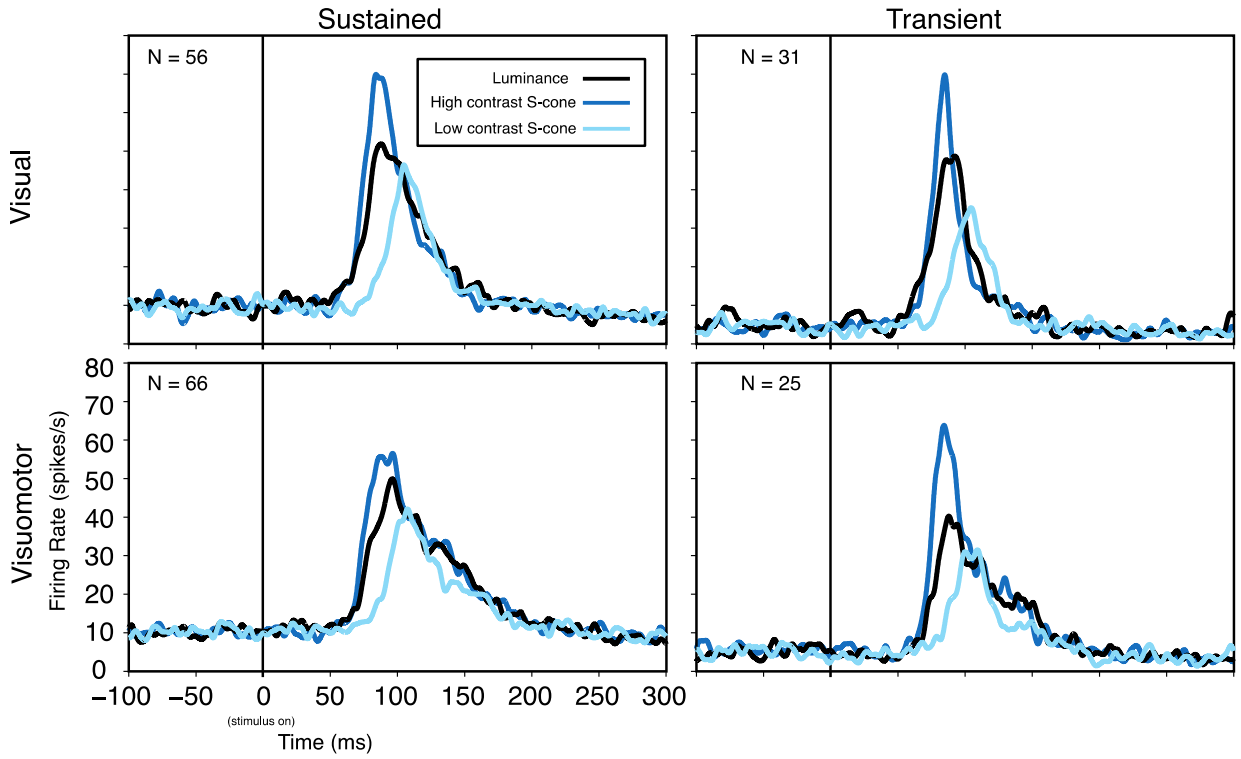

Figure 9. Average SDFs for responses to the three stimulus types (luminance, black; high contrast S-cone, dark blue; low contrast S-cone, light blue). Sustained neurons are shown in the left column, and transient neurons are in the right column. Visual neurons are shown in the top row, and visuomotor neurons are in the bottom row. All SDFs are aligned on stimulus presentation.

We were concerned that using mean responses could affect our analysis of the interaction between class and stimulus type. The mean response of transient neurons is likely to be weaker than that of the sustained neurons in a large time window because sustained neurons were defined to have greater response duration. Indeed, the 2-way ANOVA on average firing rates showed a strong main effect of cell class ($p < 0.0001$), which would be expected if sustained neurons fired more spikes to the stimuli than transient neurons. Post-hoc comparisons revealed that SVM cells had stronger responses than both transient classes while SV neurons exceeded the response of TV neurons (HSD, all $p < 0.05$). Yet the average peak responses of each cell class are qualitatively congruent (figure 9). White et al. (2009) reported a peak firing rate modulation of SC neuronal responses to colored stimuli. It is possible that many SC neurons distinguish the stimuli by modulation of their peak firing rate rather than mean rate.

We performed a second 2-way ANOVA on the peak firing rates of the SC neurons to address this issue. The analysis showed that peak firing rate differences are invariant across cell classes (main effect of class, $p = 0.4950$). We again saw that the 4 cell classes treated the 3 stimulus types similarly in their peak response modulation (interaction of class and stimulus, $p = 0.9973$). Thus differential responses to the 3 stimuli over the population of SC neurons are independent of cell class.

3.3.4 SC Population Responses Differentiate All 3 Stimuli

We wanted to know whether SC responses to S-cone stimuli could be greater than those to luminance at the population level. The 2-way ANOVA on mean responses revealed a strong effect of stimulus type across all 4 classes of SC neurons (main effect of stimulus, $p = 0.0153$). Post-hoc analysis revealed that this discrimination was the same as for within class comparisons: response

to the high contrast S-cone stimulus was significantly greater than the low (HSD, $p < 0.05$) but not the luminance stimuli (HSD, $p > 0.05$), while response to the luminance stimulus did not differ significantly from the low S-cone contrast (HSD, $p > 0.05$). The results were similar and even stronger when peak responses were analyzed (main effect of stimulus, $p = 0.0001$). Post-hoc analysis further confirmed that peak firing rate modulation follows the same pattern as mean firing rate modulation. Peak responses are greater to the high than low contrast S-cone stimulus (HSD, $p < 0.001$), while peak responses to the luminance vs. low S-cone and luminance vs. high S-cone were not significantly different (HSD, $p > 0.05$).

The population spike density function response for each cell class is stronger for the high contrast S-cone stimulus than the luminance stimulus (figure 9). Yet these differences were not significant within any given class or in the 2-way ANOVA pooling the SC population across classes. To determine whether these differences were significant, we performed an analysis that is not confounded by variance across neurons. Because neuronal responses across cell classes did not significantly differ in their modulation by stimulus type, we discarded the factor of class and performed a repeated measures one-way ANOVA on the entire population of 178 SC neurons. In this analysis we are not sorting by cell class and the irrelevant variance across neurons is eliminated. The only effect under inquiry is that of stimulus type. We found that the high contrast S-cone stimulus response was greater than the luminance, which in turn exceeded the low contrast S-cone stimulus response (HSD, all $p < 0.001$). This pattern was identical and even more striking when peak activation was considered instead of mean response (HSD, all $p < 1.0 \times 10^{-9}$). Together these results show that the most important characteristics to SC neurons are the total contrast of stimuli, regardless of the types of cones excited. Responses scale with S-cone contrast, and sufficiently high S-cone contrast stimuli can evoke stronger responses than a low contrast

luminance stimulus.

3.3.5 All Cell Classes Shift Response Latency with S-cone Contrast

It is typical of visual neurons to modulate both response magnitude and latency as a function of contrast. As contrast increases, latency decreases. If SC neurons are truly sensitive to S-cone contrast, their response latency should change as S-cone isolating contrast changes. We plotted cumulative distributions of neuronal response latencies for each class of neuron and found that this was indeed the case (figure 10). Within each class, response latency was significantly modulated across the 3 stimulus types (Friedman test, all classes $p < 1.0 \times 10^{-6}$). Neuronal response latencies to high contrast S-cone and luminance stimuli were much shorter than to the low contrast S-cone for all classes (HSD, both $p < 0.01$). In addition, the transient visual neurons had significantly shorter latency responses to the high contrast S-cone than to the luminance stimulus (HSD, $p < 0.05$). These results mirror those found with neuronal activity, namely that responses to the high contrast S-cone stimulus significantly differed from those to the low contrast S-cone stimulus within each cell class.

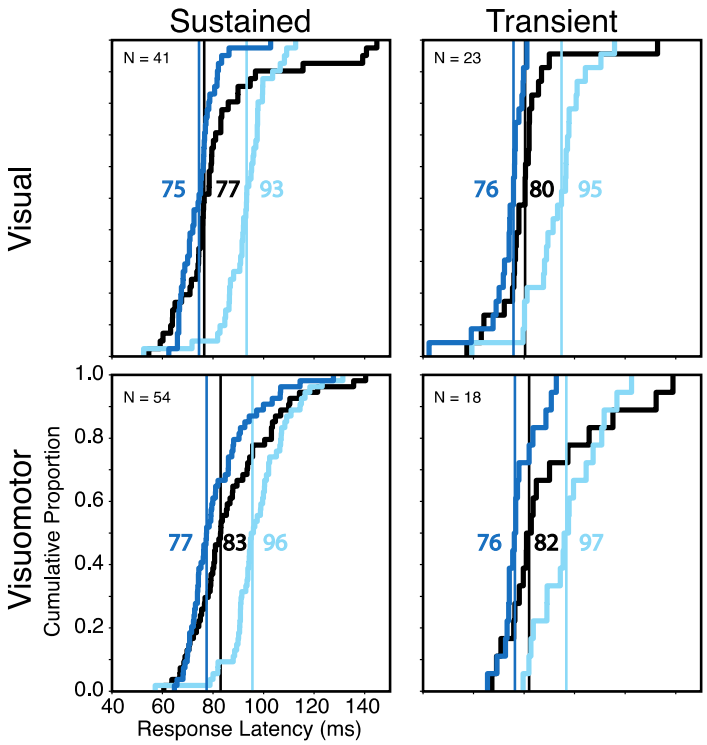

Figure 10. Cumulative distributions of neuronal response latency. Conventions are the same as in Figure 9. Colored numbers and vertical lines indicate the mediate response latency to each corresponding stimulus type. Neurons are drawn from the same population and cell classes as in Figure 9. Neurons were excluded if the response to at least one stimulus type was too weak for latency analysis.

3.3.6 Neuronal Response Latency Shifts are Greater for Visual Neurons

Given that all classes had response latencies modulated by S-cone contrast, we wanted to know whether there were any differences across the neuron classes. To that end, we compared the neuronal latency distributions to each stimulus type across the 4 cell classes. We found that neuronal latency to the luminance and low contrast S-cone stimuli were roughly the same across classes (Kruskal-Wallis, $p = 0.0563$ and $p = 0.1759$, respectively). For the high S-cone contrast stimulus, neuronal latencies differed significantly (Kruskal-Wallis, $p = 0.0169$), with SV neurons responding earlier than SVM-neurons (HSD, $p < 0.05$). Although this comparison yielded the only significant difference, neuronal latency differences to the luminance stimulus across cell classes approached significance. It is likely that our sample of transient neurons was inadequate to detect

any small differences in latency between transient visual and visuomotor neurons. Furthermore, because stimuli that elicit the largest visual responses (the high S-cone and luminance stimulus) produced the greatest differences across classes, nonlinearities in contrast sensitivity between transient and sustained neurons may have obscured differences between neuronal classes. Qualitatively, the median latencies of the TV neurons were all less than or equal to those of the TVM neurons. These data suggest that visual neurons may respond sooner than visuomotor neurons to high contrast stimuli, though the differences appear small.

3.3.7 SC Population Latencies Differentiate All 3 Stimuli

Finally, we wondered whether the small differences seen in median response latency between the luminance and high contrast S-cone stimuli were meaningful at the population level, independent of cell class. To increase statistical power we grouped response latencies across all cell classes, despite the possibility of small differences in neuronal response latency between visual and visuomotor neurons. This analysis yielded a highly significant result for latency differences across the stimulus types (Friedman, $p < 1x10^{-33}$). Further analysis confirmed that response latencies to each of the 3 stimulus types significantly differed from one another (HSD, all $p < 0.001$). In particular the neuronal response latencies to the high contrast S-cone stimulus were shorter than to the luminance stimulus. SC neurons within each class responded with shorter latency to high than to low S-cone contrasts. At the class independent population level, increasing S-cone contrast elicited responses with shorter latency compared to the luminance contrast stimulus.

3.3.8 S-cone Contrast Sensitivity Increases with Transience

Throughout the visual system, there is a tendency for transient visual neurons to be more sensitive to changes in contrast. We asked whether this would be true of SC neurons using S-cone isolating contrasts. We plotted the high vs. low S-cone contrast sensitivity index of each neuron against its transience index separately for visual and visuomotor neurons (figure 11, top row). Nearly all neurons tested had a stronger mean response to high than to low S-cone contrasts (73/87 visual and 82/90 visuomotor contrast sensitivity indices > 0). This shows that although only about 1/3 of neurons significantly distinguished the 2 contrasts (Table 2), nearly all neurons increased their response as S-cone contrast increased. In addition, the degree to which neurons modulated their response with S-cone contrast was correlated with their level of transience (visual cells, $r = 0.2121$, $p = 0.0486$; visuomotor cells, $r = 0.2885$, $p = 0.0058$). SC neurons with more transient responses were more sensitive to changes in S-cone contrast.

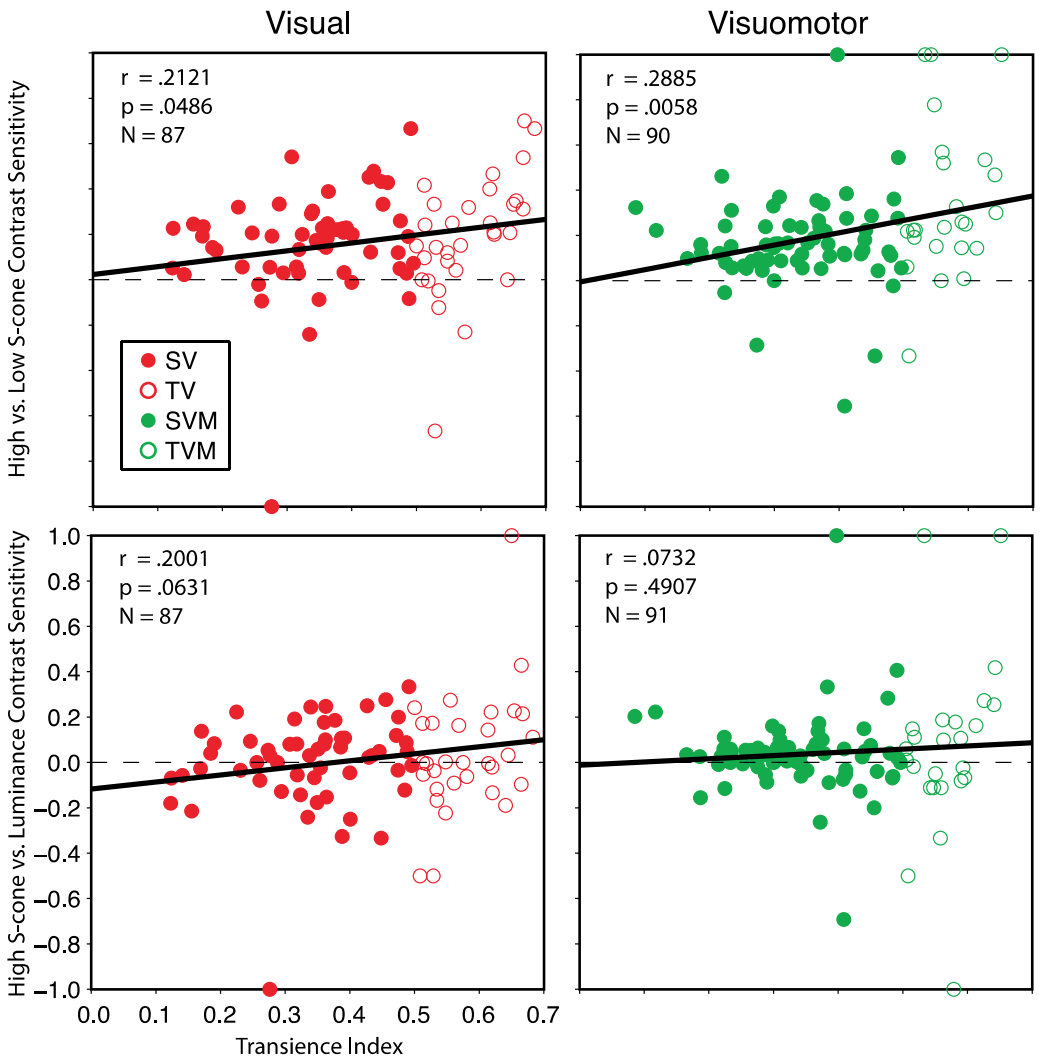

Figure 11. Contrast sensitivity indices as a function of transience index. Top row: High versus low S-cone contrast sensitivity index. Each point plots a neuron's contrast sensitivity index against its transience index. Colors indicate each neuron's classification as visual or visuomotor. Filled circles indicate neurons classified as sustained and open circles indicate neurons classified as transient. Solid black lines are the least squares linear regression line of best fit. Dashed horizontal black lines correspond to a contrast sensitivity index of 0, indicating equal responses to high and low contrast S-cone stimuli. Bottom row: High S-cone versus luminance contrast sensitivity index. Conventions are the same as top row.

3.3.9 S-cone Contrast Sensitivity is Weaker than Luminance

In addition to response modulations with S-cone contrast, we asked how the high contrast S-cone stimulus responses compared with those to the luminance stimulus. We examined this question

by plotting the high S-cone vs. luminance contrast sensitivity index of each neuron against its transience index separately for visual and visuomotor neurons (figure 11, bottom row). These data indicate that SC neuronal responses were much more similar for the high S-cone and luminance stimuli than between the two S-cone stimuli (45/87 visual and 55/91 visuomotor contrast sensitivity indices > 0). Correlations for visual and visuomotor neurons in this instance were not significant (visual cells, $r = 0.2001$, $p = 0.0631$; visuomotor cells, $r = 0.0732$, $p = 0.4907$), although visual neurons trend in the positive direction. The contrast of the high S-cone stimulus was much greater than the luminance in DKL space. The contrast of the low S-cone stimulus was only slightly less than the luminance stimulus contrast. Our results indicate that SC neurons as a whole treated the high S-cone and luminance stimuli as being more similar than the low S-cone and luminance stimuli, in opposition to their definition in DKL space. These data suggest that overall SC neurons may be more sensitive to luminance contrast than to S-cone contrast. Nevertheless, response magnitude can be made greater or smaller to an S-cone compared to a luminance stimulus by appropriately manipulating contrast.

3.4 DISCUSSION

3.4.1 SC and extrastriate cortex play a role in blindsight

Blindsight is defined as the ability to detect, localize and discriminate visual stimuli despite visual field defects produced by damage to primary visual cortex (V1). The term is used to acknowledge the fact that patients with V1 lesions may have quite good residual visual capabilities despite their inability to report visual detection verbally (Sanders et al., 1974, Weiskrantz, 2004, Cowey, 2010).

Consistent with a lack of conscious awareness of visual stimuli, blindsight is distinctly different from impaired normal vision, such as near threshold detection (Weiskrantz, 1986, Azzopardi and Cowey, 1997). Blindsight has been studied in both humans and macaque monkeys, and is believed to be similar in both species (Cowey and Stoerig, 1995, Moore et al., 1995, Stoerig and Cowey, 1997, Gross et al., 2004). Despite substantial efforts, the exact pathways and mechanisms responsible for blindsight are not completely resolved (Leopold, 2012).

Many studies have suggested an essential role for the SC in the mediation of blindsight (Vaughan and Gross, 1969, Gross, 1991, Weiskrantz, 2004, Yoshida et al., 2008, Cowey, 2010, Leopold, 2012). This evidence comes in large part from early lesion studies. It has long been known that ventral stream visual areas, like inferotemporal cortex, are more dependent on visual input from V1 as compared to dorsal stream areas in parietal cortex (Vaughan and Gross, 1969). Visual responses in inferotemporal cortex are abolished by V1 lesions (Rocha-Miranda et al., 1975) and visual discriminations dependent on ventral stream processing are impaired (Cowey and Gross, 1970).

Neural Responses in dorsal stream visual areas are less affected by V1 lesions. This is because dorsal stream areas are able to utilize their input from the SC in the absence of V1 (Gross, 1991). Neurons in the superior temporal polysensory area (STP) show reduced responses and selectivity after V1 lesions, but these responses break down completely after additional SC lesions (Bruce et al., 1986). Similarly, lesion or cooling of V1 alone has almost no effect on neurons in middle temporal (MT) area. However, when V1 lesions are combined with SC lesions, MT responses are eliminated (Rodman et al., 1989, 1990).

How are these neurophysiological observations related to blindsight? Reversible inactivation of the SC abolishes blindsight behavior in monkeys with V1 lesions (Kato et al.,

2011). Interestingly, an SC lesion alone has little or no effect on either MT or MST neuronal responses, suggesting that removal of V1 may enhance the role of the SC in visual function (Gross, 1991). Residual dorsal extrastriate activation has been observed in both monkey and human blindsight subjects using fMRI (Goebel et al., 2001, Schmid et al., 2010). Studies of more expansive cortical lesions demonstrate that activity in dorsal stream extrastriate areas is important for blindsight. Lesions that include V1 and extrastriate cortex deplete residual visual capacities and often eliminate blindsight (Stoerig et al., 1996, Weiskrantz, 2004, Leh et al., 2006). In sum, extrastriate cortex and its input from the SC are likely to play a pivotal role in blindsight (Gross et al., 2004, Yoshida et al., 2008, Leopold, 2012).

3.4.2 Examining the role of SC in blindsight using chromatic stimuli

To pinpoint the role of the SC in blindsight, several investigators have attempted to block visual input to the SC by using colored stimuli. For example, the speeding of reaction time produced by redundant targets disappears in blindsight for both red and purple colored stimuli (Marzi et al., 2009). A similar result was found while measuring pupil and fMRI responses (Tamietto et al., 2010). The conclusion is that the SC plays an essential role in blindsight because it is selectively discriminated against by the use of colored stimuli. These data stand in contrast to several other investigations of the effects of color in blindsight.

Numerous investigators have asked whether blindsight patients can discriminate any color at all. Their results provide an apparent contradiction with studies attempting to block visual input to the SC in blindsight subjects using chromatic stimuli. Color opponency is present in human blindsight (Stoerig and Cowey, 1989, 1991) and results are similar in macaques (Cowey and Stoerig, 1999). Results in monkeys and humans reveal a role for the S-cone opponent system and

suggest that, if anything, this system may be stronger in blindsight than the L-M opponent mechanism (Cowey and Stoerig, 2001). In fact, responses to green stimuli appeared to be weakest among the blue, green, and red stimuli tested . Effects of color have also been observed via fMRI activations of the SC to red, but not green, stimuli (Barbur et al., 1998). Together, these studies support a role for color in blindsight (Stoerig and Cowey, 1997). Nevertheless, the effects of cone contrast and luminance are difficult to resolve in these studies because stimuli were not specific to any cone or visual mechanism, specifically the S-cone mechanism.

3.4.3 S-cone discrimination in blindsight

Precise cone activation was addressed more directly using uncalibrated S-cone contrast stimuli (Leh et al., 2006). In hemispherectomized subjects these investigators found a lack of spatial summation effect in blindsight using S-cone stimuli as compared to luminance stimuli (Leh et al., 2006). This result, combined with others using colored stimuli, suggests that color may be treated differently in blindsight than in normal vision, where V1 input to SC is available. It is difficult to say whether these results in hemispherectomized patients apply generally to blindsight because color specific effects may depend on the presence of color selective areas in extrastriate cortex (Gross, 1991, Gross et al., 2004). Nevertheless, these results suggest that without any cortical input available, sensitivity of SC neurons to colored stimuli is diminished.

In another effort to better isolate the S-opponent mechanism, narrowband stimuli were used to address color discrimination in blindsight (Alexander and Cowey, 2010). These researchers found that color discrimination is possible, even for short wavelength stimuli. Interestingly, when the cone contrast of stimuli was specifically addressed, discrimination appeared to be better for stimuli with larger effects on the S-opponent system. Contrary to evidence from

hemispherectomized subjects, these data indicate that blindsight can make use of signals that preferentially excite S-cones.

Behavioral studies in monkeys provide further evidence for the utility of S-cone isolating information in blindsight. Monkeys with blindsight can make saccades to color defined targets (Yoshida et al., 2012). These targets include uncalibrated S-cone isolating stimuli, as defined in DKL color space. Although the S-cone stimulus was not individually calibrated, Yoshida et al. (2012) performed 3 manipulations designed to rule out stimulus detection due to artifacts. **1)** Luminance contrast was varied to rule out the possibility of detection by luminance contrast. **2)** Gaussian stimuli were used that eliminate the effects of presenting hard edges. **3)** Luminance noise masking was used to eliminate artifacts of sudden stimulus onset, residual contrasts, and hard edge presentation. Despite efforts to ascribe blindsight detection of S-cone stimuli to other stimulus attributes, monkeys consistently demonstrated blindsight detection of S-cone stimuli. These findings are consistent with a role for chromatic detection and the SC in blindsight.

3.4.4 Pathways for S-cone signals in blindsight

What are the pathways through which S-cone signals could contribute to blindsight? From studies of neuronal degeneration patterns it might be expected that L-M opponency would decline, while S-opponency remained stable or strengthened (Stoerig and Cowey, 1997). After V1 lesions, there is widespread degeneration of LGN and retinal ganglion cells in pathways that carry L- and M-opponent signals, while those in S-cone pathways are less damaged (Cowey, 2010, Cowey et al., 2011). This is presumably because afferent and efferent neurons of the koniocellular layers of the LGN are preferentially spared after V1 lesions (Cowey, 2010). Not only is the koniocellular LGN less damaged by V1 lesions, neurons there may actually enhance and strengthen their role as

indicated by their change in size (Leopold, 2012). Many of the neurons in LGN that survive retrograde degeneration after V1 lesions are those that project directly to extrastriate areas (Cowey and Stoerig, 1989). Direct projections from the LGN to extrastriate visual areas stem primarily from the koniocellular layers, whereas the magnocellular and parvocellular layers project predominantly to V1 (Hendry and Reid, 2000, Cowey, 2010, Leopold, 2012). The intact subcortical input from the SC also terminates predominantly in the koniocellular layers of the LGN (Hendry and Reid, 2000, Leopold, 2012).

Intriguing evidence for the role of the SC and koniocellular neurons in blindsight comes from the spatial and temporal response properties of these neurons. Koniocellular and SC neurons, which closely resemble each other (as outlined above), are similar to those most desirable for eliciting blindsight, namely, low pass filtered spatial tuning responses with sensitivity peaks around 1 cycle/degree, abrupt transient stimuli, and hard edges (Weiskrantz, 2004, Alexander and Cowey, 2010). Thus patterns of neuronal degeneration and visual abilities after V1 lesions strongly suggest an enhanced, rather than diminished, role for S-cone and SC pathways in blindsight.

3.4.5 Neuronal pathways for blindsight

Although the exact pathways for blindsight are not known, observations of neuronal degeneration in the LGN and retina after V1 lesions advocate a crucial role for reorganization in blindsight. Neuronal pathways for blindsight could be affected by the substantial reorganization that takes place after V1 lesions (Gross et al., 2004). Evidence for the importance of reorganization stems from V1 lesions in infancy, which generally produce more effective blindsight in monkeys (Moore et al., 1996, Moore et al., 2001). This is presumably because reorganization is faster and more

effective in early life. An example of differential reorganization later in life is seen in the complex task of color discrimination. Color discrimination takes a considerable amount of time to stabilize in blindsight, suggesting that reorganization of color systems is slow to take hold (Stoerig and Cowey, 1997). While it is difficult to reconcile the contradicting results of color discrimination and SC contributions to blindsight (described above), reorganization could be a confounding factor. Reorganization of visual systems, and the koniocellular system in particular, is likely to have a powerful impact on the residual visual abilities and critical structures of blindsight. Understanding how the visual system reorganizes in blindsight is critical to understanding the underlying mechanisms.

One of the most elusive aspects of the blindsight puzzle is the precise pathway(s) involved. Even after neuronal degeneration and reorganization, a number of visual pathways remain possibilities (Stoerig and Cowey, 1997, Leopold, 2012). Both the LGN and pulvinar nuclei of the thalamus project to extrastriate cortex and receive direct retinal input. Both nuclei also receive input from the SC. The SC and extrastriate visual cortex both appear to be indispensable for blindsight (Vaughan and Gross, 1969, Goebel et al., 2001, Weiskrantz, 2004, Yoshida et al., 2008, Cowey, 2010). Recent fMRI evidence in monkeys points additionally to a critical role for the LGN. Visual stimuli induce widespread activation of extrastriate cortex after V1 lesions (Schmid et al., 2010). The critical finding is that when V1 lesions are combined with inactivation of the LGN, responses in extrastriate cortex are abolished. Our data show that SC neurons are responsive to S-cone stimuli. The discovery that blindsight monkeys, and blindsight patients in some studies, are able to detect stimuli that preferentially activate S-cones would cast doubt on the well established role of the SC in blindsight if the SC were not sensitive to S-cones. Our data show that even during color discriminations, the SC could retain a central role in blindsight. Together

these findings suggest that the blindsight pathway follows a route from the SC, to the koniocellular layers of the LGN, to extrastriate cortex (Leopold, 2012), and can carry color signals from S-cones. This proposal completes a picture whereby the SC, extrastriate cortex, and the LGN are all essential to blindsight.

3.4.6 What Pathway(s) carries S-cone signals to the SC?

Our data do not address the pathway(s) that carry S-cone signals to the SC. There are 2 major pathways that carry visual input to the SC. Either or both of these pathways could be responsible for the observed activation of SC neurons to S-cone stimuli. It has been argued that the SC depends on the indirect pathway via LGN to V1 to generate saccades (Schiller et al., 2008). The finding that saccades can be generated to S-cone stimuli (Yoshida et al., 2012) would suggest that S-cone input can reach the SC through the indirect pathway via V1. To test whether the direct retinotectal pathway carries S-cone input to the SC would likely involve testing a function that depends on this pathway with S-cone stimuli. One example would be express saccades, which are thought to make use of the direct retinotectal pathway [(Yoshida et al., 2008) but see (Schiller et al., 2008) for a counter view]. Under this assumption, if express saccades can be generated to S-cone isolating stimuli then this would indicate that S-cone signals are carried in the retinotectal pathway.

3.5 CONCLUSIONS

We found that neurons in the SC respond to individually calibrated S-cone isolating stimuli on a luminance noise masking background. The population of SC neurons is able to discriminate high

from low S-cone contrasts and respond more strongly to appropriately chosen S-cone than luminance stimuli. The neuronal response latency of SC neurons correspondingly modulates with the contrast of an S-cone stimulus, with shorter latencies at higher contrasts. The sensitivity of SC neurons to changes in S-cone contrast depends on their level of transience, such that more transient neurons are more sensitive to changes in contrast. Our experimental procedures provide a direct link between our electrophysiological results and previous human psychophysical studies. Our finding that S-cone stimuli activate SC neurons rules out the possibility of blocking visual input to the SC by using S-cone isolating stimuli. Therefore, further studies are required to elucidate the neuronal foundations of, and SC contributions to, phenomena that have been widely studied with the use of S-cone stimuli, such as blindsight.

4.0 EXPRESS SACCADES ARE SENSITIVE TO S-CONE CONTRAST

First published in: Hall NJ and Colby CL (2016). Express saccades and SC responses are sensitive to S-cone contrast. Proceedings of the National Academy of Sciences (In Press).

4.1 INTRODUCTION

Decades of oculomotor research have led to an incongruous conclusion: the oculomotor system does not use color information to guide the eyes (Schiller, 1998, White et al., 2006). Yet it is natural to direct one's gaze to objects defined by color. Color vision in primates evolved because of the tremendous benefit of being able to discriminate colors and direct our actions accordingly (Mollon, 1989, Dominy and Lucas, 2001). The superior colliculus (SC) is a brainstem structure with a central role in the transformation of visual sensory signals into saccadic eye movements (Schiller, 1998). Visual projections to the SC lack color opponent responses and appear to be dominated by luminance information (Finlay et al., 1976, Schiller and Malpeli, 1977, De Monasterio, 1978b, a, Schiller et al., 1979b). Luminance signals arise almost exclusively from long and medium wavelength sensitive cones (L- and M-cones) in the retina, but not short wavelength sensitive cones (S-cones) (Calkins, 2001). Instead, S-cones evolved to contribute to color vision (Hunt and Peichl, 2014). The takeaway is that the SC does not use color or S-cone input to guide saccades. This conclusion is surprising because both the SC and S-cones are

evolutionarily ancient, and the SC has a central role in visually guided orienting behavior (Schiller, 1998, Hunt and Peichl, 2014).

The proposition that the SC cannot detect S-cone stimuli has been leveraged to test SC function in diverse clinical and human psychophysical studies (Hall and Colby, 2014, Smithson, 2014). The scope of these investigations has ranged from neural mechanisms of blindsight (Leh et al., 2006, Marzi et al., 2009, Alexander and Cowey, 2010) and interhemispheric transfer in patients without a corpus callosum (Savazzi et al., 2007), to inhibition of return (Sumner et al., 2004), nasotemporal asymmetry (Bompas et al., 2008), and the gap effect (Anderson and Carpenter, 2008). The rationale for these experiments comes from an influential study by Sumner et al. (2002) who noted that previous physiological and anatomical experiments had failed to find S-cone input to the SC (Sumner et al., 2002). The idea is to present subjects with either a luminance or an S-cone stimulus on separate trials of a visual-oculomotor task. If behavior (usually saccadic reaction time, or RT) is different in response to the S-cone stimulus, the conclusion is that the phenomenon under study depends on the SC. The argument is that because the SC cannot detect the S-cone stimulus, it cannot generate a behavior that depends on the S-cone stimulus.

The major appeal of this strategy is that, if it were true, it would allow researchers to selectively "lesion" the SC on a trial by trial basis in healthy human (or animal) subjects. Under this assumption, *any* observed visual-oculomotor behavioral phenomenon could theoretically be tested to assess whether it arises from brainstem mechanisms in the SC. Clinically, after cortical damage, an experimenter could test whether recovery or survival of *any* visual-oculomotor behavior is the result of neural plasticity in the SC, allowing it to take over control of the behavior.

Only recently have studies begun to challenge the view that the oculomotor system is

confined to luminance channels (White et al., 2006, White et al., 2009). White et al. (2009) demonstrated color sensitivity in SC neurons. Their goals did not involve testing the assumption that the SC can be blocked using S-cone stimuli, nor did they examine how an SC-dependent behavior changes with color contrast. Our recent work shows that SC neurons in the macaque do respond to calibrated S-cone stimuli under conditions identical to those used in human psychophysics CHAPTER 3 (Hall and Colby, 2014). We showed that manipulating S-cone contrast modulates SC neural responses. The key piece of information missing from these previous physiological studies of color in the SC, and specifically S-cone sensitivity, is how it relates to behavior. Behavior is the fundamental output measured in human psychophysics. No study has demonstrated a relationship between S-cone driven activity in the SC and an SC-dependent behavior. Researchers have continued to consider it a good strategy to use S-cone stimuli to isolate the SC (Mizzi and Michael, 2014, Smithson, 2014, Spering and Carrasco, 2015). Observed differences in behavioral RT between S-cone and luminance stimuli seem to contradict the finding that S-cone and luminance stimuli activate SC neurons equally well (Mizzi and Michael, 2014). It has instead been argued that S-cone stimuli reach the SC via longer, slower visual pathways than luminance stimuli.

Although the SC plays a role in all saccadic behavior, there is a specific subclass of saccades, known as express saccades (Fischer and Boch, 1983), that depend critically on the SC (Schiller et al., 1987). Express saccades are saccades with extremely short RTs (as short as 70 ms), approaching minimum sensory and motor neuron conduction delays (Fischer and Weber, 1993). Express saccades are not eliminated by lesions of the frontal eye fields or several other areas (Schiller and Lee, 1994). In contrast, express saccades are completely and selectively abolished after SC inactivation or lesion (Schiller et al., 1987). Fittingly, two hallmark neural

correlates of express saccade behavior have been observed in the SC. First, after target presentation, SC neurons generate a large single burst of visual and oculomotor activity, as compared to the two smaller distinct visual and oculomotor bursts generated on regular latency saccade trials (Edelman and Keller, 1996). Second, SC neurons exhibit greater preparatory activity on express saccade trials than regular saccade trials. SC neurons begin to increase their activity before the saccade target is presented (Dorris et al., 1997).

In the present study, we capitalized on the tight relationship between express saccade behavior and the SC to test whether SC neurons actually use the S-cone input they receive to direct behavior. We reasoned that if the SC is able to transform S-cone input into a behavioral output, then we should observe express saccades to psychophysically calibrated S-cone isolating targets. Further, express saccades to S-cone targets should depend on S-cone contrast, as has been shown for luminance contrast (Boch et al., 1984, Marino et al., 2015). The two SC neural hallmarks of express saccade generation should also be present when S-cone targets are used. If the SC uses S-cone input to drive express saccades, varying S-cone contrast should modulate SC neuronal hallmarks of express saccades in parallel with behavior. We tested these hypotheses using the methods standard in human psychophysical studies, and demonstrate that the SC can use S-cone contrast to drive express saccades in the same manner, and as rapidly, as luminance contrast.

4.2 MATERIALS AND METHODS

Two adult male rhesus monkeys (*macaca mulatta*) were used in these experiments. Animals were cared for in accordance with National Institutes of Health guidelines. The University of Pittsburgh Institutional Animal Care and Use Committee approved all experimental protocols. Monkeys

weighed 13 and 8.5 kg (monkey CA and monkey FS, respectively). Surgical procedures and chamber placement have been described elsewhere in CHAPTER 3 (Hall and Colby, 2014).

4.2.1 Data Acquisition and Analysis

Task timing and behavioral monitoring were continuously monitored and controlled online (NIMH Cortex software, provided by Dr. Robert Desimone). Timing accuracy of our setup was verified with a photodiode to be within +/- 4 ms. Data were saved for offline analysis on a Plexon MAP system (Plexon Inc., Dalls, TX) along with spike timing. Our neuronal recording procedure, physiological identification of the SC, and CRT monitor calibration have been described previously in CHAPTER 3 (Hall and Colby, 2014). All data analyses were performed offline using custom MATLAB® software (Mathworks; Natick, MA).

4.2.2 Stimuli and Background

The target and background presentation and calibration procedures have been described in full in CHAPTER 2 and CHAPTER 3 (Hall and Colby, 2013, 2014). Briefly, targets were defined by either luminance or S-cone contrast with respect to an equal energy gray (EEG) background of luminance noise (Birch et al., 1992, Sumner et al., 2002). The background was a full screen array of 1 x 1^{o} squares whose individual luminance changed at random every 4 monitor frames (~47 ms at 85 Hz). This flickering background removes potential artifacts created by stimuli that are not exactly equiluminant with the background. Luminance values ranged from 18.78 to 22.55 cd/m^2, spaced in increments of approximately 0.5 cd/m^2. The mean background luminance across all possible values was 20.73 cd/m^2.

We converted targets and background to DKL contrast space in order to make the effects of contrast explicit (Derrington et al., 1984, Brainard, 1996). The mean color and luminance of the background was used as the basis for conversion to DKL space. Following the procedure described by Brainard (1996), we normalized DKL space such that a stimulus isolating a specific mechanism in DKL space with unit pooled cone contrast would correspond to a contrast of 100%. Contrasts are given in terms of each DKL visual mechanism with coordinates of the form (L+M, L-M, S-(L+M)). The maximum decrement of the luminance noise background was (-16.2298, 0.0091, 1.0320) and the maximum increment was (15.3497, -0.0402, -0.2187). Targets were 1 x 1^{o} squares embedded in the luminance noise background. The luminance contrast target (24.92 cd/m^2) isolates the luminance mechanism (35.1922, 0.1817, 0.5641). The other 2 targets isolated the S-cone opponent mechanism. Their exact DKL coordinates varied by session and animal but spanned a relatively narrow range. The high contrast S-cone target coordinates ranged from (-5.4318, 0.0157, 95.7475) to (-8.7634, -0.1684, 95.9704). The low contrast S-cone target coordinates ranged from (-2.7450, 0.0462, 28.3539) to (-6.2916, -0.2824, 29.5714). Both S-cone targets slightly decreased DKL luminance and contained only small, inconsistent contrasts in the DKL L-M-opponent mechanism. Both deviations remained within the range covered by the background noise. S-cone targets presented on the noisy background were therefore detectable only on the basis of S-cone contrast, and are thus S-cone isolating.

4.2.3 Behavioral Tasks

Receptive fields of recorded SC neurons were identified with a standard memory guided saccade task. The memory guided gap saccade task was used to measure behavioral and neuronal responses to the 3 target types. The fixation cross was 1 x 1^{o} in size and black (< 0.01 cd/m^2). Animals

fixated the central cross for 300-500 ms and then the fixation cross was turned off. This marks the beginning of the 200 ms (17 frame) gap period during which the background continued to flicker but no other stimuli were presented on the screen. The targets appeared for 4 frames synchronously with changes in the luminance noise background. Animals were required to maintain fixation within a 1.5 x 1.5^{o} square window for the duration of the fixation, gap and target presentation. This procedure discouraged early guesses (only ~1% of all trials were aborted during this interval across both animals) and ensured that the monkeys were presented with the target before being allowed to choose a saccade location. The monkeys were given 300 ms to initiate a saccade after the target was turned off. After leaving the fixation window, subjects were required to reach the 2 x 2^{o} square target window within 30 ms to prevent corrective saccades. Monkeys maintained fixation within the target window for 200-400 ms to receive a liquid reward. During the ITI the computer screen was uniform EEG and the same luminance as the mean luminance of the background noise.

The memory guided gap task parameters and brief ITI motivate the monkeys to make rapid saccades to targets but also prevent guessing and maintain accuracy. All target types, especially the low contrast S-cone target, were subjectively difficult to detect for a human observer and this was reflected in the monkeys' behavior. Behavior was correct for 72-80% of the low contrast S-cone target trials, and 85-93% of the high contrast S-cone and luminance target trials. Errors were typically the result of failure to detect the target largely due to their low contrast. Nearly all errors were failures to initiate a saccade after target presentation or failures to reach the correct target.

4.2.4 Behavioral Reaction Time

We analyzed behavior by computing saccadic reaction time (RT) on correct trials of the memory

guided gap saccade task. RT was measured as the time between target onset and the time at which the eye velocity first exceeded 30 deg/s. Trials with RTs less than 80 ms or less than 2 standard deviations from the mean express saccade mode (see below) were considered anticipations and RTs greater than 300 ms were considered late. Both were removed from further analysis. RTs were combined across the 2 possible spatial locations for each target type. This left a total of 2018 luminance trials (1701 monkey CA, 317 monkey FS), 2009 low contrast S-cone trials (1709 monkey CA, 300 monkey FS), and 2023 high contrast S-cone trials (1711 monkey CA, 312 monkey FS).

Reciprocal RT data were fit with a mixture of two Gaussians (Carpenter, 1981) using Maximum Likelihood Estimates (MLE). The MLEs were performed using a 5 parameter probability density function (PDF) of the form:

Equation 3.
$$f(x) = P\frac{1}{\sigma_1\sqrt{2\pi}}e^{-\frac{(x-\mu_1)^2}{2{\sigma_1}^2}} + (1-P)\frac{1}{\sigma_2\sqrt{2\pi}}e^{-\frac{(x-\mu_2)^2}{2{\sigma_2}^2}}$$

Where x is the reciprocal RT (1/RT), μ_1, μ_2 are the mean of the first and second modes of the distribution (express and regular RTs), and σ_1, σ_2 represent their standard deviations. The parameter P determines the proportion of the total probability that lies in each mode, and corresponds to the proportion of express saccades. The parameter P was constrained to lie on the interval [0,1] and σ_1, σ_2 were constrained to be positive. To eliminate additional outliers, trials with RTs 2 standard deviations below the mean express saccade modality were removed (22-30 trials per target type). The data were then fit again with these outliers removed. The means and probabilities of the express and regular RTs are reported as the values of these fitted parameters. All behavioral statistical analyses reported in the manuscript were derived from the simultaneous 95% confidence intervals of the MLE parameters (Sidak corrected for 3 comparisons: low S-cone vs. high S-cone, low S-cone vs. luminance, and high S-cone vs. luminance; i.e. 98.3% confidence

intervals). Confidence intervals were obtained using a parametric bootstrap procedure performed by resampling (with sample size equal to the original sample) the fitted distribution 1000 times and performing a MLE of the parameters for each sample.

4.2.5 Neuronal Analyses

We recorded from 138 neurons (112 monkey CA, 26 monkey FS) in the intermediate layers of the SC. Neuronal data were only considered for trials in which the target appeared in the receptive field of the recorded neuron. The spike trains from each neuron for each trial were sorted as belonging to either an express or regular saccade trial. Sorting for each trial was based on the fit of the Gaussian mixture PDF to the RT distributions. Only trials whose posterior probability of being in one of the two modes was at least 95% were included in the neuronal analysis. The remaining ambiguous trials were not included.

Our neural analysis has 3 target types, and in addition, express and regular saccades to each target type, yielding a total of 6 possible trial categories. We cannot control the number of express saccades generated to each target type in a given session or the number of trials excluded as ambiguous. Express saccades also varied with target type. We aimed to perform statistical tests using a repeated measures design to reduce the impact of different firing rates across neurons and increase statistical power. Each neural analysis included as many neurons as possible given these constraints. Many analyses were thus performed on subsets of the total recorded neural population. Neurons from both animals showed qualitatively similar neuronal response profiles and target differences during the gap task and were pooled for further analysis. It should be noted that despite the relatively smaller contribution of neurons from monkey FS, his data contributed signal to the main results. Inclusion of his neurons in the analysis decreased p-values of the statistical tests

performed beyond what would be expected by a simple increase in sample size. This was assayed by resampling data from monkey CA (leaving out data from monkey FS) with n = the total number of neurons from both animals. Resampled results from monkey CA were compared with results using the full data set including data from monkey FS.

To create the spike density functions (SDF) in Figure 15, spike trains for each neuron were placed in 5 ms bins. The average firing rate in each bin was computed and smoothed by convolving with a Gaussian kernel with $\sigma = 10$ ms. The SDFs for each individual neuron were then averaged together to create the population SDF. This was done separately for each of the 6 categories, including all neurons with at least 1 trial in a given category. For express saccade trials this was 104 neurons on luminance trials (91 monkey CA; 13 monkey FS), 116 neurons on high contrast S-cone trials (103 monkey CA; 13 monkey FS), and 110 neurons on low contrast S-cone trials (97 monkey CA; 13 monkey FS). For the regular saccade trials data were included from 138 neurons on luminance trials (112 monkey CA; 26 monkey FS), 135 neurons on high contrast S-cone trials (112 monkey CA; 23 monkey FS), and 135 neurons on low contrast S-cone trials (112 monkey CA; 23 monkey FS).

Neuronal response latency was determined by finding the time at half height of the peak response for the population SDF in the window from 25 to 150 ms after target onset. Half height was considered half the peak SDF rate plus the average SDF rate from 200 to 0 ms before fixation offset. Statistical analysis for neuronal latency was performed by using bootstrap resampling (1000 samples) of neurons for each category to create Sidak corrected (for 3 comparisons) simultaneous 95% confidence intervals.

Rate comparisons between express and regular saccade trials (i.e. tests to establish the presence of neural hallmarks) were performed on the subset of neurons with at least 1 regular and

1 express trial to a given target type. This included 104 neurons on luminance trials (91 monkey CA; 13 monkey FS), 116 neurons on high contrast S-cone trials (103 monkey CA; 13 monkey FS), and 110 neurons on low contrast S-cone trials (97 monkey CA; 13 monkey FS). Peak activity analysis was performed on the SDF, computed as above, but for each neuron individually. The peak activity was defined as the maximum rate in a 50 ms window beginning at the population neuronal response latency for each of the 6 trial categories. Average preparatory activity was computed on the same subsets of neurons. The mean rate from 125 ms before to 25 ms after target onset was used in this case.

We used a Monte Carlo shuffling procedure with a repeated measures design to determine activity differences between express and regular trials. The same procedures were used for both peak activity and mean preparatory activity comparisons. The activity of each neuron during express and regular latency trials was randomly shuffled, i.e. the label of being an express or regular trial was randomly assigned within each neuron. The test statistic was computed as the difference in median neuronal activity between the randomly assigned express and regular trials. The test statistic was computed 10,000 times to create the null distribution. Reported p-values are given as the number of null distribution samples that equaled or exceeded the test statistic computed on the actual data, divided by 10,000. We then used binomial tests to determine the proportion of neurons that demonstrated this effect. The proportion of neurons with strictly greater express than regular trial activity ("successes") was compared against an expected random proportion of 0.50. For both tests we report raw actual p-values and the Holm-Bonferroni (HB) corrected p-values for 3 comparisons at an alpha level of 0.05.

We also tested for differences between the low contrast S-cone target activity and the *combined* luminance and high S-cone activity during express saccade trials. Neurons included in

these analyses were required to have at least one express saccade trial to all three of the target types (94 neurons; 84 monkey CA, 10 monkey FS). To test whether activity differed between the target types we again used a matched pairs Monte Carlo shuffling procedure. This time the activity of each neuron to each of the three target types was randomly shuffled, i.e. the label of being a luminance, high S-cone, or low S-cone trial was randomly assigned within each neuron. The test statistic was computed as the difference between the randomly assigned low S-cone trials' median and the median of the combined randomly assigned luminance and high S-cone trials. The null distribution and p-values were computed as above. We used binomial tests to determine the proportion of neurons that demonstrated a contrast effect. Neurons with lower peak activity (higher preparatory activity) on low contrast S-cone trials than *both* luminance and high S-cone trials were counted as "successes". All other neurons, including cases of strictly equal activity, were considered "failures". The proportion of successes was compared to a null proportion of 0.25. This value represents the uniform probability of low contrast S-cone activity falling into one of four possible categories: 1) less than high S-cone and luminance; 2) less than high S-cone and greater than luminance; 3) greater than high S-cone and less than luminance; 4) greater than high S-cone and luminance.

4.3 RESULTS

We asked whether the primate SC uses S-cone input to guide behavior. We measured behavioral responses from two monkeys and neuronal responses from 138 intermediate layer SC neurons (112 monkey CA, 26 monkey FS). Behavioral and neural responses were measured while monkeys performed a memory guided gap task (Figure 12), a task that frequently elicits express saccades.

Removing the fixation cross at a fixed time before target presentation both frees

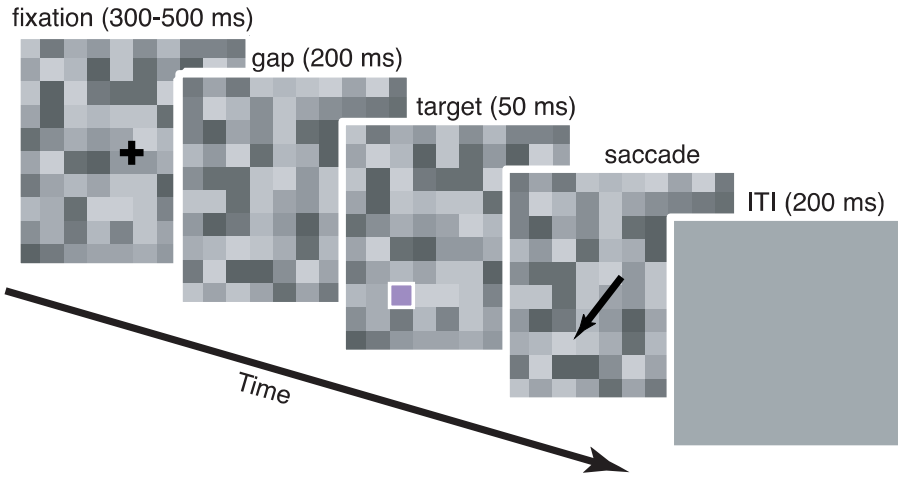

Figure 12. Memory guided gap saccade task with luminance noise. After the initial fixation period, the fixation cross disappeared. After fixation offset, a fixed gap period began followed by target presentation (outlined in white for clarity). The target was either in the receptive field of the recorded SC neuron or in the mirrored location in the opposite hemifield. Monkeys then made a saccade to the remembered target location. Target color and location were selected randomly interleaved on each trial. Locations were 45º above, 45º below, or on the horizontal meridian. Targets were 4º eccentricity in monkey FS and 6º eccentricity in monkey CA.

fixation related inhibition and creates a temporal cue, which allows visual stimulation to drive quick behavioral responses, including express saccades (Sommer, 1994, Pare and Munoz, 1996, Dorris et al., 1997, Sommer, 1997). Three different saccade targets were used: a luminance target, a high contrast S-cone target, and a low contrast S-cone target. S-cone targets were psychophysically calibrated at 6 spatial locations in each monkey (Hall and Colby, 2013). Calibration is critical because a true S-cone isolating stimulus varies across individuals and retinal locations. Using a luminance target in addition allows us to compare results using S-cone isolating targets with a large body of evidence linking the SC and express saccades. All targets were only presented at retinal locations where S-cone stimuli had been calibrated in each animal. SC neurons with receptive fields at calibrated target locations were sought for recording. The targets were presented on a flickering background of luminance noise in order to mask target luminance

artifacts and replicate methods previously used in human subjects (Sumner et al., 2002).

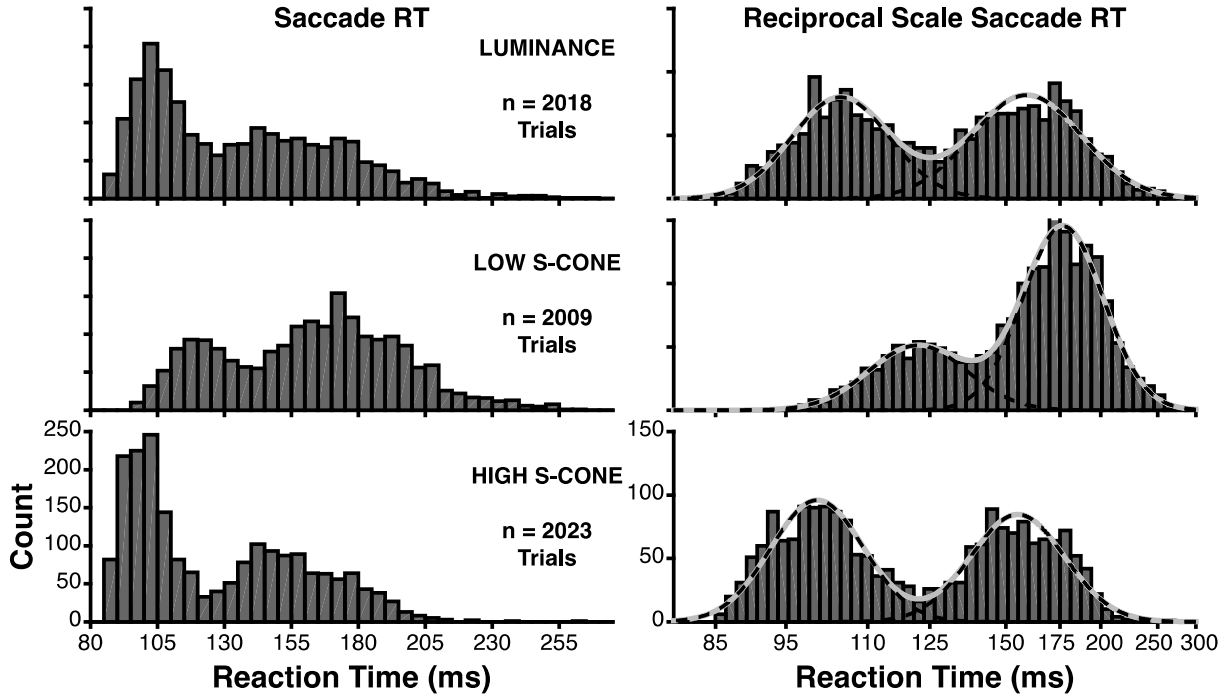

Figure 13. Saccadic reaction time distributions during the gap task to the three target types. Distributions include data pooled across both monkeys, and both spatial locations (in RF and mirrored), for each target type. Left column shows the raw RT distributions in 5 ms bins. Right column shows the same RT data on a reciprocal time scale, which creates a normal distribution. Data are shown in 50 bins evenly spaced on a reciprocal scale. Solid gray curves show the best fit of a Gaussian mixture model. Dashed black lines show the fit of each individual component of the Gaussian mixture. Gaussian fits were rescaled to overlay the raw histograms for visualization purposes.

We computed saccadic RT during the gap task to determine whether express saccades were present to S-cone defined targets (Figure 13). The early mode of each RT distribution represents express saccades (Fischer and Boch, 1983). Both animals exhibited express saccades to all three target types with qualitatively similar modes (Figure 14) and were pooled in further analyses. The low contrast of our targets yielded express saccades with relatively long latencies compared to previous work using high contrast white targets on black backgrounds (Boch et al., 1984). We used the luminance target trials as a baseline for express saccade generation (Figure 13, top row). The novel finding is that express saccades are induced by S-cone targets (Figure 13, bottom two rows). Importantly, express saccades depend critically on the S-cone contrast of the target. To measure

this dependency, we plotted RTs on a reciprocal scale (Figure 13, right column), which makes RTs follow a Gaussian distribution (Carpenter, 1981). We then fit a sum of two Gaussian distributions to quantify the latency and probability of express and regular RTs to each target type. Both the latency and probability of express saccades is modulated by the amount of S-cone contrast. Compared to luminance target trials, high S-cone contrast reduced the average latency (luminance 104.5 ms, high S-cone 100.2 ms, $p < .05$) and increased the proportion of express saccades (luminance 46.4% of trials, high S-cone 52.8% of trials, $p < .05$). When S-cone contrast was reduced, the latency of express saccades increased (121.8 ms) and their probability decreased (29.9% of trials) compared to both the high contrast S-cone (latency and proportion both $p < .05$) and luminance target trials (latency and proportion both $p < .05$).

The first neural hallmark of express saccades is a larger initial burst of activity on express saccade trials compared to regular saccade trials. Trials were classified as either regular or express saccade latency using the distributions fit in the right hand column of Figure 13. This was done separately for each of the three target types, creating 6 separate categories of trials. During regular saccade trials (Figure 15, dashed curves), average neuronal activity to the 3 target types showed an initial visual response, followed by a second burst indicative of a saccadic command.

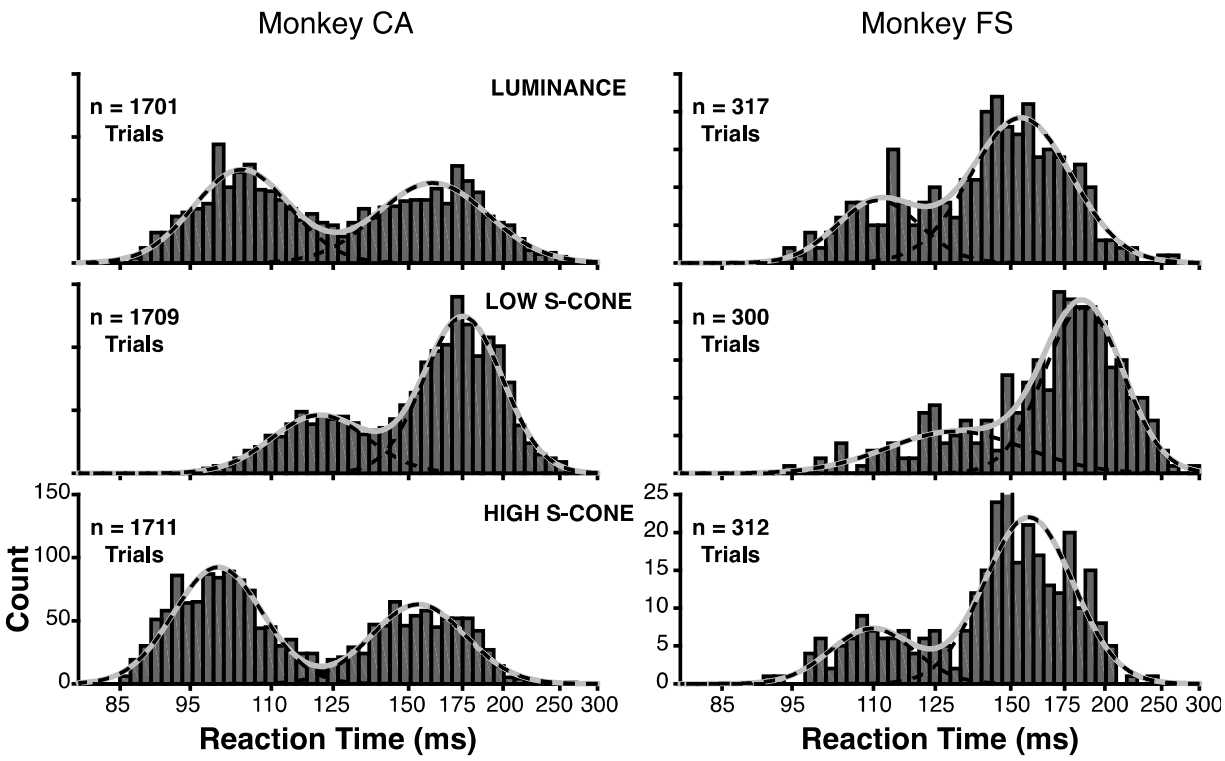

Figure 14. Individual animal saccadic reaction time distributions during the gap task to the three target types. Left column shows data from monkey CA. Right column shows data for monkey FS. Conventions are the same as in the right column of Figure 13. The MLE for both animals shows that the mean express saccade RT to the low contrast S-cone target was significantly later than to the luminance and high contrast S-cone targets. No significant differences between the luminance and high contrast S-cone target are detectable within the individual animals, but are present in data pooled across both animals (Figure 13).

During express saccade trials (Figure 15, solid curves) neural activity manifested as a larger unified burst. The express trial peak burst activity exceeds that on regular trials as expected for the luminance target (Figure 15, black curves and Figure 16A, black circles; Monte Carlo, $p = 0.0002$; Holm-Bonferroni (HB) corrected, $p < 0.05$). The S-cone target responses show the same neural hallmark. Express saccades to both the high contrast S-cone and the low contrast S-cone targets showed a greater peak than regular saccade trials (high S-cone: Figure 15, magenta curves and Figure 16A, magenta circles; Monte Carlo, $p = 0.0232$; low S-cone: Figure 15, blue curves and Figure 16A, blue circles; Monte Carlo, $p < 0.0001$; both HB corrected, $p < 0.05$). This effect was found throughout the neuron population for all target types (Figure 16A, most data points lie above the unity line). A majority of neurons tested had greater peak burst on express saccade trials to all

three target types (luminance: 70/104, binomial test, $p = 2.671e^{-4}$; high S-cone: 70/116, binomial test, $p = 0.0161$; low S-cone: 71/110, binomial test, $p = 0.0015$; all HB corrected $p < 0.05$).

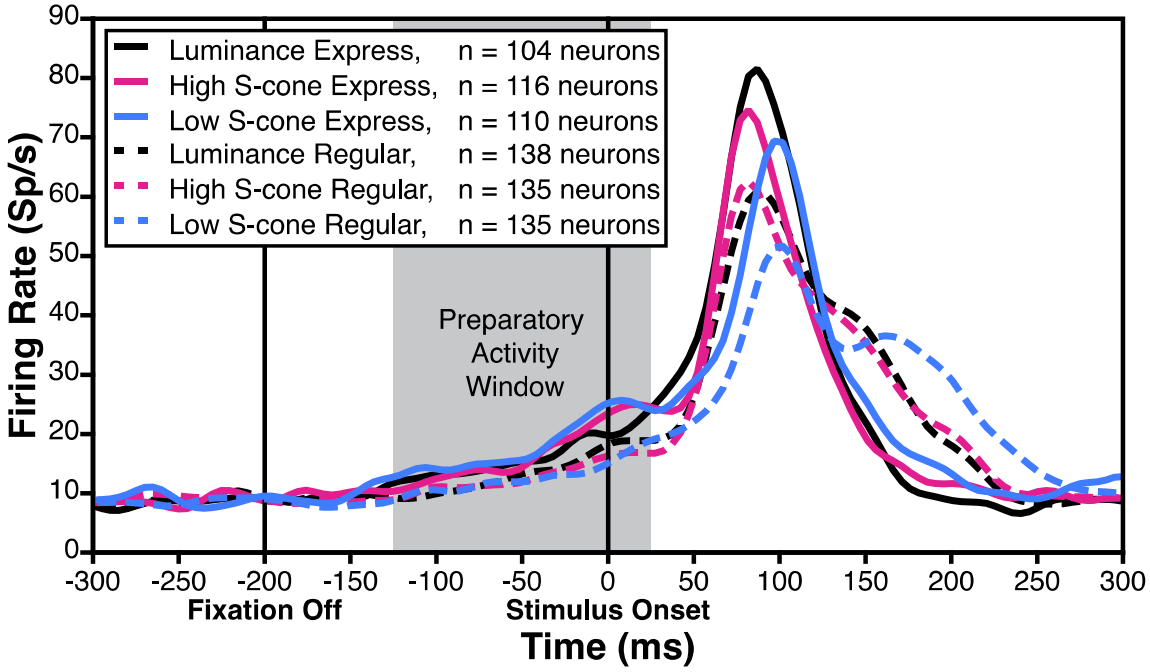

Figure 15. Neural responses to the three target types during express and regular latency saccade trials. Curves shows the spike density function across all neurons aligned on target onset for trials in which the target appeared in the RF. Gray shaded region indicates the preparatory activity analysis window.

We next asked whether the first hallmark depends on the amount of S-cone contrast. We observed that the low contrast S-cone target burst was later (72.9 ms) than both the high S-cone and luminance target bursts (Figure 15, solid blue curve lags behind solid magenta and black; high S-cone: 60.0 ms; bootstrap, $p < .05$; luminance 61.0 ms; bootstrap, $p < .05$). This is in direct correspondence with the differences observed in express saccade RTs as S-cone contrast decreased (Figure 13). Neural latency increased by 12.9 ms and behavioral RT increased by 21.5 ms. Effects of S-cone target intensity on peak burst were examined in the subset of neurons with express saccade data to all three target types (94 neurons). We considered peak responses to the high contrast S-cone and luminance targets together because they were similar and combining them increases statistical power. The median peak response was significantly lower to the low contrast

S-cone target than to the other targets combined (solid curves Figure 15, blue peak is less than the median of black and magenta peaks; Figure 16A, blue circles fall lower along the vertical axis than black and magenta; Monte Carlo, p = 0.0005). In fact the majority of this neural subset had lower peak activity to the low contrast S-cone target than to both the luminance and high S-cone targets considered separately (57/94, binomial test, p = $2.833e^{-13}$). Express saccade bursts in most SC neurons are present in response to S-cone targets, and sensitive to changes in S-cone contrast.

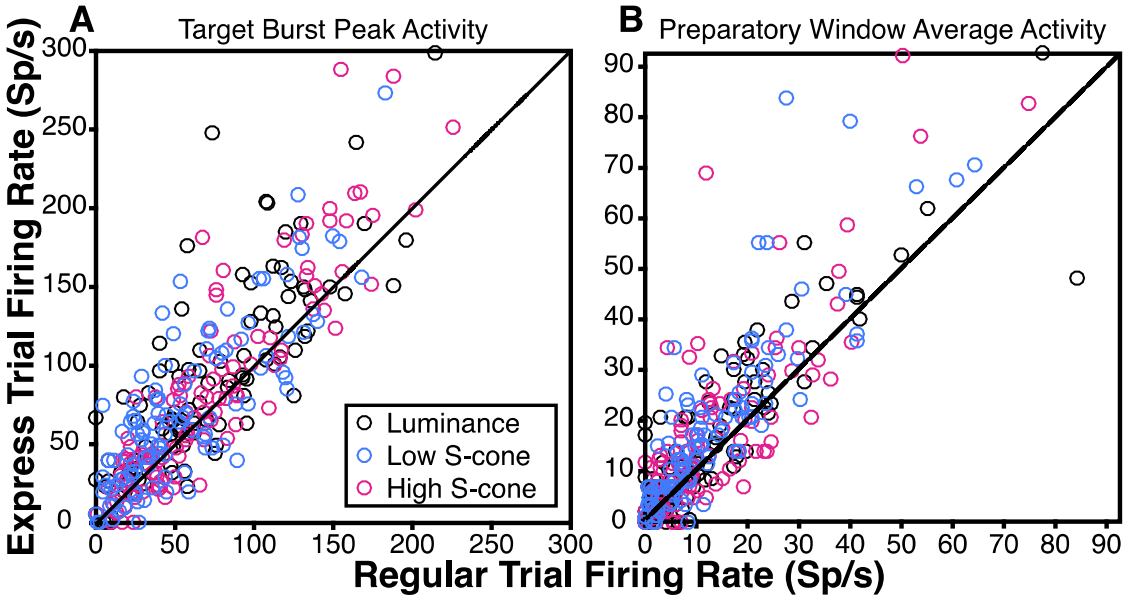

Figure 16. Individual neuron activity differences between express and regular saccade trials to each target type. Points above the unity line indicate neurons with greater response during express saccade trials for either the initial activity burst peak (A) or average preparatory window activity (B). n = 104 luminance, 116 high S-cone, and 110 low S-cone neurons.

The second neural hallmark of express saccade generation is stronger preparatory activity in SC neurons on express saccade trials. Preparatory activity is reflected in the slow rise of the solid curves compared to the dashed curves in the preparatory window leading up to target response (gray shading Figure 15, 125 ms before to 25 ms after target presentation). We confirmed the expected presence of greater express than regular trial preparatory activity to the luminance target (Figure 15, black curves and Figure 16B, black circles; Monte Carlo, p = 0.0030; HB

corrected, $p < 0.05$). We then inspected the data for preparatory activity on S-cone target trials. Preparatory activity was considerably greater on express compared to regular trials for both contrasts of S-cone target (high S-cone: Figure 15, magenta curves and Figure 16B, magenta circles, Monte Carlo, $p = 0.0053$; low S-cone: Figure 15, blue curves and Figure 16B, blue circles, Monte Carlo, $p < 0.0001$; both HB corrected, $p < 0.05$). Preparatory activity was evident at the single neuron level (Figure 16B, most data points lie above the unity line). The majority of SC neurons exhibited express saccade trial preparatory activity to all three target types (luminance: 66/104, binomial test, $p = 0.0039$; high S-cone: 74/116, binomial test, $p = 0.0019$; low S-cone: 85/110, binomial test, $p = 3.916e^{-4}$; all HB corrected $p < 0.05$).

Perhaps more important than the presence of the preparatory activity per se, is whether preparatory activity is greater when S-cone contrast is low. If preparatory activity brings SC neurons closer to saccadic threshold, then greater preparatory activity should be required to trigger an express saccade when visual input is weaker (Carpenter and Williams, 1995, Dorris et al., 1997, Marino et al., 2015). This predicts greater preparatory activity during express saccade trials to the low contrast S-cone target because the visual burst is smaller. Our data provide resounding support for this hypothesis. Preparatory activity on express saccade trials was greater for the low contrast S-cone target than for the luminance and high S-cone targets combined (solid curves Figure 15, blue preparatory activity is greater than the median of black and magenta; Figure 16B, blue circles tend to lie higher along the vertical axis than black and magenta; Monte Carlo, $p = 0.0294$). Moreover, many SC neurons in this subset exhibited greater preparatory activity on low S-cone express trials than both the luminance and high S-cone trials considered separately (42/94, binomial test, $p = 2.603e^{-5}$). The SC displays express saccade preparatory activity that varies according to S-cone contrast and the effects are present in individual cells.

4.4 DISCUSSION

S-cone targets can drive express saccades, a behavior that depends on the SC. Two hallmarks of express saccade related neural activity in the SC are present when S-cone targets are used: 1) a single visual-motor burst and 2) preparatory activity. Both express saccade behavior and SC neural correlates depended on the amount of S-cone contrast in the target. This contrast modulation indicates that our results do not stem from trivial target selection or attention factors that could be computed at higher cortical levels. We conclude that the SC uses S-cone input to guide visual-oculomotor behavior.

Express saccade RTs can be made arbitrarily shorter or longer than those to a luminance target by changing the amount of S-cone contrast. The total cone contrast of the luminance target in our study fell between the total cone contrast of the S-cone targets. Correspondingly, express saccade RTs to the luminance target were between those to the S-cone targets. It has been suggested that express saccades to S-cone targets are guesses or anticipations in human subjects (Anderson and Carpenter, 2008). The fact that RT changed with S-cone contrast in the present experiments rules out this possibility. The shift in reaction time with contrast demonstrates that express saccades to S-cone targets were stimulus dependent. Our data indicate that SC-dependent behavior hinges upon total cone contrast in the retina, rather than a special presence or absence of S-cone input.

The two SC neuronal hallmarks of express saccade generation changed in concert in an S-cone contrast dependent manner. Previous models of saccadic RT (Carpenter, 1981, Carpenter and Williams, 1995) and the role of intermediate layer SC neurons in generating express saccades (Sommer, 1994, Edelman and Keller, 1996, Dorris et al., 1997, Dorris and Munoz, 1998, Marino et al., 2015) predict a specific relationship between the initial burst and preparatory activity. If the

initial visual burst is sufficient to push SC activity over saccadic threshold, an express saccade is triggered. Preparatory activity brings SC neurons closer to saccadic threshold, making it more likely that the initial burst will breach threshold and an express saccade will occur. This model offers a critical test of whether express saccades truly depend on SC responses to S-cone targets: greater preparatory activity should be present in order for the weak visual burst to the low contrast S-cone target to push SC activity over threshold. This was indeed the case. Decreasing S-cone contrast decreased the visual burst and greater preparatory activity was required to trigger an express saccade. Increasing S-cone contrast generated a large burst that required less preparatory activity to trigger an express saccade. Our findings support previous models of saccade generation and expand them to include color specific contrast. The fact that data using S-cone targets fits well with a large body of research based on luminance targets implies that the SC makes use of S-cone contrast as it does luminance contrast.

Reaction time differences between S-cone and luminance stimuli in previous studies can likely be interpreted as the result of using an S-cone stimulus that was too weak compared to the luminance control. This would lead to weaker SC neuronal responses and slower RTs to the S-cone stimulus. Our data show that behavioral and neural responses to the luminance and high contrast S-cone target were very similar, despite the fact that the high contrast S-cone target contained much greater total cone contrast in DKL space. Total cone contrast of the luminance and low contrast S-cone targets were much more similar, but their neural and behavioral results were very different. Most previous behavioral studies did not test different levels of S-cone contrast, and matching stimuli in contrast across cone types and visual mechanisms is a very difficult problem (Brainard, 1996). Even when stimuli are equated in detectability (Bompas and Sumner, 2008), it is likely that S-cone and luminance channels function at different speeds

(Calkins, 2001, Smithson and Mollon, 2004). To avoid the contrast matching problem, we have shown that behavior and SC neuronal responses are sensitive to changes in S-cone contrast and can be shifted relative to a fixed luminance contrast. This sensitivity predicts that increasing S-cone contrast and/or decreasing luminance contrast could reverse results from previous psychophysical work that compared S-cone and luminance stimuli.

It has been argued that SC-dependent behavior to luminance stimuli might employ the faster direct retinotectal pathway, whereas SC-dependent behavior to S-cone stimuli is slowed by rerouting through cortex (Mizzi and Michael, 2014). While our experiments cannot distinguish whether S-cone stimuli traverse the retinotectal or corticotectal pathway, they do indicate that it is impossible to infer a specific pathway behaviorally. Express saccades are among the most rapid visual-motor behaviors, and approach the minimum required visual and motor neuron conduction delays via the corticotectal route (Fischer and Weber, 1993). We have demonstrated that S-cone and luminance stimuli can trigger express saccades at the same latency. The parsimonious explanation is that both stimulus types utilize the same pathway(s). Reaction times of SC-dependent behavior to S-cone and luminance stimuli depend principally on the level of contrast. S-cone stimuli cannot be used to stop the SC from participating in behavior, nor can they be used to deduce the contributions of specific visual pathways.

5.0 GENERAL DISCUSSION

Adapted from: Hall NJ and Colby CL (2014). S-cone visual stimuli activate superior colliculus neurons in old world monkeys: implications for understanding blindsight. Journal of Cognitive Neuroscience (26): 1234-1256.

Neurons in the SC are sensitive to S-cone isolating stimulus contrasts. SC visual responses are a function of total cone contrast that does not discriminate against S-cones. This finding raises questions about the visual properties of, and visual inputs to, SC neurons. It has a direct bearing on studies that have used S-cone isolating stimuli to probe the role of the SC in visual and oculomotor phenomena, such as blindsight.

5.1 HOW COULD S-CONE STIMULI REACH THE SC?

There are two major pathways by which visual input from the retina reaches neurons in the SC. The SC receives direct input from retinal ganglion cells, primarily to the superficial layers (Hendrickson et al., 1970, Bunt et al., 1975, Hubel et al., 1975, Marrocco and Li, 1977). It also receives indirect, cortical input from striate and extrastriate cortex. Striate cortex targets more superficial neurons while extrastriate cortex targets the intermediate and deeper layers (Kuypers and Lawrence, 1967, Fries, 1984, Sommer and Wurtz, 2004). Either or both of these pathways could contribute to the collicular activation we observed using S-cone stimuli.

5.1.1 Early studies of SC visual afferents and properties

In early studies, the ganglion cells comprising the direct, retinotectal pathway were reported to lack chromatic sensitivity. Pioneering physiological investigations of the direct pathway to SC recorded retinal ganglion cells, studied their properties, and confirmed tectal projection by antidromic activation from the SC (Schiller and Malpeli, 1977, De Monasterio, 1978b, a). They found that direct projections to SC arose primarily from non-opponent ganglion cells that sum input from L- and M-cones. SC-projecting ganglion cells had transient responses and generally lacked a strong center-surround organization. Many of these ganglion cells were classified as the broad band type now associated with the magnocellular "luminance" pathway. The conclusion was that the direct pathway to the SC carries primarily, or exclusively, luminance contrast information from L- and M-cones.

Cortical projections to the SC also appear to stem from luminance channels in the LGN (Finlay et al., 1976). Antidromically activated corticotectal neurons in V1 are mostly complex cells that have large receptive fields, weak orientation selectivity and lack color opponency. Lesion or cooling of striate cortex causes a powerful, selective decrease in visual sensitivity of neurons in deeper SC layers while sparing sensitivity of the superficial layers (Schiller et al., 1974). Similar deficits were found after inactivation of the magnocellular layers of the LGN, but not the parvocellular layers, where color opponent neurons are found (Schiller et al., 1979b). The conclusion was that visual inputs to the SC from striate cortex arise from the magnocellular layers of the LGN, summing achromatic signals from L- and M-cones in the retina.

The properties of neurons projecting to the SC through both the direct and indirect pathways are reflected in those of visual SC neurons (Cynader and Berman, 1972, Goldberg and Wurtz, 1972, Marrocco and Li, 1977). Visual neurons in the SC have comparatively large RFs

with a weak or absent inhibitory surround. They are relatively insensitive to stimulus size, shape, orientation, and lack color opponency. Observations of SC neurons and their primary visual inputs have led to the belief that SC neurons do not get input from S-cones.

5.1.2 "Rarely encountered cells"

Initial reports on both direct and indirect pathways showed a lack of color opponent input with no contribution from S-cones. From an evolutionary perspective, the lack of S-cone input to the SC is a curious finding. Both the SC (Kaas, 2004) and S-cones are evolutionarily ancient (Mollon, 1989). The SC shares similarities across many mammalian species, and the ganglion cell types that carry S-cone signals in modern primates were more prominent in early primates (Kaas, 2004). Genes encoding the S-cone in macaques and humans are highly homologous and conserved across mammals, though not all mammals express this gene (Nathans et al., 1986, Yokoyama and Yokoyama, 1989). Across new and old world monkeys, systems for opponent S-cone vision appear conserved, again hinting at its early origins among primates (Silveira et al., 1999, Jacobs, 2007), with the notable exception of some new world species (Jacobs, 1998, Levenson et al., 2007). The conservation of S-cones and the SC in mammals would appear to make their interaction likely.

Why have S-cone inputs to the SC gone undetected? The most likely explanation stems from the properties of the S-cone subsystem. S-cones, and the ganglion cells that carry their output, are rare in the retina, comprising only about 5-10% of cells (Bumsted and Hendrickson, 1999, Calkins, 2001). Ganglion cells that project to the SC are also scarce and tend to have broad, sparse dendritic fields (Leventhal et al., 1981, Perry and Cowey, 1984, Rodieck and Watanabe, 1993). To make matters worse, ganglion cells carrying S-cone signals are a heterogeneous population that tend to have small axons and low firing rates (Hendry and Reid, 2000). As noted

by Schiller and Malpeli (1977), these properties are likely to create a severe bias against detecting such ganglion cells in non-targeted extracellular recordings. Nevertheless, these researchers reported a population of "rarely encountered cells" with small axons and slow conduction velocity that projected to the SC in unusually high proportions. Another early report on retinal ganglion cells that project to SC called them "atypical", with on and off responses to visual stimuli and non-concentric RFs (De Monasterio, 1978b). These cells seem to correspond well with earlier reports of less numerous non-concentric ganglion cells with phasic responses, large receptive fields and no color opponency (De Monasterio and Gouras, 1975). Although not color opponent, some of these cells responded well to stimuli of any color, as do visual neurons in the SC (Marrocco and Li, 1977, White et al., 2009). Some atypical ganglion cells were reported to receive input from all cone types and even project directly to the SC (De Monasterio, 1978a). More recent studies have confirmed these findings, revealing a heterogeneous population of numerous ganglion cell types that project to the SC (Leventhal et al., 1981, Perry and Cowey, 1984, Rodieck and Watanabe, 1993). Many properties of SC projecting ganglion cells closely resemble those of ganglion cells known to carry S-cone related signals to the koniocellular layers of the LGN (Hendry and Reid, 2000, Dacey and Packer, 2003). Chromatic sensitivity in the SC could arise from this small population of ganglion cells that have proven especially difficult to characterize.

5.1.3 Recent characterization of S-cone input to retinal ganglion cells

Advances in technique have allowed targeted, intracellular recordings of retinal ganglion cells. Targeted recording led to the identification of the first class of ganglion cell that carries S-cone specific signals (Dacey and Lee, 1994, Dacey, 1996). Modern tracing techniques allow morphological identification of recorded neurons. Targeted recording combined with chromatic

adaption and silent substitution (older studies used monochromatic lights to study color opponency, not cone isolation techniques) allows physiological characterization of cone inputs in addition to anatomical imaging (Dacey, 1999). Without these methods, it is difficult to measure cone specific input, especially if S-cone input is weak, and nearly impossible to classify ganglion cell types (Calkins, 2001, Dacey et al., 2003, Klug et al., 2003). It is now known that a diverse population of ganglion cells carries both S-cone ON and OFF inputs to the more recently recognized koniocellular layers of the LGN, which lie between the magnocellular and parvocellular layers (Martin et al., 1997, Hendry and Reid, 2000, Szmajda et al., 2006). The majority of SC projecting ganglion cells have been classified as the P gamma cell type (Perry and Cowey, 1984). This heterogeneous population is most commonly associated with the diverse cell types that receive S-cone input and project to the koniocellular layers of the LGN. Whether the cells so far classified as receiving S-cone input also project to the SC is not yet known.

There are a large number of cell types and cell specific interactions in the retina whose properties are still being characterized (Dacey, 1999, Dacey and Packer, 2003). Efforts to study these interactions have revealed a variety of sparse cell types that carry input from S-cones and are similar in many respects to those known to project to the SC. Additional studies suggest that S-cones may influence other visual subsystems more than originally believed. For example, S-cones contribute to a number of functions commonly associated with the luminance channel, and it has been suggested that they may contribute to this pathway (Calkins, 2001). S-cone OFF bipolar cells have been found that contact midget ganglion cells and hence may influence the parvocellular pathway (Klug et al., 2003). Other research has uncovered bipolar cells that could contact all cone types (Joo et al., 2011) and melanopsin expressing ganglion cells that carry color signals derived from S-cones and may contribute to perception (Dacey et al., 2005). At least 8 other

types of ganglion cells were recently discovered, representing only 1-2% of the population, and at least two of these are sensitive to S-cone specific excitation (Dacey and Packer, 2003, Dacey et al., 2003). In addition, two more types of achromatic ganglion cells have been reported that sum input from all cone types (Calkins and Sterling, 2007). Many of these cells have wide dendritic fields, suggesting broad summation and large receptive fields, as would be expected for SC projecting cells and is common among koniocellular projecting cells (Szmajda et al., 2008). Many other types of small ganglion cells have been observed, but await further classification to determine their cone sensitivity and possible tectal projections (Crook et al., 2008a, Crook et al., 2008b). Ongoing research makes it clear that the types of cells and signals leaving the retina are not fully understood. Some of these newly discovered ganglion cell types, or those yet to be fully characterized, could be the source of S-cone input observed in the SC.

5.2 COMPARISONS TO PREVIOUS RESULTS

Several previous studies have examined the effect of color and S-cone stimuli on visual responses in the SC. These studies have used a variety of techniques. None have used S-cone stimuli calibrated individually for each observer and spatial location combined with dynamic luminance noise. Our focus was on using techniques from human psychophysics to make our results directly comparable.

5.2.1 Chromatic sensitivity in macaque SC

Only one previous study has investigated color sensitivity in SC neurons recorded in awake

behaving macaques (White et al., 2009). Isoluminant Gaussian patches were presented in the receptive field of SC neurons. The color of the patches was chosen from across DKL space, including stimuli near and along the theoretical, uncalibrated, S-cone isolating direction. Recorded SC neurons were broadly sensitive to color, including colors that should most strongly modulate the S-cone opponent mechanism. White et al. (2009) further reported that achromatic stimuli produce shorter latency visual responses than chromatically defined stimuli. This latency result may reflect the use of only a maximum contrast luminance stimulus. We used a low contrast luminance stimulus and varied the contrast of our chromatic S-cone stimulus. Our data show that while low contrast S-cone stimuli evoke longer latency responses than luminance stimuli, a high contrast S-cone stimulus can evoke shorter latency responses than a luminance stimulus. When comparing chromatic vs. achromatic response latency, stimulus contrast must be taken into account. Our results indicate that neuronal responses in the SC are largely determined by a contrast-dependent broadband summation of cone activation that includes S-cones.

Sustained and transient SC neurons differ in their sensitivity to color as compared to luminance (White et al., 2009). White et al. (2009) found that transient visual neurons are much less sensitive to color than to luminance. We performed a similar neuronal classification on our visual SC neurons. We found that the most transient neurons are more sensitive to changes in S-cone isolating contrast. Differences between the high and low contrast S-cone stimuli in the present results and the findings between the luminance and chromatic stimuli of White et al. (2009) are similar on the grounds of contrast. In both studies, transient visual neurons were more sensitive to contrast. Our data show that contrast sensitivity is not specific to the particular visual mechanism activated by the stimulus. We conclude that transient visual neurons are more sensitive to contrast than sustained neurons and this includes chromatic sensitivity to S-cone input.

5.2.2 Chromatic sensitivity in marmoset SC

Interesting recent investigations in new world monkeys measured cone input to SC neurons in anesthetized marmosets, with emphasis on input from S-cones (Tailby et al., 2012). S-cone responses were observed only after presentation of flashed S-cone stimuli. These responses were typically weak, although the S-cone response was stronger to stimulus offset. The relatively weak response of SC neurons to S-cone stimuli was attributed to residual contrast in long wavelength cones, and not true S-cone input. When drifting gratings were used to measure response characteristics of SC neurons, responses to changes in S-cone contrast were not observed. The authors concluded that SC neurons are not driven by S-cones.

Residual contrast in longer wavelength cones seems insufficient to account for our data. The SC neurons we recorded frequently exhibit on and off responses to S-cone stimuli. These responses are as large as those to stimuli designed to specifically modulate contrast in the long wavelength sensitive cones. We used 2 levels of S-cone contrast and, across animals and spatial locations, presented 6 radiometrically distinct S-cone stimuli. The effects of these stimuli on the luminance and L-M opponent channels were small and, due to limitations of the 8-bit DAC, inconsistent across stimuli. S-cone stimuli were presented on a checkered background that was constantly changing luminance in order to mask residual responses in luminance channels by deliberately creating luminance contrast artifacts (Birch et al., 1992). Because the monitor calibration is not perfect and equiluminant points vary between neurons (Schiller and Colby, 1983), the noise had small additional effects on L-M opponent channels. Yet we observed consistent and large SC neuronal response modulation with changes in S-cone contrast. Considering that our use of luminance noise is, by design, better suited to control for residual luminance effects than L-M opponent effects, it is worth noting what would be expected of residual

L-M opponent activation. The L-M opponent channel is slower than the luminance channel, both psychophysically and electrophysiologically (Maunsell and Gibson, 1992, Schmolesky et al., 1998, Smithson and Mollon, 2004, Bompas and Sumner, 2008). This suggests that it would take a large amount of residual L-M opponent contrast for SC neurons to exhibit shorter response latencies to the high contrast S-cone stimulus than to the luminance stimulus. Taken together with the relatively large response magnitude to chromatic stimuli observed in our data and in that of White et al. (2009), it is difficult to attribute our responses entirely to residual activation of L- and M-cones.

The conclusion that S-cone input does not reach the SC is surprising when one considers the other physiological and anatomical aspects of this structure. In addition to their analysis of cone inputs, Tailby et al. (2012) rigorously characterized the temporal, spatial and direction preferences of SC neurons in a way not previously done. They found that spatio-temporal properties of SC neurons more closely match those of koniocellular layer neurons, which are known to receive input from S-cone sensitive ganglion cells, than those of the magnocellular or parvocellular layers, which do not. These data in isolation would predict the presence of S-cone input to the SC if neuronal responses are largely a reflection of the properties of their afferent visual neurons.

Two major differences in experimental procedure compared to the awake behaving macaque model were noted by Tailby et al. (2012). **1)** Their subjects were anesthetized and the effects of anesthesia are prejudiced against cortical structures. Such an effect could disproportionately reduce cortically dependent color sensitivity in the SC. **2)** Despite their many similarities to macaques, it is possible that new world marmoset monkeys have organizational differences in their visual system. This possibility is emphasized by discrepancies between new

world and old world monkeys in their S-cone and koniocellular layer organization (Hendry and Reid, 2000, Jacobs, 2007). Especially of interest here is that the projection from SC to koniocellular LGN neurons appears stronger in macaques than in new world monkeys, suggesting possible differences for the role of S-cone input and tectal influence between these species (Hendry and Reid, 2000). The observation that S-cone input was not present in the marmoset SC could be a result of either of these factors.

5.2.3 Chromatic sensitivity in human SC

How are physiological results in monkeys reflected in human fMRI responses? This question has been directly addressed in two recent studies. In both studies S-cone isolating stimuli were presented while measuring fMRI activation in the SC. Leh et al. (2010) compared activation to achromatic and S-cone stimuli where the achromatic stimulus was of greater cone contrast. They found that activation of the SC was absent using S-cone compared to achromatic stimuli (Leh et al., 2010). Interestingly, a second fMRI study appears to have measured a BOLD signal response change to S-cone stimuli in the same direction as luminance stimuli during pro and antisaccade tasks (Anderson et al., 2008). Their effect suggests stronger activation to luminance than to S-cone stimuli that were matched for subjective salience. The conclusion from both studies was that the human SC is not activated by S-cone isolating stimuli.

Three major concerns arise when considering fMRI activation of the SC to visual stimuli. **1)** The SC is a difficult structure to measure using fMRI (Anderson and Rees, 2011), although rough topography and visual responses have been measured (DuBois and Cohen, 2000, Schneider and Kastner, 2005). **2)** Visual responses in the SC rapidly habituate (Boehnke et al., 2011, Tailby et al., 2012), which is likely to reduce measured visual responses given the temporal resolution of

fMRI. **3)** The final, and most important concern is stimulus contrast. Our data, and those from other human fMRI studies (Schneider and Kastner, 2005), demonstrate that contrast has a major effect on SC activation. Even when cone contrast is matched, it is difficult to make comparisons between cone mechanisms (Brainard, 1996), particularly because the luminance mechanism shows a steeper, saturating contrast sensitivity function (Tailby et al., 2008b, Tailby et al., 2012). Data from these two fMRI studies rely on changes relative to activation during a luminous background presentation and not absolute activity. This would make it easy to miss responses in the SC to S-cone stimuli that are weaker than responses to other stimuli. Indeed, it appears Leh et al. (2010) observed diminished responses to the S-cone stimulus in several visual areas, and both studies show weak activation of the SC, which could be accounted for by differences in contrast.

In sum, direct tests of input to the SC show a number of differences likely to stem from the use of different species as well as stimulus presentation and measurement techniques. Whether there are actually large differences between species and stimulus presentation techniques requires further research. We chose to follow closely techniques used in human psychophysics in order to relate our data to this line of work. Unlike previous studies in non-human primates, we calibrated S-cone stimuli for each animal and spatial location and used a relatively strong luminance noise background to reduce residual response artifacts. Our technique revealed strong modulation of SC neurons with changes in S-cone contrast that contradict several other findings.

5.3 BLOCKING VISUAL INPUT TO THE SC WITH S-CONE STIMULI

Beginning with the innovative work of Sumner and colleagues (2002), many human psychophysical studies have taken advantage of an apparent lack of S-cone input to explore the

role of SC. The rationale for these experiments is that the SC can be effectively "lesioned" by using visual stimuli that the SC cannot perceive. Collicular "lesions" are performed by presenting stimuli that are only detectable through use of retinal S-cones. Behavioral responses to S-cone stimuli are then compared with those to luminance stimuli, to which the SC is not blind. If differences (typically reaction time differences) are observed between behavioral responses to the S-cone and luminance stimuli, the conclusion is that the SC mediates the behavior under investigation because the SC cannot resolve the S-cone stimulus. A negative result using S-cone stimuli (reaction times to luminance and S-cone stimuli are equal) is taken to mean that the SC does not mediate the behavioral effect in question. Our data show that the assumption that the SC is insensitive to stimuli that activate only S-cones is incorrect. Nevertheless, several studies have reported behavioral effects using S-cone stimuli.

The first experiments to use S-cone stimuli to block the SC reported distinct behavioral effects for luminance compared to S-cone stimuli. The first study to use S-cone stimuli to block visual input to SC investigated two phenomena: the oculomotor distractor effect and exogeneous orienting of attention (Sumner et al., 2002). The oculomotor distractor effect is characterized by increases in saccadic reaction time to a visual target when a second visual stimulus, the distractor, is presented elsewhere in the visual field. Sumner et al. (2002) reported the absence of the oculomotor distractor effect when the distractors were S-cone isolating stimuli. This result was found only for saccadic responses, and not when manual responses were required. Exogenous orienting of attention is the phenomenon whereby an irrelevant stimulus briefly presented at the target location just before the go cue decreases reaction time. In contrast to the distractor effect, S-cone and luminance cues both produced exogenous orienting of attention. The conclusion was that the SC has a primary role in the oculomotor distractor effect when saccadic responses are

required but not in exogenous cueing of attention.

The initial success in finding distinct outcomes with S-cone compared to luminance stimuli prompted further studies. Inhibition of return is the tendency to avoid returning to previously attended locations. Inhibition of return was absent when saccadic responses were required to a previously attended S-cone stimulus location (Sumner et al., 2004). In contrast, inhibition of return was observed after attending an S-cone stimulus when manual responses were required. This distinction suggested the possibility of two distinct mechanisms for inhibition of return: a saccadic mechanism mediated through the SC and a separate mechanism for manual responses independent of the SC (Sumner, 2006).

Continued use of S-cone isolating stimuli to block SC input showed no effect of using S-cone isolating stimuli on the gap effect and naso-temporal asymmetry (Sumner et al., 2006, Bompas et al., 2008). The gap effect is seen when a fixation target is extinguished before target presentation, providing a temporal gap between fixation release and motor response. The result is faster saccadic reaction time. Studies of the gap effect using S-cone stimuli as the fixation point were similar to those using a luminance defined fixation point (Sumner et al., 2006). Although fixation of the luminance stimulus provided a stronger effect, it could not be ruled out that the gap effect was sensitive to S-cone stimulus fixation. Nasotemporal asymmetry is seen when observers, monocularly presented with two stimuli, preferentially choose the target in the temporal visual field. This effect is thought to reflect an asymmetry in retinotectal projections. Nasotemporal asymmetry was found to be similarly present using both S-cone and luminance defined targets (Bompas et al., 2008). Results from these two studies suggested that the SC does not play a pivotal role in the gap effect or nasotemporal asymmetry.

The idea that visual input to the SC could be blocked or altered using S-cone stimuli, as

cleverly set forth by Sumner and colleagues, proved highly influential. Numerous other groups have used S-cone stimuli to investigate SC function under the assumption that the SC is insensitive to S-cone stimuli. Phenomena studied range from the redundant target effect (Leo et al., 2008) and pro-antisaccade cost (Anderson et al., 2008) to more clinical applications such as interhemispheric transfer in callosotomy patients (Savazzi and Marzi, 2004, Savazzi et al., 2007) and mediation of blindsight (discussed below), among many others.

5.4 HOW CAN PSYCHOPHYSICAL WORK BE RECONCILED

Our experimental methods were modeled after human psychophysics studies using S-cone stimuli with the goal of testing the assumption that the SC is blind to S-cone stimuli. Yet our data show that SC neurons are responsive to S-cone isolating stimuli under these conditions. This means that the SC cannot be blocked by using an S-cone stimulus in this manner.

How could psychophysical studies find positive results if S-cone activation does reach the SC? This is an important question given the widespread use of S-cone stimuli now present in the literature. Many of these studies did not use precisely measured or individually calibrated S-cone stimuli. They simply used "blue" or "purple" stimuli whose retinal activation properties are not known. Several also used low levels of luminance noise, which could lead to influence from rods. If we focus on those that closely follow the techniques proposed by Sumner and colleagues there are 2 explanations. Both hinge on the fact that nearly all psychophysical studies using the S-cone stimulus technique rely heavily on reaction time measurements.

5.4.1 Stimulus contrast affects reaction time and neuronal response

It has long been known that reaction time is strongly dependent on stimulus contrast, or magnitude (Hovland and Bradshaw, 1937). Our data show that the response latency of SC neurons is largely determined by stimulus contrast, including chromatic contrast that isolates S-cones. Therefore, if S-cone and luminance stimuli are not matched, reaction times could vary as a simple matter of contrast and neuronal latency.

It is noteworthy that several studies found negative results using S-cone stimuli when manual responses were required, but positive effects using saccadic responses. Saccadic eye movements are executed with shorter reaction time and greater velocity than typical manual responses. Our data demonstrate that neuronal latencies in the SC (as in other brain regions) are influenced by cone contrast. Furthermore, our data suggest that luminance signals are likely to reach the SC faster than S-cone signals of comparable strength. These small differences in transmission time would be more likely to affect motor systems with simple, rapid processing like the saccadic eye movement system. Thus it is possible that manual and saccadic reaction time are differentially influenced by S-cone stimuli due to differences in timing precision, rather than their explicit use of the SC visual pathways.

Supporting the idea that contrast-dependent neuronal response latency plays a critical role, the gap effect and nasotemporal asymmetry showed no effect of S-cone stimuli. In both tasks, the impact of differential processing time between the luminance and S-cone stimulus is likely to be negligible. For the gap task, the fixation point is turned off and the subject has 200 ms to release fixation and prepare for the saccade. As long as this process takes less time than is actually allotted, differences in S-cone and luminance processing time would not be reflected in behavioral reaction time. The investigation of nasotemporal asymmetry actually avoided confounds of direct

comparison between luminance and S-cone stimuli entirely. Using this paradigm, saccade bias was measured through comparisons within stimulus type. No behavioral differences were observed between S-cone and luminance stimuli when the differential processing time of luminance and S-cone stimuli did not affect the results. This further supports the conclusion that positive behavioral effects may have underlying causes that stem from neuronal response latency and stimulus contrast, rather than the role of SC in the behavior.

5.4.2 S-cone and luminance processing channels differ

The S-cone processing system appears slower than the luminance system. Several studies using S-cone stimuli have attempted to account for confounds of stimulus contrast by equating stimuli for subjective salience or objective contrast (Sumner et al., 2006, Anderson et al., 2008, Bompas and Sumner, 2008, Thirkettle et al., 2013). Nevertheless, differences in reaction time are often observed between subjectively matched S-cone and luminance stimuli. This could be attributed to differences in the S-cone opponent and luminance channels in the brain. Even subjectively matched luminance and S-cone stimuli vary in processing time psychophysically (Smithson and Mollon, 2004, Bompas and Sumner, 2008). Physiologically, differences are also observed in S-cone signal processing in V1 (Cottaris and De Valois, 1998) and through retinal ganglion cells and koniocellular neurons in the LGN (Hendry and Reid, 2000). Estimates of these differences typically indicate that S-cone processing is about 20 to 40 ms slower than luminance processing, which could have a substantial impact on measured reaction time.

Some investigators using S-cone stimuli have acknowledged the differential processing of S-cone and luminance signals. Attempts to account for the slowness of the S-cone system have involved manipulating cue timing and stimulus onset asynchronies to allow more time for S-cone

signal processing (Sumner et al., 2004, Bompas and Sumner, 2009). Indeed, this technique has revealed that, contrary to Sumner et al. (2002), the oculomotor distractor effect *is* present when S-cone stimuli are used (Bompas and Sumner, 2009). This finding validates the importance of reaction time effects caused by stimulus contrast and processing in separate visual channels. The combination of subjective salience matching and stimulus onset asynchronies for S-cone stimuli appears to be a necessary and valuable technique for comparing reaction time between S-cone and luminance stimuli.

5.4.3 How can psychophysical results be reinterpreted?

Our finding that S-cone stimuli activate SC neurons requires a re-evaluation of results using such stimuli to block the SC. Despite the concerns raised above, there are positive results demonstrating differences in the use of S-cone and luminance contrasts that are likely attributable to the use of S-cone stimuli. Instead of these psychophysical findings being directly attributable to the SC per se, they are likely a reflection of the S-cone processing system itself. Three simple lines of evidence support the view that the S-cone and luminance systems should process stimuli differently. **1)** The visual system can be subdivided into multiple distinct subsystems, where luminance and color are processed separately (Derrington, 2002, Nassi and Callaway, 2009). **2)** Even the individual chromatic channels have evolved separately for their own purposes, being distinct anatomically, morphologically and immunologically (Smithson and Mollon, 2004). **3)** Most importantly, the S-opponent system is known to exhibit a number of properties different from luminance and L-M opponent channels (Hendry and Reid, 2000, Calkins, 2001, Nassi and Callaway, 2009). On these grounds, behavioral and neuronal response differences between S-cone and luminance stimuli should be expected independent of collicular mediation. Because our data

show that S-cone stimuli are able to drive SC neurons, previous results might be better interpreted in light of the peculiarities of the S-opponent subsystem as a whole, rather than as an indicator of SC contribution.

BIBLIOGRAPHY

Alexander I, Cowey A (2010) Edges, colour and awareness in blindsight. Consciousness and Cognition 19:520-533.

Anderson AJ, Carpenter RHS (2008) The effect of stimuli that isolate S-cones on early saccades and the gap effect. Proceedings of the Royal Society London B Biological Sciences 275:335-344.

Anderson EJ, Husain M, Sumner P (2008) Human intraparietal sulcus (IPS) and competition between exogenous and endogenous saccade plans. NeuroImage 40:838-851.

Anderson EJ, Rees G (2011) Neural correlates of spatial orienting in the human superior colliculus. Journal of Neurophysiology 106:2273-2284.

Anstis SM, Cavanagh P (1983) A Minimum Motion Technique for Judging Equiluminance. In: Colour Vision: Physiology and psychophysics (Mollon, J. D. and Sharpe, L. T., eds), pp 156-166 London: Academic Press London.

Azzopardi P, Cowey A (1997) Is blindsight like normal, near-thresholdâ€‰vision? Proceedings of the National Academy of Sciences 94:14190-14194.

Barbur JL, Sahraie A, Simmons A, Weiskrantz L, Williams SCR (1998) Residual processing of chromatic signals in the absence of a geniculostriate projection. Vision Research 38:3447-3453.

Bilodeau L, Faubert J (1997) Isoluminance and chromatic motion perception throughout the visual field. Vision Research 37:2073-2081.

Birch J, Barbur JL, Harlow AJ (1992) New method based on random luminance masking for measuring isochromatic zones using high resolution colour displays. Ophthalmic and Physiological Optics 12:133-136.

Boch R, Fischer B, Ramsperger E (1984) Express-saccades of the monkey: Reaction times versus intensity, size, duration, and eccentricity of their targets. Exp Brain Res 55:223-231.

Boehnke SE, Berg DJ, Marino RA, Baldi PF, Itti L, Munoz DP (2011) Visual adaptation and novelty responses in the superior colliculus. European Journal of Neuroscience 34:766-779.

Bompas A, Sterling T, Rafal RD, Sumner P (2008) Naso-Temporal Asymmetry for Signals Invisible to the Retinotectal Pathway. J Neurophysiol 100:412-421.

Bompas A, Sumner P (2008) Sensory sluggishness dissociates saccadic, manual, and perceptual responses: An S-cone study. Journal of Vision 8:1-13.

Bompas A, Sumner P (2009) Oculomotor Distraction by Signals Invisible to the Retinotectal and Magnocellular Pathways. Journal of Neurophysiology 102:2387-2395.

Bowmaker JK, Dartnall HJ (1980) Visual pigments of rods and cones in a human retina. The Journal of Physiology 298:501-511.

Bowmaker JK, Dartnall HJ, Lythgoe JN, Mollon JD (1978) The visual pigments of rods and cones in the rhesus monkey, Macaca mulatta. The Journal of Physiology 274:329-348.

Brainard DH (1996) Cone contrast and opponent modulation color spaces. In: Human Color Vision (Kaiser, P. K. and Boynton, R. M., eds), pp 563-579 Washington, D.C.: Optical Society of America.

Bruce CJ, Desimone R, Gross CG (1986) Both striate cortex and superior colliculus contribute to visual properties of neurons in superior temporal polysensory area of macaque monkey. Journal of Neurophysiology 55:1057-1075.

Bumsted K, Hendrickson A (1999) Distribution and development of short-wavelength cones differ between *Macaca* monkey and human fovea. The Journal of Comparative Neurology 403:502-516.

Bunt AH, Hendrickson AE, Lund JS, Lund RD, Fuchs AF (1975) Monkey retinal ganglion cells: Morphometric analysis and tracing of axonal projections, with a consideration of the peroxidase technique. The Journal of Comparative Neurology 164:265-285.

Calkins DJ (2001) Seeing with S cones. Progress in Retinal and Eye Research 20:255-287.

Calkins DJ, Sterling P (2007) Microcircuitry for Two Types of Achromatic Ganglion Cell in Primate Fovea. The Journal of Neuroscience 27:2646-2653.

Carpenter RHS (ed.) (1981) Oculomotor procrastination. Hillsdale, NJ: L. Erlbaum Associates.

Carpenter RHS, Williams MLL (1995) Neural computation of log likelihood in control of saccadic eye movements. Nature 377:59-62.

Cavanagh P, MacLeod DIA, Anstis SM (1987) Equiluminance: spatial and temporal factors and the contribution of blue-sensitive cones. J Opt Soc Am A 4:1428-1438.

Cottaris NP, De Valois RL (1998) Temporal dynamics of chromatic tuning in macaque primary visual cortex. Nature 395:896-900.

Cowey A (2010) The blindsight saga. Experimental Brain Research 200:3-24.

Cowey A, Alexander I, Stoerig P (2011) Transneuronal retrograde degeneration of retinal ganglion cells and optic tract in hemianopic monkeys and humans. Brain 134:2149-2157.

Cowey A, Gross CG (1970) Effects of foveal prestriate and inferotemporal lesions on visual discrimination by rhesus monkeys. Experimental Brain Research 11:128-144.

Cowey A, Stoerig P (1989) Projection patterns of surviving neurons in the dorsal lateral geniculate nucleus following discrete lesions of striate cortex: implications for residual vision. Experimental Brain Research 75:631-638.

Cowey A, Stoerig P (1995) Blindsight in monkeys. Nature 373:247-249.

Cowey A, Stoerig P (1999) Spectral sensitivity in hemianopic macaque monkeys. European Journal of Neuroscience 11:2114-2120.

Cowey A, Stoerig P (2001) Detection and discrimination of chromatic targets in hemianopic macaque monkeys and humans. European Journal of Neuroscience 14:1320-1330.

Crook JD, Peterson BB, Packer OS, Robinson FR, Gamlin PD, Troy JB, Dacey DM (2008a) The Smooth Monostratified Ganglion Cell: Evidence for Spatial Diversity in the Y-Cell Pathway to the Lateral Geniculate Nucleus and Superior Colliculus in the Macaque Monkey. The Journal of Neuroscience 28:12654-12671.

Crook JD, Peterson BB, Packer OS, Robinson FR, Troy JB, Dacey DM (2008b) Y-Cell Receptive Field and Collicular Projection of Parasol Ganglion Cells in Macaque Monkey Retina. The Journal of Neuroscience 28:11277-11291.

Curcio CA, Sloan KR, Packer O, Hendrickson AE, Kalina RE (1987) Distribution of cones in human and monkey retina: individual variability and radial asymmetry. Science 236:579-582.

Cynader M, Berman N (1972) Receptive-field organization of monkey superior colliculus. Journal of Neurophysiology 35:187-201.

Dacey DM (1996) Circuitry for color coding in the primate retina. Proceedings of the National Academy of Sciences 93:582-588.

Dacey DM (1999) Primate retina: cell types, circuits and color opponency. Progress in Retinal and Eye Research 18:737-763.
Dacey DM (2004) Origins of perception: retinal ganglion cell diversity and the creation of parallel visual pathways. In: The Cognitive Neurosciences (Gazzaniga, M., ed), pp 281-301 Cambridge, MA: MIT Press.
Dacey DM, Lee BB (1994) The 'blue-on' opponent pathway in primate retina originates from a distinct bistratified ganglion cell type. Nature 367:731-735.
Dacey DM, Liao H-W, Peterson BB, Robinson FR, Smith VC, Pokorny J, Yau K-W, Gamlin PD (2005) Melanopsin-expressing ganglion cells in primate retina signal colour and irradiance and project to the LGN. Nature 433:749-754.
Dacey DM, Packer OS (2003) Colour coding in the primate retina: diverse cell types and cone-specific circuitry. Current Opinion in Neurobiology 13:421-427.
Dacey DM, Peterson BB, Robinson FR, Gamlin PD (2003) Fireworks in the Primate Retina: In Vitro Photodynamics Reveals Diverse LGN-Projecting Ganglion Cell Types. Neuron 37:15-27.
De Monasterio FM (1978a) Properties of concentrically organized X and Y ganglion cells of macaque retina. J Neurophysiol 41:1394-1417.
De Monasterio FM (1978b) Properties of ganglion cells with atypical receptive-field organization in retina of macaques. J Neurophysiol 41:1435-1449.
De Monasterio FM, Gouras P (1975) Functional properties of ganglion cells of the rhesus monkey retina. The Journal of Physiology 251:167-195.
De Valois RL, Morgan HC, Polson MC, Mead WR, Hull EM (1974) Psychophysical studies of monkey vision--I. Macaque luminosity and color vision tests. Vision Research 14:53-67.
Derrington AM (2002) Visual System: S is not for Saccades. Current biology : CB 12:R591-R592.
Derrington AM, Krauskopf J, Lennie P (1984) Chromatic mechanisms in lateral geniculate nucleus of macaque. The Journal of Physiology 357:241-265.
Dominy NJ, Lucas PW (2001) Ecological importance of trichromatic vision to primates. Nature 410:363-366.
Dorris MC, Munoz DP (1998) Saccadic Probability Influences Motor Preparation Signals and Time to Saccadic Initiation. The Journal of Neuroscience 18:7015-7026.
Dorris MC, Paré M, Munoz DP (1997) Neuronal Activity in Monkey Superior Colliculus Related to the Initiation of Saccadic Eye Movements. The Journal of Neuroscience 17:8566-8579.
DuBois RM, Cohen MS (2000) Spatiotopic Organization in Human Superior Colliculus Observed with fMRI. NeuroImage 12:63-70.
Dunn CA, Hall NJ, Colby CL (2010) Spatial Updating in Monkey Superior Colliculus in the Absence of the Forebrain Commissures: Dissociation Between Superficial and Intermediate Layers. J Neurophysiol 104:1267-1285.
Edelman JA, Keller EL (1996) Activity of visuomotor burst neurons in the superior colliculus accompanying express saccades. Journal of Neurophysiology 76:908-926.
Eisner A, MacLeod DIA (1980) Blue-sensitive cones do not contribute to luminance. J Opt Soc Am 70:121-123.
Field GD, Gauthier JL, Sher A, Greschner M, Machado TA, Jepson LH, Shlens J, Gunning DE, Mathieson K, Dabrowski W, Paninski L, Litke AM, Chichilnisky EJ Functional connectivity in the retina at the resolution of photoreceptors. Nature 467:673-677.

Finlay BL, Schiller PH, Volman SF (1976) Quantitative studies of single-cell properties in monkey striate cortex. IV. Corticotectal cells. Journal of Neurophysiology 39:1352-1361.
Fischer B, Boch R (1983) Saccadic eye movements after extremely short reaction times in the monkey. Brain Research 260:21-26.
Fischer B, Weber H (1993) Express saccades and visual attention. Behavioral and Brain Sciences 16:553-567.
Franke TM, Ho T, Christie CA (2011) The Chi Square Test: Often Used and More Often Misinterpreted. American Journal of Evaluation.
Fries W (1984) Cortical projections to the superior colliculus in the macaque monkey: a retrograde study using horseradish peroxidase. J Comp Neurol 230:55-76.
Goebel R, Muckli L, Zanella FE, Singer W, Stoerig P (2001) Sustained extrastriate cortical activation without visual awareness revealed by fMRI studies of hemianopic patients. Vision Research 41:1459-1474.
Goldberg ME, Wurtz RH (1972) Activity of superior colliculus in behaving monkey. I. Visual receptive fields of single neurons. J Neurophysiol 35:542-559.
Goodman LA (1964) Simultaneous Confidence Intervals for Contrasts Among Multinomial Populations. The Annals of Mathematical Statistics 35:716-725.
Gross CG (1991) Contribution of striate cortex and the superior colliculus to visual function in area MT, the superior temporal polysensory area and inferior temporal cortex. Neuropsychologia 29:497-515.
Gross CG, Moore T, Rodman HR (2004) Visually guided behavior after V1 lesions in young and adult monkeys and its relation to blindsight in humans. Progress in Brain Research Volume 144:279-294.
Hall NJ, Colby CL (2013) Psychophysical definition of S-cone stimuli in the macaque. Journal of Vision 13:1-18.
Hall NJ, Colby CL (2014) S-cone Visual Stimuli Activate Superior Colliculus Neurons in Old World Monkeys: Implications for Understanding Blindsight. Journal of Cognitive Neuroscience 26:1234-1256.
Hendrickson A, Wilson ME, Toyne MJ (1970) The distribution of optic nerve fibers inMacaca mulatta. Brain Research 23:425-427.
Hendry SHC, Reid RC (2000) The Koniocellular Pathway in Primate Vision. Annual Reviews of Neuroscience 23:127-153.
Hovland C, Bradshaw D (1937) Visual reaction time as a function of stimulusbackground contrast. Psychologische Forschung 21:50-55.
Huang X, MacEvoy SP, Paradiso MA (2002) Perception of Brightness and Brightness Illusions in the Macaque Monkey. The Journal of Neuroscience 22:9618-9625.
Hubel DH, LeVay S, Wiesel TN (1975) Mode of termination of retinotectal fibers in macaque monkey: An autoradiographic study. Brain Research 96:25-40.
Hunt DM, Peichl L (2014) S cones: Evolution, retinal distribution, development, and spectral sensitivity. Visual Neuroscience 31:115-138.
Jacobs G (2007) New World Monkeys and Color. International Journal of Primatology 28:729-759.
Jacobs GH (1998) A perspective on color vision in platyrrhine monkeys. Vision Research 38:3307-3313.

Joo HR, Peterson BB, Haun TJ, Dacey DM (2011) Characterization of a novel large-field cone bipolar cell type in the primate retina: Evidence for selective cone connections. Visual Neuroscience 28:29-37.
Judge S, Richmond B, Chu F (1980) Implantation of magnetic search coils for measurement of eye position: an improved method. Vision Research 20:535-538.
Kaas JH (2004) The Evolution of the Visual System in Primates. In: The Visual Neurosciences, vol. 1 (Chalupa, L. M. and Werner, J. S., eds), pp 1563-1572 Cambridge: MIT Press.
Kato R, Takaura K, Ikeda T, Yoshida M, Isa T (2011) Contribution of the retino-tectal pathway to visually guided saccades after lesion of the primary visual cortex in monkeys. European Journal of Neuroscience 33:1952-1960.
Klug K, Herr S, Ngo IT, Sterling P, Schein S (2003) Macaque Retina Contains an S-Cone OFF Midget Pathway. The Journal of Neuroscience 23:9881-9887.
Kuypers HGJM, Lawrence DG (1967) Cortical projections to the red nucleus and the brain stem in the rhesus monkey. Brain Research 4:151-188.
Lee BB (2011) Visual pathways and psychophysical channels in the primate. Journal of Physiology 589:41-47.
Lee BB, Martin PR, Valberg A (1988) The physiological basis of heterochromatic flicker photometry demonstrated in the ganglion cells of the macaque retina. Journal of Physiology 404:323-347.
Lee J, Williford T, Maunsell JHR (2007) Spatial Attention and the Latency of Neuronal Responses in Macaque Area V4. The Journal of Neuroscience 27:9632-9637.
Leh SE, Mullen KT, Ptito A (2006) Absence of S-cone input in human blindsight following hemispherectomy. European Journal of Neuroscience 24:2954-2960.
Leh SE, Ptito A, Schönwiesner M, Chakravarty MM, Mullen KT (2009) Blindsight Mediated by an S-Cone-independent Collicular Pathway: An fMRI Study in Hemispherectomized Subjects. Journal of Cognitive Neuroscience 0:1-13.
Leh SE, Ptito A, Schönwiesner M, Chakravarty MM, Mullen KT (2010) Blindsight Mediated by an S-Cone-independent Collicular Pathway: An fMRI Study in Hemispherectomized Subjects. Journal of Cognitive Neuroscience 22:670-682.
Leo F, Bertini C, di Pellegrino G, La davas E (2008) Multisensory integration for orienting responses in humans requires the activation of the superior colliculus. Experimental Brain Research 186:67-77.
Leopold DA (2012) Primary Visual Cortex: Awareness and Blindsight*. Annual Review of Neuroscience 35:91-109.
Levenson DH, Fernandez-duque E, Evans S, Jacobs GH (2007) Mutational changes in S-cone opsin genes common to both nocturnal and cathemeral Aotus monkeys. American Journal of Primatology 69:757-765.
Leventhal AG, Rodieck RW, Dreher B (1981) Retinal ganglion cell classes in the Old World monkey: morphology and central projections. Science 213:1139-1142.
Logothetis NK, Charles ER (1990) The minimum motion technique applied to determine isoluminance in psychophysical experiments with monkeys. Vision Research 30:829-838.
MacLeod DIA, Boynton RM (1979) Chromaticity diagram showing cone excitation by stimuli of equal luminance. J Opt Soc Am 69:1183-1186.
Marino RA, Levy R, Munoz DP (2015) Linking express saccade occurance to stimulus properties and sensorimotor integration in the superior colliculus. Journal of Neurophysiology 114:879-892.

Marrocco RT, Li RH (1977) Monkey superior colliculus: properties of single cells and their afferent inputs. J Neurophysiol 40:844-860.
Martin PR, White AJR, Goodchild AK, Wilder HD, Sefton AE (1997) Evidence that Blue-on Cells are Part of the Third Geniculocortical Pathway in Primates. European Journal of Neuroscience 9:1536-1541.
Marzi CA, Mancini F, Metitieri T, Savazzi S (2009) Blindsight following visual cortex deafferentation disappears with purple and red stimuli: A case study. Neuropsychologia 47:1382-1385.
Maunsell JH, Gibson JR (1992) Visual response latencies in striate cortex of the macaque monkey. Journal of Neurophysiology 68:1332-1344.
Mizzi R, Michael GA (2014) The role of the collicular pathway in the salience-based progression of visual attention. Behavioural Brain Research 270:330-338.
Mollon JD (1989) Tho' she kneel'd in that place where they grew: The uses and origins of primate colour vision. Journal of Experimental Biology 146:21-38.
Mollon JD, Polden PG (1975) Colour illusion and evidence for interaction between cone mechanisms. Nature 258:421-422.
Moore T, Rodman HR, Gross CG (2001) Direction of Motion Discrimination after Early Lesions of Striate Cortex (V1) of the Macaque Monkey. Proceedings of the National Academy of Sciences of the United States of America 98:325-330.
Moore T, Rodman HR, Repp AB, Gross CG (1995) Localization of visual stimuli after striate cortex damage in monkeys: parallels with human blindsight. Proceedings of the National Academy of Sciences 92:8215-8218.
Moore T, Rodman HR, Repp AB, Gross CG, Mezrich RS (1996) Greater residual vision in monkeys after striate cortex damage in infancy. Journal of Neurophysiology 76:3928-3933.
Nassi JJ, Callaway EM (2009) Parallel processing strategies of the primate visual system. Nat Rev Neurosci 10:360-372.
Nathans J, Thomas D, Hogness DS (1986) Molecular Genetics of Human Color Vision: The Genes Encoding Blue, Green, and Red Pigments. Science 232:193-202.
Pare M, Munoz DP (1996) Saccadic reaction time in the monkey: advanced preparation of oculomotor programs is primarily responsible for express saccade occurrence. Journal of Neurophysiology 76:3666-3681.
Perry VH, Cowey A (1984) Retinal ganglion cells that project to the superior colliculus and pretectum in the macaque monkey. Neuroscience 12:1125-1137.
Ripamonti C, Woo WL, Crowther E, Stockman A (2009) The S-cone contribution to luminance depends on the M- and L-cone adaptation levels: Silent surrounds? Journal of Vision 9.
Rocha-Miranda CE, Bender DB, Gross CG, Mishkin M (1975) Visual activation of neurons in inferotemporal cortex depends on striate cortex and forebrain commissures. Journal of Neurophysiology 38:475-491.
Rodieck RW, Watanabe M (1993) Survey of the morphology of macaque retinal ganglion cells that project to the pretectum, superior colliculus, and parvicellular laminae of the lateral geniculate nucleus. The Journal of Comparative Neurology 338:289-303.
Rodman HR, Gross CG, Albright TD (1989) Afferent basis of visual response properties in area MT of the macaque. I. Effects of striate cortex removal. The Journal of Neuroscience 9:2033-2050.

Rodman HR, Gross CG, Albright TD (1990) Afferent basis of visual response properties in area MT of the macaque. II. Effects of superior colliculus removal. The Journal of Neuroscience 10:1154-1164.
Sanders MD, Warrington E, Marshall J, Wieskrantz L (1974) "Blindsight": Vision in a Field Defect. The Lancet 303:707-708.
Savazzi S, Fabri M, Rubboli G, Paggi A, Tassinari CA, Marzi CA (2007) Interhemispheric transfer following callosotomy in humans: Role of the superior colliculus. Neuropsychologia 45:2417-2427.
Savazzi S, Marzi CA (2004) The superior colliculus subserves interhemispheric neural summation in both normals and patients with a total section or agenesis of the corpus callosum. Neuropsychologia 42:1608-1618.
Schiller PH (1998) The neural control of visually guided eye movements. In: Cognitive neuroscience of attention: a developmental perspective (Richards, J. E., ed), pp 3-50 Mahwah, New jersey: Lawrence Erlbaum Associates.
Schiller PH, Colby CL (1983) The responses of single cells in the lateral geniculate nucleus of the rhesus monkey to color and luminance contrast. Vision Research 23:1631-1641.
Schiller PH, Kendall GL, Slocum WM, Tehovnik EJ (2008) Conditions that alter saccadic eye movement latencies and affect target choice to visual stimuli and to electrical stimulation of area V1 in the monkey. Visual Neuroscience 25:661-673.
Schiller PH, Koerner F (1971) Discharge characteristics of single units in superior colliculus of the alert rhesus monkey. J Neurophysiol 34:920-936.
Schiller PH, Lee K (1994) The effects of lateral geniculate nucleus, area V4, and middle temporal (MT) lesions on visually guided eye movements. Visual Neuroscience 11:229-241.
Schiller PH, Malpeli JG (1977) Properties and tectal projections of monkey retinal ganglion cells. J Neurophysiol 40:428-445.
Schiller PH, Malpeli JG (1978) Functional specificity of lateral geniculate nucleus laminae of the rhesus monkey. Journal of Neurophysiology 41:788-797.
Schiller PH, Malpeli JG, Schein SJ (1979a) Composition of geniculostriate input ot superior colliculus of the rhesus monkey. J Neurophysiol 42:1124-1133.
Schiller PH, Malpeli JG, Schein SJ (1979b) Composition of geniculostriate input to superior colliculus of the rhesus monkey. J Neurophysiol 42:1124-1133.
Schiller PH, Sandell JH, Maunsell JH (1987) The effect of frontal eye field and superior colliculus lesions on saccadic latencies in the rhesus monkey. Journal of Neurophysiology 57:1033-1049.
Schiller PH, Stryker M (1972) Single-unit recording and stimulation in superior colliculus of the alert rhesus monkey. J Neurophysiol 35:915-924.
Schiller PH, Stryker M, Cynader M, Berman N (1974) Response characteristics of single cells in the monkey superior colliculus following ablation or cooling of visual cortex. J Neurophysiol 37:181-194.
Schmid MC, Mrowka SW, Turchi J, Saunders RC, Wilke M, Peters AJ, Ye FQ, Leopold DA (2010) Blindsight depends on the lateral geniculate nucleus. Nature advance online publication.
Schmolesky MT, Wang Y, Hanes DP, Thompson KG, Leutgeb S, Schall JD, Leventhal AG (1998) Signal Timing Across the Macaque Visual System. Journal of Neurophysiology 79:3272-3278.

Schneider KA, Kastner S (2005) Visual Responses of the Human Superior Colliculus: A High-Resolution Functional Magnetic Resonance Imaging Study. Journal of Neurophysiology 94:2491-2503.
Silveira LCL, Lee BB, Yamada ES, Kremers JAN, Hunt DM, Martin PR, Gomes FL (1999) Ganglion cells of a short-wavelength-sensitive cone pathway in New World monkeys: Morphology and physiology. Visual Neuroscience 16:333-343.
Smith VC, Pokorny J (1975) Spectral sensitivity of the foveal cone photopigments between 400 and 500 nm. Vision Research 15:161-171.
Smithson HE (2014) S-cone psychophysics. Visual Neuroscience 31:211-225.
Smithson HE, Mollon JD (2004) Is the S-opponent chromatic sub-system sluggish? Vision Research 44:2919-2929.
Smithson HE, Sumner P, Mollon JD (2003) How to find a tritan line. In: Normal and Defective Colour Vision (Mollon, J. D. et al., eds), pp 279-287 Oxford: Oxford University Press.
Snodderly DM, Auran JD, Delori FC (1984a) The macular pigment. II. Spatial distribution in primate retinas. Investigative Ophthalmology & Visual Science 25:674-685.
Snodderly DM, Brown PK, Delori FC, Auran JD (1984b) The macular pigment. I. Absorbance spectra, localization, and discrimination from other yellow pigments in primate retinas. Investigative Ophthalmology & Visual Science 25:660-673.
Sommer MA (1994) Express saccades elicited during visual scan in the monkey. Vision Research 34:2023-2038.
Sommer MA (1997) The spatial relationship between scanning saccades and express saccades. Vision Research 37:2745-2756.
Sommer MA, Wurtz RH (2004) The Dialogue between Cerebral Cortex and Superior Colliculus: Implications for Saccadic Target Selection and Corollary Discharge. In: The Visual Neurosciences, vol. 2 (Chalupa, L. M. and Werner, J. S., eds), pp 1466-1484 Cambridge: MIT Press.
Spering M, Carrasco M (2015) Acting without seeing: eye movements reveal visual processing without awareness. Trends in Neurosciences 38:247-258.
Stoerig P, Cowey A (1989) Wavelength sensitivity in blindsight. Nature 342:916-918.
Stoerig P, Cowey A (1991) Increment-threshold Spectral Sensitivity in Blindsight: Evidence for Colour Opponency. Brain 114:1487-1512.
Stoerig P, Cowey A (1997) Blindsight in man and monkey. Brain 120:535-559.
Stoerig P, Faubert J, Ptito M, Diaconu V, Ptito A (1996) No blindsight following hemidecortication in human subjects? NeuroReport 7:1990-1994.
Sumner P (2006) Inhibition versus attentional momentum in cortical and collicular mechanisms of IOR. Cognitive Neuropsychology 23:1035-1048.
Sumner P, Adamjee T, Mollon JD (2002) Signals Invisible to the Collicular and Magnocellular Pathways Can Capture Visual Attention. Current Biology 12:1312-1316.
Sumner P, Nachev P, Castor-Perry S, Isenman H, Kennard C (2006) Which Visual Pathways Cause Fixation-Related Inhibition? J Neurophysiol 95:1527-1536.
Sumner P, Nachev P, Vora N, Husain M, Kennard C (2004) Distinct Cortical and Collicular Mechanisms of Inhibition of Return Revealed with S Cone Stimuli. Current Biology 14:2259-2263.
Sun H, Smithson HE, Zaidi Q, Lee BB (2006) Specificity of Cone Inputs to Macaque Retinal Ganglion Cells. Journal of Neurophysiology 95:837-849.

Szmajda BA, Buzas P, FitzGibbon T, Martin PR (2006) Geniculocortical relay of blue-off signals in the primate visual system. Proceedings of the National Academy of Sciences 103:19512-19517.

Szmajda BA, Grünert U, Martin PR (2008) Retinal ganglion cell inputs to the koniocellular pathway. The Journal of Comparative Neurology 510:251-268.

Tailby C, Cheong SK, Pietersen AN, Solomon SG, Martin PR (2012) Colour and pattern selectivity of receptive fields in superior colliculus of marmoset monkeys. The Journal of Physiology 590:4061-4077.

Tailby C, Solomon SG, Lennie P (2008a) Functional Asymmetries in Visual Pathways Carrying S-Cone Signals in Macaque. The Journal of Neuroscience 28:4078-4087.

Tailby C, Szmajda BA, Buzas P, Lee BB, Martin PR (2008b) Transmission of blue (S) cone signals through the primate lateral geniculate nucleus. The Journal of Physiology 586:5947-5967.

Tamietto M, Cauda F, Corazzini LL, Savazzi S, Marzi CA, Goebel R, Weiskrantz L, de Gelder B (2010) Collicular Vision Guides Nonconscious Behavior. Journal of Cognitive Neuroscience 22:888-902.

Thirkettle M, Walton T, Shah A, Gurney K, Redgrave P, Stafford T (2013) The path to learning: Action acquisition is impaired when visual reinforcement signals must first access cortex. Behavioural Brain Research 243:267-272.

Trieschmann M, van Kuijk FJGM, Alexander R, Hermans P, Luthert P, Bird AC, Pauleikhoff D (2007) Macular pigment in the human retina: histological evaluation of localization and distribution. Eye 22:132-137.

Vaughan HG, Jr., Gross CG (1969) Cortical responses to light in unanesthetized monkeys and their alteration by visual system lesions. Experimental Brain Research 8:19-36.

Weiskrantz L (1986) Blindsight. A Case Study and Implications. Oxford: Oxford University Press.

Weiskrantz L (2004) Blindsight. In: The Visual Neurosciences, vol. 1 (Chalupa, L. M. and Werner, J. S., eds), pp 657-669 Cambridge: MIT Press.

White B, Kerzel D, Gegenfurtner K (2006) Visually guided movements to color targets. Exp Brain Res 175:110-126.

White BJ, Boehnke SE, Marino RA, Itti L, Munoz DP (2009) Color-Related Signals in the Primate Superior Colliculus. The Journal of Neuroscience 29:12159-12166.

Yokoyama S, Yokoyama R (1989) Molecular evolution of human visual pigment genes. Molecular Biology and Evolution 6:186-197.

Yoshida M, Itti L, Berg David J, Ikeda T, Kato R, Takaura K, White BJ, Munoz Douglas P, Isa T (2012) Residual Attention Guidance in Blindsight Monkeys Watching Complex Natural Scenes. Current Biology 22:1429-1434.

Yoshida M, Takaura K, Kato R, Ikeda T, Isa T (2008) Striate Cortical Lesions Affect Deliberate Decision and Control of Saccade: Implication for Blindsight. The Journal of Neuroscience 28:10517-10530.